The Relationship Between Herpes Simplex Virus 1 and the Cellular DNA Damage Response

HARVARD UNIVERSITY
Graduate School of Arts and Sciences

DISSERTATION ACCEPTANCE CERTIFICATE

The undersigned, appointed by the

Division of Medical Sciences

Committee on Virology

have examined a dissertation entitled

The Relationship Between Herpes Simplex Virus 1 and the Cellular DNA Damage Response

presented by Max Eldon Mertens

candidate for the degree of Doctor of Philosophy and hereby certify that it is worthy of acceptance.

Signature: Lee Gehrke

Typed Name: Dr. Lee Gehrke

Signature: Samuel Rabkin
Samuel Rabkin (Dec 18, 2020 11:39 EST)

Typed Name: Dr. Samuel Rabkin

Signature: JACapr
James DeCaprio (Dec 18, 2020 11:27 EST)

Typed Name: Dr. James DeCaprio

Signature: Karl Munger

Typed Name: Dr. Karl Münger

Date: December 14, 2020

The Relationship Between Herpes Simplex Virus 1 and the Cellular DNA Damage Response

A dissertation presented

by

Max Eldon Mertens

to

The Division of Medical Sciences

in partial fulfillment of the requirements

for the degree of

Doctor of Philosophy

in the subject of

Virology

Harvard University

Cambridge, Massachusetts

December 2020

Dissertation Advisor: Dr. David M. Knipe Max Eldon Mertens

The Relationship Between Herpes Simplex Virus 1 and the Cellular DNA Damage Response

Abstract

Cellular DNA is under constant threat from many different agents that can cause damage to the genome. Damage to the DNA can inhibit the ability of the cell to replicate its genome, which usually leads to death of the cell. Consequently, cells have evolved complex pathways of machinery, collectively termed the DNA damage response (DDR), with the sole purpose to fix any damaged DNA. DNA virus infection also activates the DDR. In this dissertation, we explore the relationship between the DDR and herpes simplex virus 1 (HSV-1). We describe the DDR to incoming and replicating viral genomes with an emphasis on two key DDR kinases: ATM and Chk2. We observed that the DDR is biphasic with incoming and replicating viral DNA activating Chk2 and ATM, respectively. Moreover, we were surprised to find that different DDR proteins had differing effects on the replication of the virus. Canonically, Mre11, encoded by the *MRE11A* gene and a component of the MRN complex, promotes the activation of ATM in response to double-stranded DNA breaks. However, disruption of *MRE11A* and *ATM* by CRISPR-Cas9 had opposing effects on HSV-1 replication, suggesting that the DDR to infection is much more nuanced than previously thought. We also describe a novel role for the p53 tumor suppressor in regulating the expression of a key HSV-1 DNA replication gene. Our findings also allowed us to compile a detailed model of the DDR to

different stages of the HSV-1 lytic replication cycle, something not currently present in the field.

In the appendix, we describe what we thought to be a novel antiviral signaling pathway. HSV-1 infection induces an innate antiviral response presumably though recognition of the viral genome in the nucleus. While the viral DNA is sensed in the nucleus, the signal is propagated to the cytosol by an unknown mechanism. Initial evidence suggested that the Sun1 nuclear envelope protein was involved in this propagation. However, upon more rigorous investigation, we found Sun1 to be dispensable. We discovered that an off-target effect was responsible for the initial phenotype.

Table of Contents

List of Figures and Tables

For my parents Genevieve and Alan. Graduate school is not easy by any stretch of the imagination and I will forever be grateful for your love and support.

To David and the rest of the lab: thank you for helping me grow as a scientist.

Chapter 1: Introduction

1.1 The order *Herpesvirales*, the family *Herpesviridae*, and the human herpesviruses

Herpesvirales and *Herpesviridae*

The order *Herpesvirales* encompasses three families of viruses: *Herpesviridae, Alloherpesviridae,* and *Malacoherpesviridae* (Davison et al., 2009). These families share similar characteristics in that they contain linear, double-stranded DNA (dsDNA) genomes of >100 kilobase pairs (kbp). The infectious viral particle is composed of both an outer lipid bilayer envelope derived from the host, and an inner icosahedral protein capsid. Between the two is a protein-rich matrix termed the viral tegument. The outer envelope is studded with viral glycoproteins that facilitate fusion of the viral envelope with the lipid bilayers of susceptible host cells. Within the capsid lies the viral genome. The *Herpesviridae* family is divided into three sub-families: *Alphaherpesvirinae, Betaherpesvirinae,* and *Gammaherpesvirinae*, and infect a wide range of hosts including birds, reptiles, and mammals (Davison et al., 2009).

The human herpesviruses

The human herpesviruses (HHVs) are divided into the *Alpha-, Beta-,* and *Gammaherpesvirinae*. The three most notable alphaherpesviruses are herpes simplex viruses 1 and 2 (HSV-1 and HSV-2, respectively) and varicella zoster virus (VZV). Unlike the beta- and gammaherpesviruses, HSV-1, HSV-2, and VZV have a wider cellular tropism with primary infection occurring in epithelial cells followed by subsequent infection of neuronal cells where the viral genome enters a state of latency

for future reactivation (Smith, 2012). HSV-1 and HSV-2 infections are most commonly associated with oral and genital lesions, respectively, with recurrent reactivation over the life of the individual (Roizman, 2013). Individuals are typically infected with VZV early in life with a disease manifestation commonly referred to as chicken pox, with later reactivation yielding a disease termed shingles.

Human cytomegalovirus (HCMV) is a member of the *Betaherpesvirinae* with a lymphocyte tropism, different from the *Alphaherpesvirinae*. Although this virus generally does not cause pathology in healthy individuals, HCMV can cause significant congenital complications as well as pathology in immunocompromised individuals.

Two well-studied members of the *Gammaherpesvirinae* are Epstein-Barr virus (EBV) and Kaposi's sarcoma-associated herpesvirus (KSHV). EBV displays a tropism for epithelial and B cells (Möhl et al., 2016), whereas KSHV infects B cells, endothelial cells, and monocytic cells (Chakraborty et al., 2012).

1.2 Herpes simplex viruses

Epidemiology and disease

HSV-1 and HSV-2 infections are ubiquitous throughout the world. In the United States, the seroprevalence in ages 14-49 years was 48.1% for HSV-1 and 12.1% for HSV-2 (McQuillan et al., 2018). Moreover, females showed higher seroprevalence than males. For HSV-1, males and females showed 45.2% and 50.9% seroprevalence, respectively. Comparatively, males and females displayed 8.2% and 15.9% seroprevalence, respectively, for HSV-2. While HSV-1 and HSV-2 commonly cause

relatively benign oral and genital lesions, respectively, in rare cases, these viruses can spread through the nervous system to the brain and cause herpes simplex encephalitis leading to brain damage, particularly of the temporal lobe, and in some cases results in death. HSV-1 is also the leading cause of infectious corneal blindness in the United States (Roizman, 2013). The nucleoside analogs acyclovir, valaciclovir, and famciclovir are effective treatments against both HSV-1 and HSV-2 (Kimberlin and J., 2007).

HSV-1 lytic replication

Infection initiates with fusion of the virion envelope with the plasma membrane of the host cells. Glycoproteins B and C (gB and gC, respectively) first interact with cell surface markers to attach the virus (Roizman, 2013). Glycoprotein D (gD) then interacts with the cellular entry factors herpesvirus entry mediator (HVEM), nectin, or 3-O-sulfated heparan sulfate. This association then allows for fusion of the membranes catalyzed by glycoprotein H/L heterodimers (gH/gL) and glycoprotein B (gB).

Fusion of the membranes releases the capsid and the contents of the viral tegument into the cytoplasm of the host cell. The capsid is trafficked to a nuclear pore along cellular microtubules in a manner dependent on dynein and dynactin (Döhner et al., 2002). After the viral capsid is delivered to a nuclear pore, the linear viral genome is released where it rapidly circularizes (Garber et al., 1993) and begins a characteristic cascade of three stages of viral gene transcription (Honess and Roizman, 1974).

The first gene set transcribed, termed the immediate-early (IE) class, encodes ICP0, ICP4, ICP22, ICP27, and ICP47. Transcription of IE genes begins with virion protein 16 (VP16) association with the cellular Oct-1 and HCF-1 proteins. Binding of this

complex to IE gene promoters facilitates the formation of a transcription pre-initiation complex followed by subsequent elongation by cellular RNA polymerase II (Roizman, 2013).

The second class of genes expressed is the early (E) genes, which encode primarily proteins of the viral replication machinery and other proteins to increase the efficiency of the genome replication process. Transcription of E genes is largely facilitated by ICP4, ICP0, and ICP27. Following their transcription and translation, early gene products target the viral genome for replication. First, the UL9 protein binds to the viral origins of replication: *oriL* and *oriS*. *OriS* is present in a repeated region of the genome, therefore there are two copies of *oriS* and one of *oriL*. UL9 then unwinds a portion of the origin to facilitate the recruitment of the ICP8 single-stranded DNA binding protein. These two proteins then recruit the viral helicase-primase complex comprised of UL5, UL8, and UL52. The final two proteins recruited are the viral DNA polymerase UL30 and its processivity factor UL42. Together, these proteins form the viral DNA polymerase holoenzyme that proceeds to replicate the genome. It is still disputed whether replication proceeds in a rolling circle manner or a mechanism dependent on homologous recombination between the viral genomes (Roizman, 2013).

Following viral genome replication, the third class of viral genes, the late (L) class, is transcribed. Genes in this phase primarily encode virion structural proteins including capsid proteins, proteins that package the newly synthesized viral genomes into these capsids, proteins that facilitate egress of the capsid out of the nucleus, tegument proteins (such as VP16), and the viral glycoproteins that adorn the surface of progeny virions (Roizman, 2013).

After the genomes have been packaged, the new capsids are brought to, and bud through, the nuclear envelope in a manner dependent on the viral UL31 and UL34 proteins. Capsids and tegument proteins are then re-enveloped in the Golgi network and secreted from the cells by the exocytosis pathway (Roizman, 2013).

HSV-1 latent infection

Following primary infection and replication in epithelial cells, HSV-1 infects the termini of sensory neurons. The capsid moves to the nucleus of the neuron by retrograde transport, and, once inside the nucleus, the viral genome circularizes and enters a silent state absent of lytic gene expression. The latency-associated transcript (LAT; further spliced into smaller RNAs) and several micro-RNAs are transcribed which retain the viral genome in a quiescent state (Roizman, 2013). The mechanism(s) by which the virus exits latency and activates the lytic program is not well understood. Within the nucleus of the infected host cell, the viral genome is associated with cellular histone proteins whose epigenetic marks appear to control transcription of the regions of the genome they are bound to. One model of reactivation from latency involves modulation of these epigenetic marks such that, once a threshold is reached, productive lytic gene expression commences and new viruses are produced (Cliffe et al., 2015). This model along with the general role of chromatin in both lytic and latent infection will be discussed in the next section.

Chromatinization of HSV-1 DNA

Unlike polyomaviruses (Germond et al., 1975), HSV-1 DNA is not associated with histones within the viral particle. Instead, the viral DNA is compacted with positively charged polyamine molecules (Gibson and Roizman, 1971). HSV-1 DNA becomes coated with histones within an hour of infection that become unstable or are otherwise lost over the course of replication (Lacasse and Schang, 2012; Lee et al., 2016). Epigenetic marks of the histone tails serve an important role in promoting or suppressing viral gene expression. After chromatinization of the viral genome, H3 histones are tri-methylated on lysines 9 and 27 (H3K9me3 and H3K27me3, respectively) in order to repress viral gene transcription. These marks are progressively lost as infection progresses and the viral genome is replicated (Lee et al., 2016). Moreover, histones associated with viral gene promoters become acetylated, instead of methylated, in order to facilitate transcription (Cliffe and Knipe, 2008). Chromatinization and histone methylation appear to be a response by the host cell to silence transcription and will be explored further in the next section.

During latency, the viral genome is also maintained in chromatin form. However, compared to lytic infection, the viral genome contains higher levels of H3K27me3. This appears to be promoted by the viral ICP0 protein, which is intriguing as ICP0 is traditionally considered to be a lytic protein (Raja et al., 2016). HSV-1 reactivates from its latent state when some stress or other stimulus is imposed on the host neuron. Emerging evidence has implicated changes in the epigenetic marks on the viral chromatin as a mechanism for reactivation (Cliffe et al., 2015; Lee et al., 2018). One model involves phosphorylation of serine residues on the histone tails to promote low levels of transcription of lytic viral genes despite the presence of repressive marks.

Stress on the neuron activates the DLK/JIP3 pathway that culminates in JNK activation and phosphorylation of histone H3 on serine 10 on viral lytic gene promoters. This is proposed to allow for increasing amounts of viral lytic gene transcription that eventually leads to full reactivation (Cliffe et al., 2015).

Cellular sensing of HSV-1 infection

Despite being a relatively efficient process, HSV-1 replication has to overcome many cellular mechanisms that sense and respond to the viral DNA. These responses can be roughly divided into two categories: intrinsic and innate immune responses. As a part of the intrinsic response, promyelocytic leukemia nuclear bodies (PML-NBs), alternately called nuclear domain 10 (ND10), are complexes of proteins that associate with viral DNA as soon as the molecule enters the nucleus, in particular ATRX, PML, and IFI16 (Cabral et al., 2018). These proteins, along with Sp100 and Daxx, restrict replication of ICP0-null HSV-1 (Cabral et al., 2018; Everett et al., 2008; Lukashchuk and Everett, 2010; Merkl et al., 2018; Orzalli et al., 2013). An IE gene product, ICP0, is an E3 ubiquitin ligase whose primary function is to promote the disruption (Maul et al., 1993) and degradation of ND10 proteins in order to remove any restriction on viral replication. PML (Everett et al., 1998), Sp100 (Chelbi-Alix and de Thé, 1999), IFI16 (Orzalli et al., 2012), and ATRX (Jurak et al., 2012) are all degraded as a result of ICP0 activity. These intrinsic responses appear to target the viral chromatin as IFI16 and ATRX promote and maintain heterochromatic marks on the genome, respectively, to repress viral gene expression (Cabral et al., 2018; Orzalli et al., 2013).

The cellular type-I interferon (IFN) pathway is a potent innate immune response that suppresses viral replication, and HSV-1 is no exception. Both DNA and RNA can lead to the robust transcription of interferon alpha and beta (IFNα and IFNβ, respectively). Concerning DNA sensing, double-stranded DNA is bound by the sensor cyclic GMP-AMP synthase (cGAS) (Sun et al., 2013). Binding to DNA activates the catalytic activity of the protein to produce the small dinucleotide cyclic GMP-AMP (cGAMP) (Wu et al., 2013). cGAMP then binds the major adapter protein, STING (Ishikawa and Barber, 2008), on the membranes of the endoplasmic reticulum (Wu et al., 2013). Binding of cGAMP to STING triggers the recruitment of the TBK1 kinase, which then phosphorylates STING to recruit the IRF3 transcription factor. Association of IRF3 with STING allows it to also be phosphorylated by TBK1. Phosphorylated IRF3 then dimerizes and translocates to the nucleus where it promotes the transcription of type-I IFNs (Liu et al., 2015). It is currently unknown whether cGAS binds to HSV-1 DNA directly to initiate an immune response. HSV-1 infection has been observed to cause the release of mitochondrial DNA that is detected by cGAS (West et al., 2015), so this may explain the response to infection if cGAS does not bind directly to the viral genome. As type-I IFN responses can potently inhibit replication, HSV-1 has evolved an answer: the viral UL37 protein, a component of the viral tegument, specifically deamidates cGAS to impair its catalytic activity (Zhang et al., 2018).

IFI16 has been observed to sense HSV-1 DNA and elicit an IFN response through STING (Orzalli et al., 2012; Unterholzner et al., 2010) presumably by oligomerizing on the viral genome (Lum et al., 2019). As mentioned earlier, ICP0 targets IFI16 for degradation (Orzalli et al., 2012), thereby attenuating this antiviral pathway.

IFI16 senses HSV-1 DNA in the nucleus and the mechanism for STING activation in the cytosol is still largely un-resolved. A role for nuclear cGAS has emerged as it was observed to interact with IFI16 to coordinate a response to nuclear HSV-1 DNA (Orzalli et al., 2015).

Cytosolic RNA can also robustly generate an IFN response with the MAVS protein serving as the adapter (Seth et al., 2005). While viral RNAs were not directly sensed by RIG-I, an RNA helicase that binds and activates MAVS with the aid of the Zyxin protein (Kouwaki et al., 2017), HSV-1 infection causes the relocation of a cellular 5S rRNA pseudogene transcript into the cytosol where it is sensed by RIG-I (Chiang et al., 2018). In response to the inhibitory effects of type-I IFN on replication, HSV-1 has evolved numerous mechanisms to suppress the pathway. The viral US3 kinase (Peri et al., 2008; Wang et al., 2013b), ICP0 (Lin et al., 2004; Orzalli et al., 2012), ICP34.5 (γ34.5) (Verpooten et al., 2009), and ICP27 (Christensen et al., 2016) all have been shown to inhibit the IFN pathways at some stage. These findings further highlight the ongoing battle between the virus and the host.

1.3 The cellular responses to, and repair of, damaged DNA

Repair by non-homologous end-joining (NHEJ)

The integrity of the cellular genome is under constant threat from many sources. Cells have evolved complex pathways, termed the DNA damage response (DDR), in order to repair damaged DNA. One of the most devastating forms of damage to the cellular genome is a break in both strands. These can arise as a consequence of errors

during DNA replication, various drug treatments, and ionizing radiation. Double-stranded breaks can lead to chromosome translocations that can result in aberrant cell growth and cancer (Rodgers and McVey, 2016). The cell has two primary methods of fixing these types of breaks: non-homologous end-joining (NHEJ) and homologous recombination (HR), discussed in the next section.

As the name implies, NHEJ involves ligation of the free double-stranded ends of the molecule to an available pair in a manner independent of the DNA sequence. This type of repair serves as a quick fix, but is prone to error in the form of insertion-deletion (indel) mutations as it is not based on homology (Rodgers and McVey, 2016). This characteristic serves as the foundation for genetic engineering and gene deletion technologies such as CRISPR-Cas9 (Doudna and Charpentier, 2014). This nuclease introduces double-stranded breaks that, once repaired by NHEJ, may contain indels that cause a frameshift and truncate the protein or completely change the amino acid sequence, both scenarios leading to loss of function of the protein.

Initially, double-stranded breaks are sensed and bound by the Ku70/Ku80 heterodimer (Mimori and Hardin, 1986). This complex then recruits the DNA-dependent protein kinase catalytic subunit, DNA-PKcs, to form the DNA-PK holoenzyme (Gottlieb and Jackson, 1993). This complex encircles and covers approximately 30 base pairs of DNA, protecting them from degradation or any damage that may jeopardize efficient repair (Yin et al., 2017). Final ligation is performed by the XRCC4/DNA ligase IV (LigIV) complex where XRCC4 stimulates the ligase activity of LigIV to join two DNA ends (Critchlow et al., 1997; Grawunder et al., 1997). There is also an emerging role for the XLF protein in this process as well (Brouwer et al., 2016). Double-stranded breaks are

not always perfectly blunt. They can contain overhangs on either strand, and they may even have a few bases of homology to the receiving strand to be joined with, termed microhomology. Depending on the situation, the mechanisms for repair are slightly different.

Joining two blunt-ended DNA strands is a relatively straightforward process. The ends are first bound by the Ku complex and then the XRCC4/LigIV complex is recruited directly, bypassing the need for DNA-PKcs, and ligate the DNA strands together (Chang et al., 2016). Extra steps are needed if there is a 5' or 3' overhang on the ends to be joined. If there is a 5' overhang, the Ku complex still binds both DNA ends, but this time, DNA-PKcs is recruited along with the nuclease Artemis. DNA-PKcs autophosphorylation stimulates Artemis nuclease activity (Goodarzi et al., 2006). DNA-PKcs also phosphorylates Artemis itself (Ma et al., 2005), which may aid in its activation. Artemis trims the DNA overhang (Ma et al., 2002) to allow for ligation by XRCC4/LigIV. If there is a 3' overhang, it is trimmed by Artemis, and then the 3' ends are extended by polymerases μ and/or λ to generate microhomologies so the DNA can be ligated by XRCC4/LigIV (Chang et al., 2017; Ma et al., 2004).

Repair by homologous recombination (HR)

In contrast to NHEJ, double-stranded breaks can be repaired with a mechanism based on DNA homology. This involves using a complementary DNA sequence as a template, usually the sister chromatid. This method of repair results in a decreased incidence of indel mutations and therefore preserves the integrity of the genome. This repair pathway begins when a complex consisting of Mre11-Rad50-Nbs1 (MRN) binding

to free double-stranded DNA ends (Lamarche et al., 2010). This complex then recruits the ataxia telangiectasia (ATM) kinase (Lee and Paull, 2005), which is central to the double-stranded break response, via interactions with Nbs1 (You et al., 2005). ATM then generates a multi-component complex by phosphorylating the H2AX histone variant, yielding γH2AX, which is associated with the DNA surrounding the break (Burma et al., 2001). γH2AX can spread across megabases of DNA to amplify the repair signal (Rogakou et al., 1999). γH2AX is bound by the Mdc1 adapter protein that in turn serves as a signaling platform for the recruitment of additional repair proteins (Stewart et al., 2003; Stucki et al., 2005). Another major target of ATM is the Chk2 kinase. Activated Chk2 is responsible for phosphorylating many substrate proteins whose functions largely are focused on arresting cells at G1/S or G2/M in the event that the genome is damaged and needs to be repaired (Zannini et al., 2014). Chk2 also functions in promoting the eventual recruitment of RAD51, discussed in more detail below, to single-stranded DNA for homologous recombination (Zhang et al., 2004).

To allow for base pairing to a homologous DNA sequence, the DNA break needs to be resected to expose a single stranded end available for annealing. This usually occurs in two steps: initial resection followed by a more extensive resection. Initial resection begins with recruitment of the CtIP protein to the MRN complex, specifically by Nbs1 (Sartori et al., 2007; Wang et al., 2013a). ATM then phosphorylates CtIP and this promotes the initial resection of one of the DNA strands (Blackford and Jackson, 2017; Wang et al., 2013a). More extensive resection is carried out by the Exo1 nuclease in concert with the BLM helicase, whose recruitment is also dependent on phosphorylated CtIP (Gravel et al., 2008; Nimonkar et al., 2008; Wang et al., 2013a).

There is also evidence that the Dna2 nuclease can also facilitate resection (Nimonkar et al., 2011). Resected DNA is bound by the RPA protein (Huertas and Jackson, 2009) and this recruits a complex consisting of the ATRIP protein and the ATR kinase (Zou and Elledge, 2003). Resection of the double-stranded break marks the transition from an ATM- to ATR-dominant response, termed an ATM-to-ATR switch (Maréchal and Zou, 2013). ATR activity is stimulated by TopBP1 (Kumagai et al., 2006) whose recruitment is proposed to be dependent on the MRN complex (Duursma et al., 2013) as well as BLM (Blackford et al., 2015). A major target of ATR is the Chk1 kinase, whose activation inhibits cell cycle progression to allow for the repair of the damaged DNA before the cell cycle is allowed to proceed (Blackford and Jackson, 2017).

RAD51 catalyzes the recombination between the free DNA strand and a stretch of homologous DNA (Bonilla et al., 2020). With the help of BRCA2, RPA is displaced from single-stranded DNA and replaced with RAD51 (Bonilla et al., 2020). RAD51-coated DNA then invades the homologous DNA helix and binds to the complementary sequence, generating a D-loop structure, to allow for extension of the invading strand, using the homologous DNA as a template. DNA is synthesized off of the invading strand until the strand is of sufficient length to span the damaged region of the initial broken DNA (Bonilla et al., 2020). The result is an error-free correction of a double-stranded break in the DNA.

The p53 tumor suppressor

The p53 protein has been called “the guardian of the genome” for its central role in preventing aberrant cell growth. p53 is a transcriptional regulator with at least 1500

gene targets (Mirza et al., 2003) and is the most commonly mutated gene in human cancers (Hafner et al., 2019). p53 has a short half-life as it is constantly being turned over by the MDM2 E3 ubiquitin ligase (Haupt et al., 1997; Honda et al., 1997; Kubbutat et al., 1997). The DNA damage response leads to the phosphorylation of p53. Phosphorylation of serines 15 and 37 inhibits the actions of MDM2 and increases the half-life, and thereby abundance, of the protein. Moreover, phosphorylation of serine 15 is required for the transcriptional functions of p53 (Loughery et al., 2014). ATM (Canman et al., 1998), ATR (Tibbetts et al., 1999), and DNA-PK (Shieh et al., 1997) have been observed to phosphorylate p53 on this residue. In the event of DNA damage, a primary function of p53 is to halt the progression of the cell cycle until the DNA can be repaired, or induce apoptosis if the damage is too severe (Hafner et al., 2019). Therefore, this redundancy between these three kinases allows for multiple avenues of p53 activation to ensure the integrity of the genome. p53 stabilization also appears to be dependent on phosphorylation of serine 20, which is primarily due to Chk2 activity (Chehab et al., 2000; Hirao et al., 2000).

Tetrameric p53 binds to DNA (Wang et al., 1995) via its DNA binding domain to a defined sequence of nucleotides (el-Deiry et al., 1992) and recruits histone acetyltransferases (HATs), specifically PCAF and p300/CBP, which acetylate p53 (Lambert et al., 1998; Liu et al., 1999). p53 in complex with HATs promote the acetylation of histone tails, an epigenetic modification that promotes transcription, on the promoters of p53 target genes (Hafner et al., 2019). Histone acetylation was dependent on the phosphorylation of serine 15 (Loughery et al., 2014), further outlining

the pathway from initial sensing of DNA damage and ATM/ATR/DNA-PK activation, through the activation of p53 and the up-regulation of DNA repair genes.

p53 does not need to be bound directly to the promoter to promote transcription of a given gene. Association of p53 greater than 10 kbp from the transcriptional start site can still promote the expression of a target gene (Hafner et al., 2019). This explains situations where gene transcription appears dependent on p53 without a discernable binding site in the promoter.

1.4 HSV-1 and the DNA damage response

HSV-1 and NHEJ

The HSV-1 DNA genome inside the viral particle is not perfectly double-stranded. It contains nicks and gaps of various lengths as well as the free ends of the linear molecule that activate the NHEJ pathway (Smith et al., 2014). While there is no direct evidence that the Ku complex binds to HSV-1 DNA, loss of Ku70 increases the efficiency of replication, indicating that the NHEJ pathway is intrinsically antiviral (Taylor and Knipe, 2004). Furthermore, loss of DNA-PKcs increases replication as well (Parkinson et al., 1999). HSV-1 has evolved a method to subvert this antiviral pathway by degrading DNA-PKcs in a manner dependent on ICP0 (Lees-Miller et al., 1996). Interestingly, the viral ICP8 protein was observed to interact with DNA-PKcs following wild-type virus infection, indicating that ICP0 may not fully degrade DNA-PKcs in all cell types (Taylor and Knipe, 2004). As infection progresses, DNA-PKcs also localizes to viral replication compartments (Taylor and Knipe, 2004), suggesting that the activation

of NHEJ signaling recruits at least DNA-PKcs to viral genomes to suppress replication. The mechanisms of which have yet to be elucidated.

Other NHEJ proteins have opposing roles in HSV-1 replication. Depletion of either XRCC4 or LigIV reduces both viral DNA replication and progeny virus production (Muylaert and Elias, 2007), while loss of PAXX, a protein that functions with XRCC4/LigIV, increases virus production (Trigg et al., 2017). These findings indicate that these individual proteins, while having a role in cellular NHEJ, may exert their effects on the virus in unique roles outside of NHEJ. Alternatively, the proteins of the NHEJ pathway may be actively manipulated by HSV-1, as with ICP0 and DNA-PKcs, to promote the pro-viral functions of some proteins, while inhibiting the antiviral actions of others.

HSV-1 and HR

HSV-1 triggers a robust cellular DDR soon after infection that progresses over time (Lilley et al., 2005). The MRN complex associates with the viral genome by 3 hours post-infection (Dembowski and DeLuca, 2018) and remains associated throughout viral DNA replication (Dembowski and DeLuca, 2015; Dembowski et al., 2017). This is supported by microscopy experiments observing Mre11 and Nbs1 localization to viral replication compartments (Gregory and Bachenheimer, 2008). Interestingly, while cells harboring non-functional Mre11 do not support efficient replication (Lilley et al., 2005), Mre11 is degraded over the course of infection (Gregory and Bachenheimer, 2008). Perhaps Mre11 promotes the early stages of replication, and becomes dispensable as the lifecycle progresses.

ATM is activated by infection (Alekseev et al., 2014; Edwards et al., 2018; Gregory and Bachenheimer, 2008; Lilley et al., 2005), localizes to viral replication compartments (Alekseev et al., 2014; Lilley et al., 2005), and associates with replicating viral DNA (Dembowski and DeLuca, 2015). ATM appears to promote viral replication (Alekseev et al., 2014; Lilley et al., 2005), but has also been reported to be dispensable (Botting et al., 2016; Edwards et al., 2018; Gregory and Bachenheimer, 2008). Similar to the response to cellular DNA damage, Chk2 is activated by HSV-1 infection (Alekseev et al., 2014; Gregory and Bachenheimer, 2008; Li et al., 2008; Lilley et al., 2005; Shirata et al., 2005) in a manner dependent on ATM (Li et al., 2008; Lilley et al., 2005). Interestingly, Chk2 either promotes replication of HSV-1 only when ICP0 is present (Li et al., 2008), or has no effect (Edwards et al., 2018).

H2AX associates with the viral genome by two hours post-infection (Dembowski and DeLuca, 2018) as well as with replicating viral DNA (Dembowski et al., 2017) and has been suggested to promote efficient replication (Lilley et al., 2011). Another study found it to be dispensable (Botting et al., 2016), so further study is warranted. Furthermore, it has been reported that γH2AX is actively excluded from viral replication centers (Wilkinson and Weller, 2006). A major γH2AX-binding protein, Mdc1, associates with incoming viral genomes independently of ICP0 (Lilley et al., 2011). However, it remains unknown whether this protein has any role in the HSV-1 replication cycle.

RPA associates with the viral genome by one hour post-infection and remains bound throughout the course of infection, well into viral DNA replication (Dembowski and DeLuca, 2015, 2018). It can also be observed in viral replication compartments (Mohni et al., 2010), but it is currently unknown whether it regulates HSV-1 progeny

virus production. As for RAD51, it localizes to viral replication compartments (Wilkinson and Weller, 2004) and can catalyze recombination between replicating HSV-1 genomes (Tang et al., 2014). Functionally, however, it appears that RAD51 positively affects replication, but only when the virus is pre-treated with UV radiation (Muylaert and Elias, 2010), suggesting that RAD51 can repair damaged viral genomes via recombination following viral DNA replication.

HSV-1 infection also activates the ATR pathway (Edwards et al., 2018), and both ATR and ATRIP localize to viral replication compartments (Mohni et al., 2010). Chemical inhibition of ATR and the downstream Chk1 kinase significantly reduces HSV-1 replication (Edwards et al., 2018), and loss of ATRIP modestly reduces viral gene expression (Mohni et al., 2010). It is unknown whether this ATR activation is dependent on MRN and/or ATM activity, or is activated by a different stimulus.

While individual HR proteins have been studied independently, the potential interplay between them has not been thoroughly investigated and a comprehensive model of the DDR to infection in a relevant cell type for HSV-1 has not been proposed. Moreover, current conclusions about the DDR to infection are generalized to the viral lifecycle as a whole. Parental and replicated viral genomes have the potential to elicit different DDRs. A major goal of this dissertation is to not only generate DDR models to both these parental and progeny genomes, but also to compare those responses to the normal cellular DDR to double-stranded breaks.

HSV-1 and p53

Compared to NHEJ and HR, much less is known about p53 and the HSV-1 replication cycle. p53-deficient mice display less mortality when challenged intracranially with HSV-1 (Maruzuru et al., 2016). In cell culture, cells lacking p53 do not support efficient replication (Maruzuru et al., 2013). Moreover, p53 localizes to viral replication compartments (Wilcock and Lane, 1991) and binds to the viral genome (Hsieh et al., 2014), supporting the idea that p53 directly regulates viral replication. p53 binds to the origins of replication on the viral genome, adjacent to the UL9 binding sites, both *in vitro* as well as infected cells (Hsieh et al., 2014). Interestingly, while the origin sequences were sufficient to promote p53-dependent transcription of a reporter construct, lytic genes flanking the origins were transcribed more in cells deficient for p53, suggesting that association of p53 with the origins repressed viral gene transcription (Hsieh et al., 2014).

If p53 is responsible for promoting the transcription of viral genes, then a logical inference is that the p300/CBP and PCAF HATs function in complex with p53. While p300 and CBP associate with viral gene promoters (Herrera and Triezenberg, 2004), their depletion, along with depletion of PCAF, did not decrease viral gene expression (Kutluay et al., 2009), indicating that these proteins may not be required for p53 function. One caveat is that all three proteins have not been depleted simultaneously, so there exists the possibility that they may function redundantly.

Not surprisingly, p53 is also targeted by ICP0. ICP0 ubiquitinates p53 both *in vitro* and *in vivo*, and a virus not expressing ICP0 cannot suppress apoptosis following UV irradiation (Boutell and Everett, 2003). Surprisingly, despite this ubiquitination, p53 is stabilized over the course of infection, independent of ICP0 (Boutell and Everett,

2004). The mechanism by which this occurs is not known, but appears to require viral IE gene expression.

Our aim is to further determine whether p53 regulates HSV-1 replication in primary human fibroblasts and, if so, where in the lifecycle it acts. The following work dissects both p53 function and the DDR to HSV-1 infection and reveals novel functions of these pathways in the viral lytic replication cycle.

Chapter 2: Herpes Simplex Virus 1 Manipulates Host Cell Anti-viral and Pro-viral DNA Damage Responses

Max E. Mertens and David M. Knipe

Department of Microbiology and Program in Virology, Blavatnik Institute, Harvard Medical School, Boston, MA

A version of this chapter has been submitted for publication.

Abstract

Cells activate their DNA damage response (DDR) in response to DNA virus infection, including adenoviruses, papillomaviruses, polyomaviruses and herpesviruses. In this study we found that the DDR kinase pathways activated in normal human fibroblasts by herpes simplex virus (HSV-1) input genomic DNA, HSV-1 replicating and progeny DNA, and in uninfected cells treated with etoposide are different. We also found using CRISPR-Cas9 technology that different host gene products are required for the DDR in uninfected versus infected cells. Individual DDR components can be pro-viral or anti-viral in that ATM and p53 promote and Mre11 restricts replication of ICP0-null HSV-1, but ICP0 expression eliminates these DDR effects. Thus, in total these results argue that HSV-1 manipulates the host cell DDR response to utilize specific components for its optimal replication while inactivating the anti-viral aspects of the DDR.

Introduction

Cells have evolved complex pathways of machinery with the purpose of repairing breaks in the DNA to preserve the integrity of the genome. The Mre11-Rad50-Nbs1 (MRN) complex is responsible for first sensing and then binding to double-stranded DNA ends (Lamarche et al., 2010). This complex is crucial for the recruitment of a key DNA damage response (DDR) kinase, ataxia-telangiectasia mutated (ATM), via an interaction with Nbs1 (You et al., 2005). In response to DNA damage, ATM phosphorylates the H2AX histone variant (Burma et al., 2001), which is commonly used as a marker of DNA damage. Phosphorylated H2AX, termed γH2AX, is then bound by

the DDR adapter protein Mdc1 to generate a signaling platform to recruit additional repair factors including the RNF8 and RNF168 E3 ubiquitin ligases, which are required for recruitment of 53BP1 to damage loci (Doil et al., 2009; Kolas et al., 2007; Stewart et al., 2003; Stucki et al., 2005). This pathway promotes homologous recombination (HR) of complementary DNA sequences for repair of the double-stranded DNA breaks.

Double-stranded breaks are also repaired using the non-homologous end-joining (NHEJ) pathway. Free double-stranded DNA ends are first bound by the heterodimeric Ku70/Ku80 complex, which then recruits the catalytic subunit of DNA-dependent protein kinase (DNA-PKcs) (Gottlieb and Jackson, 1993; Mimori and Hardin, 1986). Through the interactions between a complex of proteins, the free DNA ends are tethered and ligated together by the XRCC4-DNA ligase IV (LIG4) complex (Critchlow et al., 1997; Graham et al., 2016; Grawunder et al., 1997).

The p53 protein is activated to regulate cellular gene expression to allow for the repair of the damage or to induce death of the cell by apoptosis (Hafner et al., 2019). Two key residues that are phosphorylated in response to DNA damage are serines 15 and 20, predominantly done by ATM/ATR, and Chk2, respectively (Canman et al., 1998; Hirao et al., 2000; Tibbetts et al., 1999). Phosphorylation of serine 15 of p53 has been suggested to regulate the transcriptional transactivation activity of p53 (Loughery et al., 2014), and serine 20 the turnover of the protein (Dumaz et al., 2001).

The genomes of DNA viruses do not go unnoticed by the DDR. High-risk human papillomaviruses (HPVs) use DDR pathways to efficiently replicate their genomes. HPV up-regulates expression of the MRN complex (Anacker et al., 2014) and promotes the activation of ATM to efficiently amplify the viral genome (Moody and Laimins, 2009). In

contrast, human adenovirus promotes both the mislocalization and degradation of the MRN complex (Stracker et al., 2002), which along with ATM restricts replication of the virus (Shah and O'Shea, 2015). The human herpesvirus Epstein-Barr virus (EBV) down-regulates the ATM pathway (Hau and Tsao, 2017), while another human herpesvirus, Kaposi's sarcoma-associated herpesvirus (KSHV), relies on the functions of Mre11 and ATM for optimal replication (Hollingworth et al., 2017). A third human herpesvirus, human cytomegalovirus (HCMV), also relies on ATM for efficient replication (E et al., 2011). The differing roles of the DDR in the lifecycles of these DNA viruses underscores how viruses manipulate the host cell to optimize their replication processes.

Herpes simplex virus 1 (HSV-1) is another large, double-stranded DNA virus with a genome approximately 152 kilobase pairs in length. Shortly following the docking of the viral capsid at the nuclear pore, the linear viral genome is released into the nucleoplasm where it rapidly circularizes and begins transcription of a characteristic cascade of three kinetic classes of genes (Roizman, 2013). The first is the immediate-early (IE) class, consisting of five genes: *ICP0*, *ICP4*, *ICP22*, *ICP27*, and *ICP47*. The ICP0 protein plays a central role in targeting host restriction factors for proteasome-mediated degradation using its E3 ubiquitin ligase activity (Chelbi-Alix and de Thé, 1999; Gu and Roizman, 2003; Jurak et al., 2012; Lukashchuk and Everett, 2010; Orzalli et al., 2012). ICP4 activates transcription of the early (E) gene class, encoding primarily the core machinery necessary to replicate the viral genome along with other miscellaneous proteins involved in optimizing the replication process (Roizman, 2013). Expressed following DNA replication, the viral late (L) gene class encodes gene

products that package the replicated genomes and assemble new particles (Roizman, 2013).

Although at least part of the input HSV-1 DNA is circularized, the host cell still initiates a double-stranded DNA break response. The homologous recombination (HR) pathway is activated soon after infection, and HR proteins localize adjacent to incoming viral genomes and the eventual viral DNA replication centers (Lilley et al., 2005; Lilley et al., 2011; Taylor and Knipe, 2004). While both ATM and the related ATR DDR kinase appear to be activated by infection, it is unclear whether they affect replication. ATM activity has been shown to promote HSV-1 gene expression and replication in some infection conditions (Alekseev et al., 2014; Lilley et al., 2005), while being dispensable in others (Botting et al., 2016; Edwards et al., 2018; Gregory and Bachenheimer, 2008). ATR has also been reported to promote replication (Edwards et al., 2018), but another study reported that infection causes the aberrant localization of this arm of the HR pathway (Wilkinson and Weller, 2006). Indeed, various DDR proteins associate with the viral DNA and localize to viral replication compartments (Dembowski and DeLuca, 2015, 2018; Gregory and Bachenheimer, 2008; Lilley et al., 2005; Taylor and Knipe, 2004), but their roles and influences on viral replication remains undescribed or at least controversial. p53 also localizes to sites of viral DNA replication (Wilcock and Lane, 1991) and positively regulates HSV-1 replication (Maruzuru et al., 2013) and the progression to encephalitis (Maruzuru et al., 2016). However, the mechanism of action has not been elucidated.

In this study, we examined and compared the DDR kinase pathways activated in normal human fibroblasts by input viral DNA, replicating/progeny viral DNA and

etoposide treatment. We observed distinct DDR kinase responses for uninfected versus infected cells including a biphasic DDR response to infection dominated by an initial Chk2 response to incoming viral DNA, which then transitioned to an ATM-dominated response to replicating viral DNA. Moreover, we observed that ATM, but not Chk2, promoted efficient viral replication. ATM was also responsible for the phosphorylation of all of the DDR proteins tested, further solidifying ATM as a dominant kinase during HSV-1 infection. Interestingly, we report Mre11-dependent restriction of replication, indicating that Mre11 and ATM may serve independent, and possibly opposing, roles during infection. Finally, we observed that p53 was phosphorylated by ATM and promoted viral transcription of the essential viral *ICP8* gene. Our results uncover novel roles for the DDR in regulating HSV-1 gene expression and overall replication.

Results

Distinct DNA damage response kinase activation to input and replicating viral DNA

The life cycle of HSV-1 can be divided into two stages: pre- and post-viral DNA replication. We sought to investigate the DDR to both parts of the lifecycle. To characterize the response to input viral DNA, we infected primary human foreskin fibroblasts (HFFs) with the HSV-1 *d*109 virus. This virus does not express any viral genes in normal cells and nuclear viral DNA persists in a quiescent state for at least 28 days in cell culture (Samaniego et al., 1998). Thus, this virus can be used as a model for the study of input viral DNA delivered by infection. By two hours after *d*109 virus infection, we observed robust Chk2 and H2AX phosphorylation, along with a substantial

up-regulation of total H2AX, low levels of p53 phosphorylation at serine 15, and low levels of ATM phosphorylation (Figure 2.1A, lane 5). This argued that Chk2 was activated by incoming viral DNA. Up-regulation of H2AX in response to an activated DDR has been described previously (Kang et al., 2012) and our results argued that *d*109 infection was sufficient to trigger this response. By 8 hours post-infection (hpi), phosphorylation of these proteins was decreased (Figure 2.1A, lane 6), presumably due to resolution of the DDR.

To investigate the responses to replicating and replicated viral DNA, we infected HFFs with HSV-1 wild type (WT) virus in either the presence or absence of the viral DNA replication inhibitor acyclovir (ACV). In infected cells undergoing viral DNA synthesis (-ACV), we observed strong Chk2 phosphorylation by 2 hpi (Figure 2.1A, lane 7), like *d*109 infection, that decreased by 8 hpi (lane 8). Interestingly, treatment with ACV to block viral DNA synthesis abrogated this reduction (lanes 9 and 10), arguing that viral DNA replication, or possibly a viral late gene product, suppressed Chk2. We observed ATM, H2AX, and p53 serine 15 and 20 phosphorylation by 8 hpi (lane 8), and all but serine 15 phosphorylation were sensitive to ACV treatment (lane 10), arguing that viral DNA replication stimulated phosphorylation of these proteins. The phosphorylation of serine 15 with ACV treatment (lane 10) suggested that phosphorylation occurred between 2 hpi and the onset of genome replication, perhaps by the prolonged presence of the parental genome or IE and E gene expression. We did not observe H2AX phosphorylation at 2 hpi following WT infection (Figure 2.1A, lane 7), as we did with *d*109. We believe that while *d*109 is an accurate model for input viral DNA, the virus prep of *d*109 likely contained a higher number of viral particles per

plaque forming unit (PFU) than the WT virus prep, evidenced by the abundance of gB glycoproteins (Figure 2.1A, lanes 5 and 7). This could have led to a stronger H2AX response than WT virus infection as a result of a higher abundance of input genomes when we used the same multiplicity of infection (MOI). Together, we observed a biphasic DDR to input and replicating viral DNA, with Chk2 being primarily activated by incoming viral genomes and ATM being activated by replicating/progeny DNA.

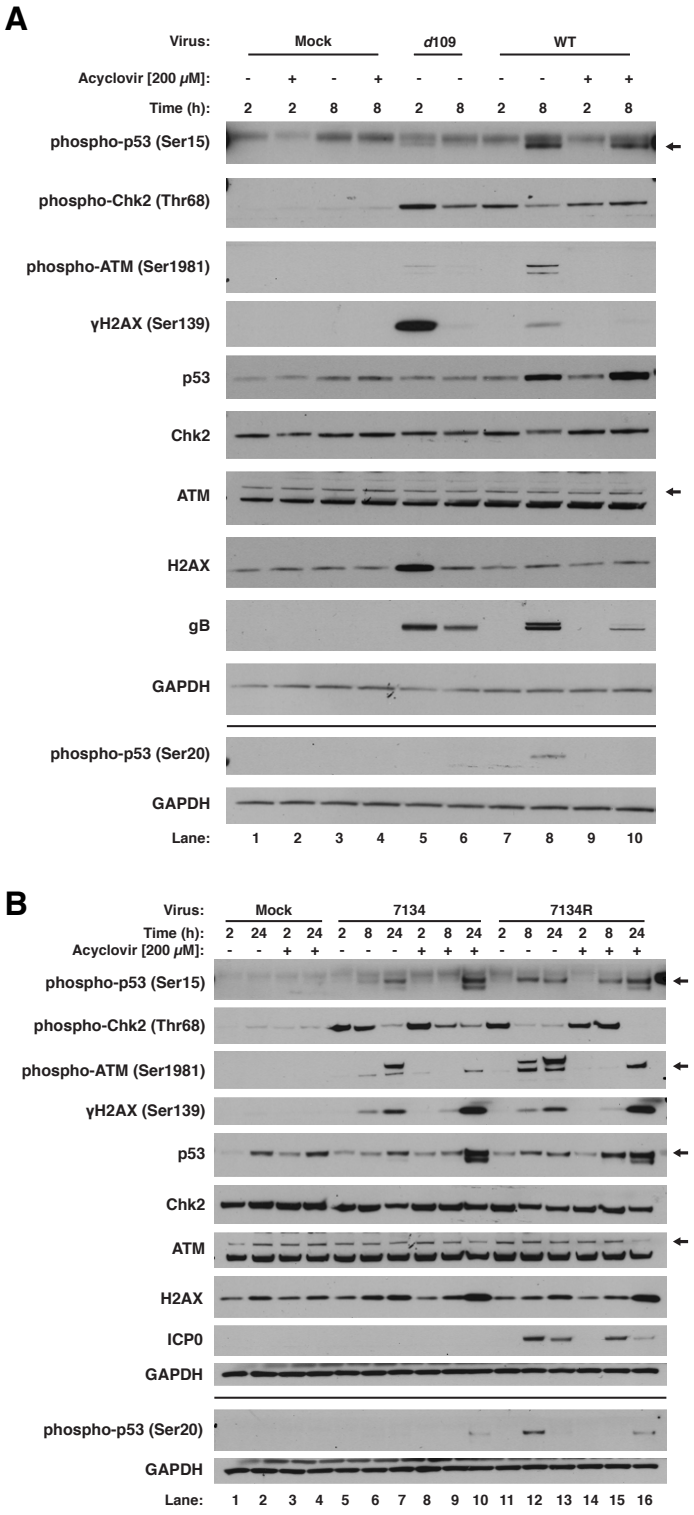

Figure 2.1. The biphasic response to incoming and replicating viral DNA. Primary HFFs were either

Figure 2.1 (continued)

mock-infected, or infected with *d*109 or WT virus at a multiplicity of infection (MOI) of 5 either in the presence or absence of 200 μM ACV added 1 hpi in the case of WT virus. Lysates were harvested for immunoblot analysis at 2 and 8 hpi (A). HFFs were also infected with 7134 or 7134R at an MOI of 5 with and without 200 μM ACV treatment 1 hpi and lysates were harvested at 2, 8, and 24 hpi (B). Presented immunoblots are representative of two independent experiments. Mock – infection medium alone, no virus.

Effect of the HSV-1 ICP0 protein on the DDR response

Prior studies had observed that the viral ICP0 E3 ubiquitin ligase is sufficient to modulate the DDR by promoting ATM and Chk2 phosphorylation (Li et al., 2008), inhibiting ATRIP/ATR function (Wilkinson and Weller, 2006), and inhibiting downstream repair processes by promoting the degradation of the RNF8 and RNF168 E3 ubiquitin ligases (Lilley et al., 2011). To investigate the effects of ICP0 in our experimental system, we infected HFFs with the ICP0-null 7134 virus and the repaired 7134R virus (Cai and Schaffer, 1989). Similar to WT virus, Chk2 was phosphorylated by 2 hpi (Figure 2.1B, lanes 5 and 11), independently of ICP0, and decreased over the course of infection (Figure 2.1B, lanes 6 and 12). The decrease was not as rapid with 7134 infection compared to 7134R, and we attributed this to the overall slower replication kinetics of the virus without ICP0. We observed ATM phosphorylation by 8 hpi with both 7134 and 7134R (Figure 2.1B, lanes 6 and 12) with the 8-hour time point being sensitive to ACV treatment (lanes 9 and 15). Interestingly, by 24 hpi in the presence of ACV, ATM was phosphorylated for both viruses (Figure 2.1B, lanes 10 and 16), suggesting that, despite replication being inhibited, prolonged presence of the viral genome, and/or prolonged expression of viral IE and E genes, led to ATM activation. H2AX phosphorylation followed a similar profile (Figure 2.1B, lanes 10 and 16). H2AX phosphorylation was reduced at 8 hpi with ACV treatment for both viruses (lanes 9 and 15), but was independent of viral DNA replication and viral late gene expression by 24 hpi (Figure 2.1B, lanes 10 and 16). Together, our results argued that the DDR kinase responses to 7134 and 7134R were largely similar, with minor differences attributed to the slower replication kinetics of the ICP0$^-$ virus.

We also observed phosphorylation of p53 serine 15 with both viruses (Figure 2.1B, lanes 7 and 13). However, phosphorylation in the absence of ICP0 occurred much more slowly, occurring primarily at 24 hpi. We also attributed this, as with Chk2 phosphorylation, to the decreased replication kinetics of the 7134 virus. Similar to WT infection, p53 serine 15 phosphorylation was not sensitive to ACV treatment for both viruses (lanes 10 and 16), arguing that phosphorylation of this residue was independent of viral DNA replication and L gene expression. Interestingly, we observed very little phosphorylation of p53 on serine 20 following infection with 7134 (Figure 2.1B, lanes 5-10). Because we observed that phosphorylation of this residue was dependent on viral DNA replication following WT infection, we hypothesized that 7134 did not undergo sufficient levels of DNA replication to stimulate phosphorylation to WT levels. In agreement with WT infection, 7134R infection stimulated phosphorylation of p53 serine 20 by 8 hpi (Figure 2.1B, lane 12) that was reduced by ACV treatment (lane 15). Interestingly, we observed low levels serine 20 phosphorylation of p53 in 7134 virus-infected cells by 24 hpi in the presence of ACV (lane 10), arguing that, as in the case for ATM phosphorylation, prolonged presence of viral DNA and/or viral gene expression can stimulate p53 phosphorylation.

Taken together, we did not observe any significant qualitative differences between ICP0-null and ICP0-expressing viruses. We observed only minor differences in the kinetics of phosphorylation of DDR proteins, most likely due to the decreased replication kinetics of the ICP0-null 7134 virus, therefore indicating that ICP0 had a minimal role in shaping these aspects of the DDR.

ATM promotes the DDR to viral infection

Having characterized the kinase pathway responses to input and replicating viral DNA, we next sought to determine the kinase(s) responsible for p53, H2AX, ATM, and Chk2 phosphorylation and whether the kinase(s) responsible are different between input and replicating DNA. We generated gene knockouts of ATM and CHEK2 in primary HFFs using CRISPR-Cas9 (Figure 2.2A). We also generated a knockout cell line for MDC1. MDC1 has been observed to localize adjacent to incoming viral genomes (Lilley et al., 2011), but its role during HSV-1 replication has not been established. To determine the kinases responsible for the response to input DNA, we infected the knockout HFFs with *d*109 for two hours. Knockout of ATM ablated Chk2 and p53 serine 15 phosphorylation (Figure 2.2B, lane 8) compared to both normal and Cas9 control HFFs (Figure 2.2B, lanes 6-7), arguing that ATM was required for the phosphorylation of both of these proteins. Knockout of MDC1 had no effect on the phosphorylation of any of the proteins investigated (Figure 2.2B, lane 10), suggesting that Mdc1 did not have a role in promoting the DDR in the first 2 hpi. Surprisingly, knockout of ATM had no effect on H2AX phosphorylation (lane 8). DNA-PK also phosphorylates H2AX in response to DNA damage (An et al., 2010; Mukherjee et al., 2006) and we hypothesized that this kinase may be responsible for the H2AX phosphorylation response to input DNA. To test this, we knocked down *PRKDC*, encoding DNA-PKcs, and infected with *d*109 virus for two hours. Compared to non-targeting siRNA, γH2AX was only partially reduced with knockdown (Figure 2.3A, lanes 3-4), arguing that DNA-PK functioned redundantly with another kinase. HSV-1 infection also activates the ATR

kinase known to also phosphorylate H2AX (Edwards et al., 2018; Ward and Chen, 2001). Therefore, DNA-PK may function redundantly with ATR and ATM.

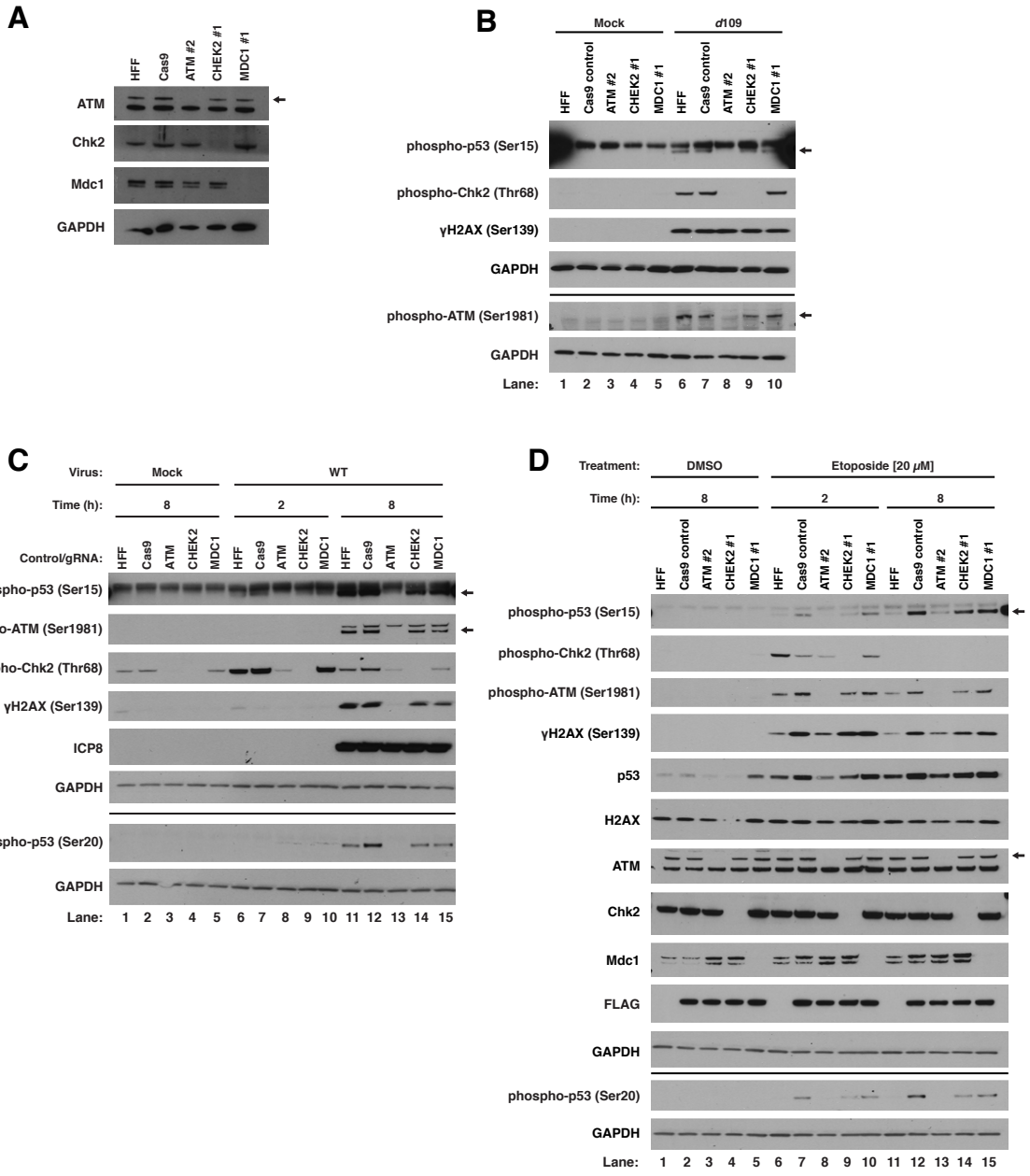

Figure 2.2. ATM promotes the DDR to both cellular DNA damage and HSV-1 infection. Primary HFFs were transduced with lentiviruses that express Cas9, a guide RNA against *ATM*, *CHEK2*, or *MDC1*, and puromycin resistance as specified in the materials and methods section. Blot images are representative

Figure 2.2 (continued)

of three passages of cells (A). Normal HFFs, Cas9 control, and knockout HFFs were mock-infected, or infected with *d*109 at an MOI of 5 and lysates harvested for immunoblot at 2 hpi (B). Control and knockout cells were either mock-infected, or infected with WT virus at an MOI of 5 and lysates harvested at the indicated hpi (C). Control and knockout HFFs were treated with either DMSO, or 20 μM etoposide, and lysates harvested at the indicated times post-treatment (D). Cas9 was FLAG-tagged. Blots are representative of two independent experiments (B-D).

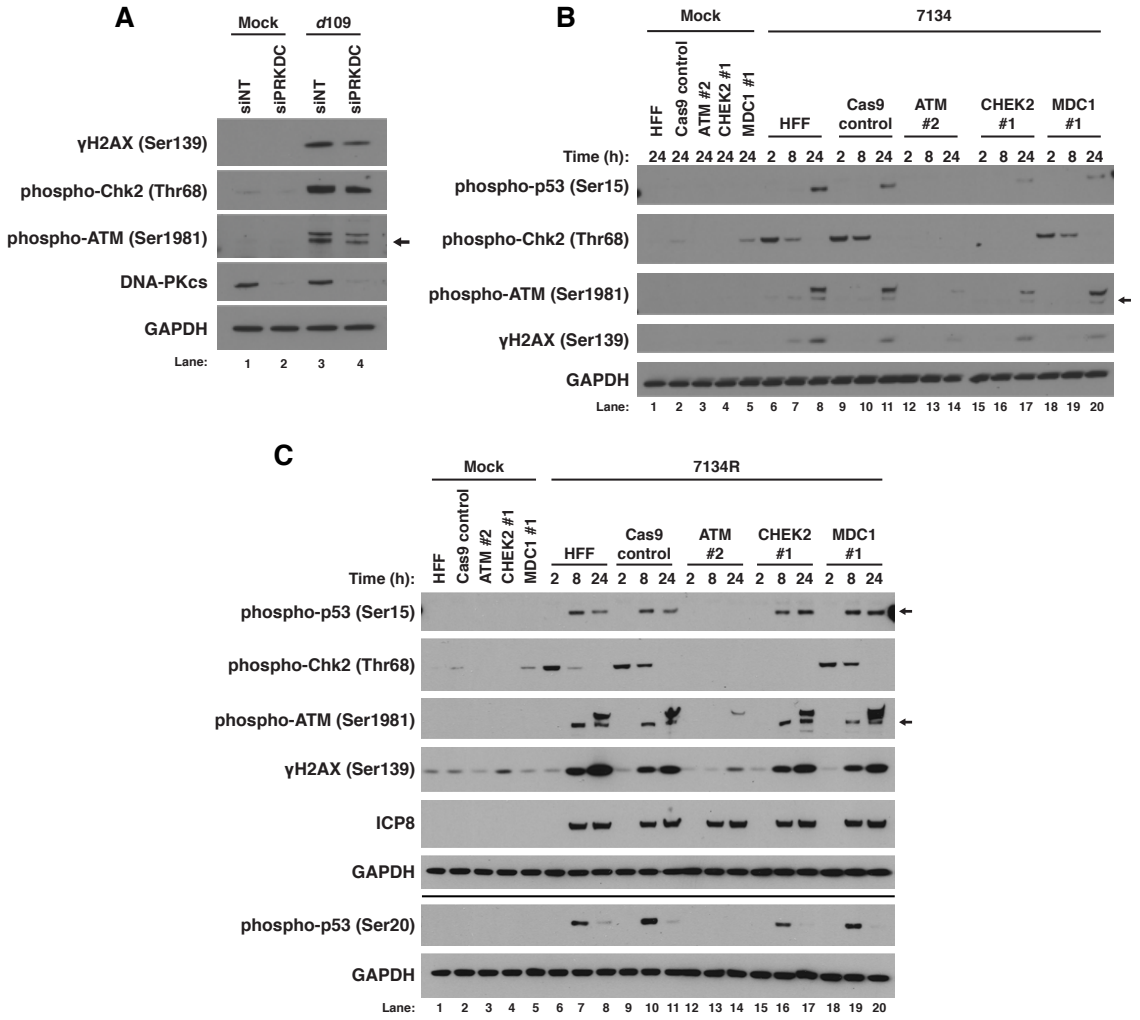

Figure 2.3. Primary HFFs were transfected with either a non-targeting siRNA pool, or a pool targeting DNA-PKcs (the gene product of *PRKDC*). Three days later, cells were infected with *d*109 at an MOI of 5, and protein lysates collected for immunoblot two hours later (A). Plain HFFs, Cas9 control, ATM #2, CHEK2 #1, and MDC1 #1 knockout cells were either mock-infected, infected with 7134 (B), or infected with 7134R (C), both at an MOI of 5, and protein lysates harvested at the indicated times post-infection. Blots are representative of two independent experiments.

To determine if ATM, Chk2, and Mdc1 serve any role following viral DNA replication, we infected the control and knockout HFFs with WT virus. By 2 hpi, the results mirrored *d*109 infection where knockout of ATM strongly reduced the phosphorylation of Chk2 (Figure 2.2C, lane 8). By 8 hpi, knockout of ATM ablated the phosphorylation of Chk2 and p53 at both serine residues (lane 13), arguing that ATM was largely responsible for progression of the DDR in response to DNA replication. Interestingly, knockout of Chk2 had no effect on the phosphorylation of p53 on serine 20 (lane 14). Because a previous publication reported that Chk2 promoted p53 phosphorylation in response to cellular DNA damage (Hirao et al., 2000), this may be an HSV-specific effect. In addition, ATM knockout abolished H2AX phosphorylation by 8 hpi (lane 13), arguing that ATM phosphorylated H2AX stimulated by replicating viral DNA, not incoming DNA. Knockout of MDC1 had no effect on any of the proteins investigated (Figure 2.2C, lanes 10 and 15), indicating a dispensable role for Mdc1 in propagating the DDR.

Having established the effects on wild-type virus, we wanted to determine whether similar results would be observed in the absence of ICP0. To test this, we infected control and knockout HFFs with 7134 and 7134R. For both viruses, ATM was still responsible for the phosphorylation of Chk2, H2AX, and both serine residues of p53 (Figures 2.3B and 2.3C, lanes 12-14), arguing that the ATM-dependency on propagating the DNA damage signal was independent of ICP0.

Etoposide induces a robust DDR in HFFs, distinct from HSV-1 infection

To investigate whether the response to cellular DNA damage was similar or different to the response to viral infection, we treated control and knockout HFFs with

etoposide to induce double-stranded DNA breaks for 2 and 8 hours. By two hours, we observed phosphorylation of ATM, Chk2, H2AX, and p53 on both serine residues (Figure 2.2D, lanes 6-7). Interestingly, unlike HSV-1 infection, Chk2 phosphorylation was minimally dependent on ATM, as ATM knockout had only a small effect on Chk2 phosphorylation compared to Cas9 control cells (Figure 2.2D, lane 8). γH2AX accumulation was also only partially dependent on ATM (lanes 8 and 13), indicating that, like for *d*109 infection, ATM may function redundantly with other DDR kinases to phosphorylate this histone variant. p53 phosphorylation on serines 15 and 20 were also dependent on ATM. Interestingly, we observed serine 20 phosphorylation at two hours (lane 7), whereas for HSV-1, it was not observed until later times during infection, primarily stimulated by viral DNA replication. ATM, H2AX, and p53 phosphorylation persisted through 8 hours post-treatment (lanes 11-12). Chk2 phosphorylation mirrored what was observed for HSV-1 infection. Its phosphorylation was observed beginning at 2 hours (lane 6-7), but was reduced by 8 hours (lane 11-12). We attributed this to a resolution in the Chk2 arm of the DDR. These observations also argued that this Chk2 arm of the response was independent of ATM activity as initial Chk2 phosphorylation was not dependent on ATM, and Chk2 phosphorylation decreased over time whereas ATM phosphorylation levels remained constant (lanes 6-7, 11-12). Phosphorylation of both p53 serine residues remained dependent on ATM at 8 hours post-treatment (lane 13).

Together, our results argued that the cellular DNA damage response, at least with respect to damage caused by etoposide, was distinct from the response to HSV-1 infection. Etoposide treatment led to robust phosphorylation of all of the proteins

investigated by 2 hours, whereas for HSV-1 infection, protein phosphorylation was temporally separated with the bulk of Chk2 and ATM phosphorylation occurring by 2 and 8 hours post-infection, respectively. Chk2 phosphorylation also displayed varying requirements for ATM depending on whether the response was triggered by cellular DNA damage or viral infection, indicating that viral gene products were manipulating the host DDR or cellular and viral DNA were treated differently by cellular surveillance pathways.

Mre11 promotes distinct DDR responses to cellular DNA damage and HSV-1 infection

Having observed the requirement of ATM for a robust DDR, we hypothesized that the MRN complex may have facilitated this phenotype by activating ATM in response to infection. Additionally, we sought to determine whether the H2AX histone variant has a role in regulating replication. One study reported that γH2AX has no impact on replication (Botting et al., 2016), but another study reported that H2AX enhanced replication (Lilley et al., 2011). To test the roles of these proteins, we generated knockout HFFs for the genes MRE11A and H2AFX, encoding Mre11 and H2AX, respectively. MRE11A #3 gave a robust knockout (Figure 2.4A, lane 2), whereas MRE11A #4 (lane 3) gave an intermediate knockout between Cas9 control and MRE11A #3 cells. H2AX levels were not detectable in H2AFX #3 cells (lane 4).

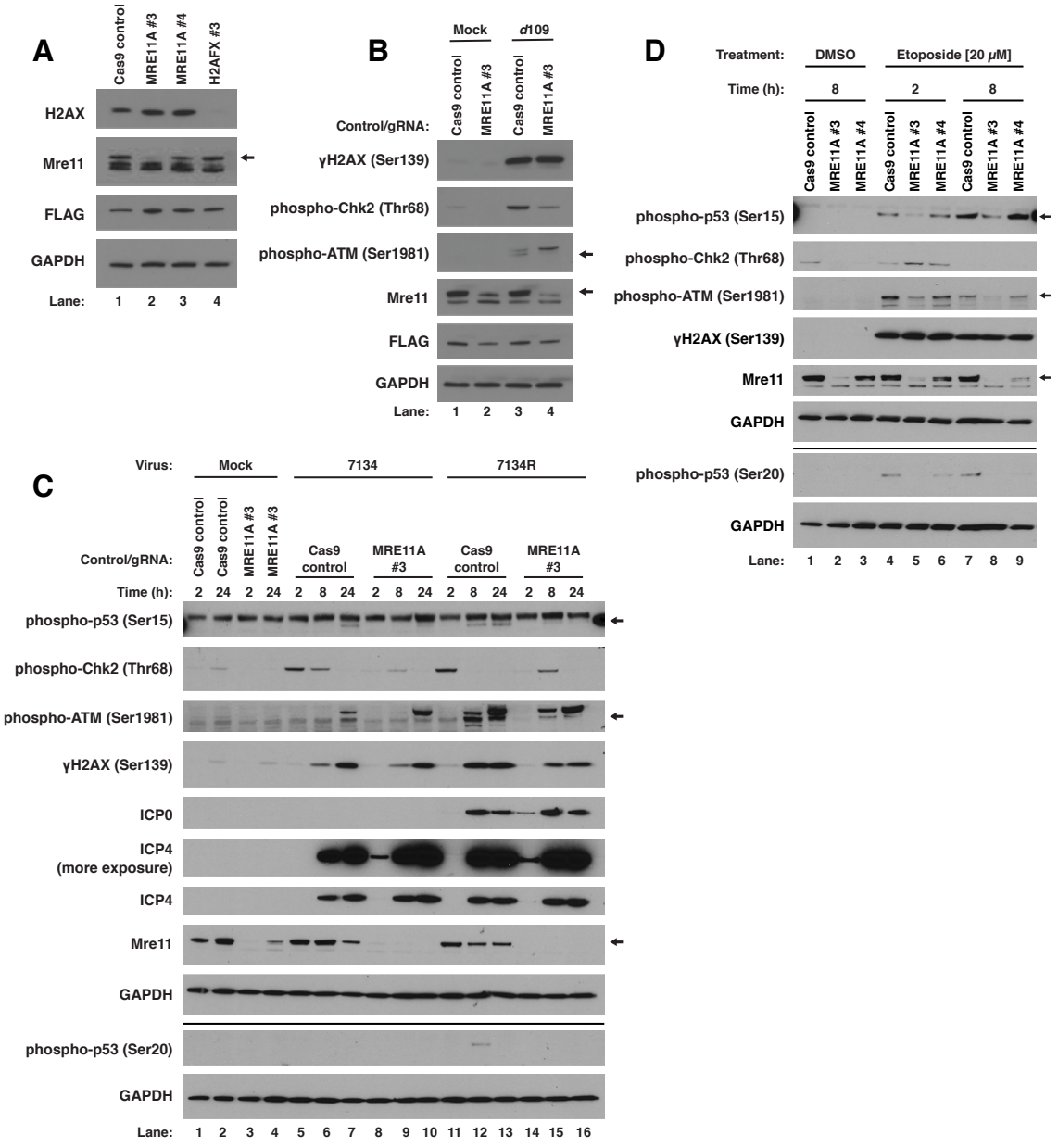

Figure 2.4. Mre11 influences the response to incoming and replicating viral DNA. Primary HFFs were transduced with lentiviruses that express Cas9 only, or Cas9 along with one of two guide RNAs against *MRE11A*, or a guide RNA against *H2AFX* as outlined in the materials and methods section. Blots are representative of three passages of cells (A). Cas9 control and MRE11A #3 cells were either mock

Figure 2.4 (continued)

infected or infected with *d*109 at an MOI of 5 and lysates harvested at 2 hpi (B). Cas9 control and MRE11A #3 cells were mock infected, or infected with 7134 or 7134R at an MOI of 5 and lysates harvested at 2, 8, and 24 hpi (C). Cas9, MRE11A #3, and MRE11A #4 cells were treated with either DMSO or 20 μM etoposide and lysates harvested at the indicated times post-treatment (D). Blots are representative of two independent experiments (B-D).

First, to determine whether the MRN complex facilitates the DDR to input viral DNA, we infected control and MRE11A #3 cells with *d*109 for 2 hours. Loss of Mre11 reduced both ATM and Chk2, but not H2AX, phosphorylation (Figure 2.4B, lane 4). This agreed with our ATM knockout results where H2AX phosphorylation was also unaffected (Figure 2.2B). Our results argued that the MRN complex was responsible for inducing an H2AX-independent DDR to incoming viral DNA.

Second, to determine whether the MRN complex promotes the DDR to replicating viral DNA, and also if ICP0 has any role in this response, we infected control and MRE11A #3 knockout HFFs with the 7134 and 7134R viruses. Mre11 promoted Chk2 phosphorylation in response to both viruses by 2 hours (Figure 2.4C, lanes 8 and 14), indicating that, as with *d*109 infection, Mre11, and presumably the MRN complex, was required for early recognition of incoming viral DNA. By 8 hpi with both 7134 and 7134R infection, ATM and H2AX phosphorylation were only weakly affected by MRE11A knockout (lane 9 and 15), arguing that there were redundant pathways for their activation. p53 serine 15 phosphorylation was strongly reduced 8 hpi with both viruses with MRE11A knockout (lanes 9 and 15), arguing that Mre11 primarily facilitated phosphorylation of this residue, most likely through ATM. p53 serine 20 phosphorylation following 7134R infection was also sensitive to Mre11 depletion at 8 hpi (lane 15), also arguing that Mre11 controlled phosphorylation of this residue of p53 as well. We also observed increased ICP4 and ICP0 protein levels with MRE11A knockout by 2 hpi for both ICP0^{-} and ICP0^{+} viruses (lanes 8 and 14), compared to the Cas9 control (lanes 5 and 11), indicating that Mre11 may have repressed viral IE gene expression.

To determine if Mre11 promoted a similar DDR to cellular damage, we treated control and MRE11A #3 and #4 cells with etoposide for 2 and 8 hours. The results were very similar to those observed for ATM knockout. MRE11 #3 cells displayed reduced ATM and p53 serine 15, and 20, phosphorylation at both 2 and 8 hours post-treatment (Figure 2.4D, lanes 5 and 8). In agreement with our ATM knockout results, Chk2 phosphorylation was not affected by the loss of Mre11 (Figure 2.4D, lane 5), in fact Chk2 phosphorylation appeared to be increased relative to the Cas9 control cell line, arguing that Mre11 repressed Chk2 activation with etoposide treatment, but promoted its activation following HSV-1 infection. γH2AX accumulation appeared to be independent of Mre11 (lane 5), again arguing for a redundancy in the kinases responsible, similar to our observations for HSV-1 infection. MRE11 #4 gave similar phenotypes to MRE11A #3 cells (lanes 6 and 9), but not as drastic. We attributed this to the incomplete knockout of MRE11A when compared to MRE11A #3 cells. Together, our results indicated that Mre11 promoted the activation of ATM following both etoposide treatment and HSV-1 infection, but were divergent with regards to Chk2 phosphorylation; ATM promoted its phosphorylation following HSV-1 infection, but not etoposide treatment. p53 phosphorylation was promoted by both Mre11 and ATM, indicating that this arm of the DDR pathway was conserved between chemical treatment and infection.

ATM and Mre11 have opposing effects on HSV-1 replication

Prior studies have reported conflicting results as to whether various DDR proteins regulate the replication of HSV-1. To address these differences, we infected

our ATM, CHEK2 and MDC1 knockout HFFs with WT, 7134R, and 7134 viruses, and measured viral replication by plaque assay. Replication of both WT and 7134R viruses were unaffected by all of the gene knockouts (Figure 2.5A). However, knockout of ATM significantly reduced replication of the 7134 virus, indicating that ATM had pro-viral functions, but only in the absence of ICP0. Interestingly, knockout of CHEK2 did not have an effect on any of the viruses. A prior study observed that loss of Chk2 decreased viral replication, but only in the presence of ICP0 (Li et al., 2008). Our results argued that although ATM promoted the activation of Chk2, the latter was ultimately dispensable for HSV-1 replication, independent of ICP0 expression. Similarly, knockout of MDC1 did not affect the replication of any of the viruses (Figure 2.5A), arguing that the recruitment of this downstream repair factor was not required for efficient viral replication.

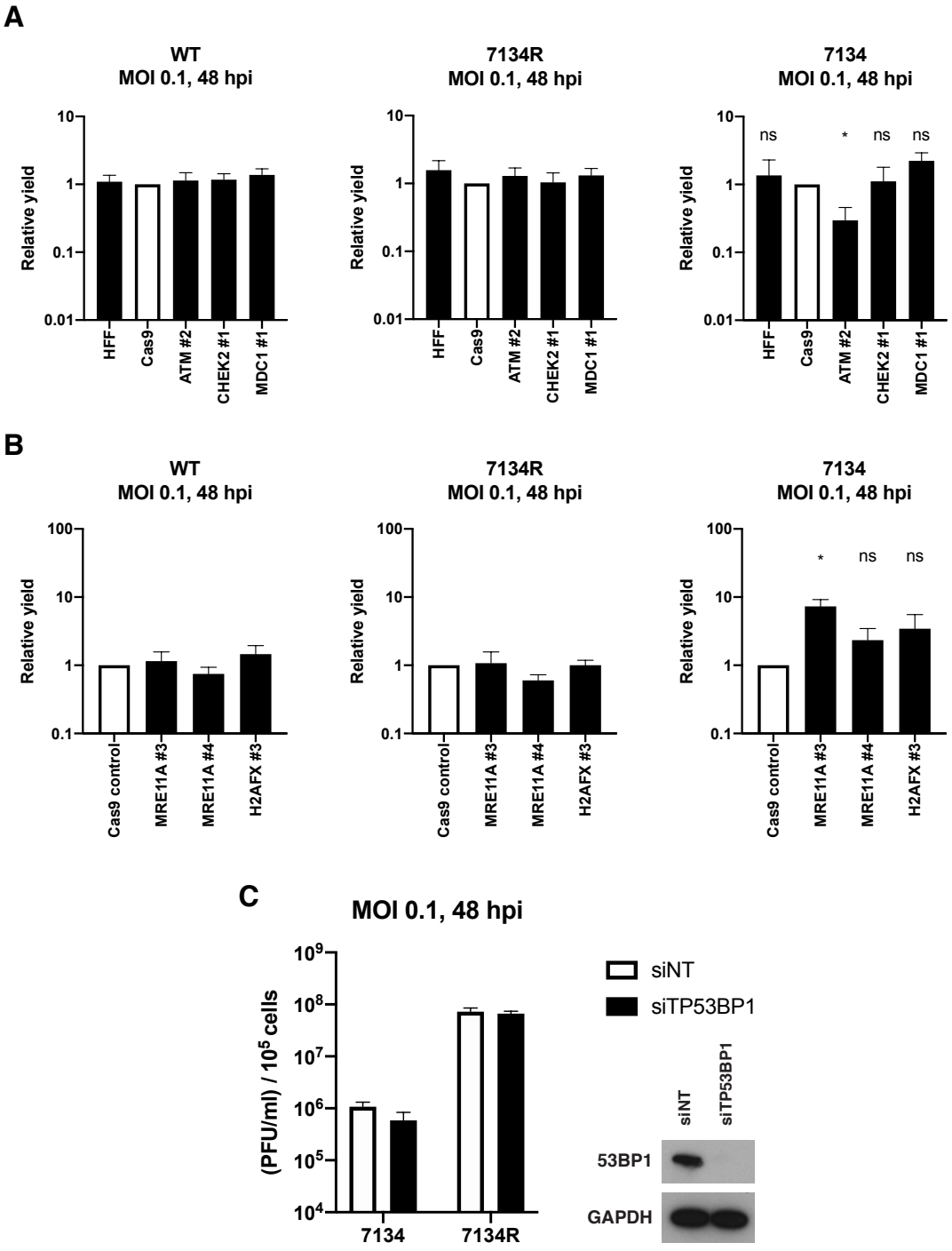

Figure 2.5. ATM and Mre11 have different roles in regulating the replication of HSV-1. Normal HFFs, Cas9 control, ATM #2, CHEK2 #1, and MDC1 #1 knockout cells were infected with WT, 7134R, and 7134

Figure 2.5 (continued)

viruses at an MOI of 0.1 and total virus was collected 48 hours later and titered on U2OS cells (A). Cas9, MRE11A #3, MRE11A #4, and H2AFX #3 cell lines were also infected with WT, 7134R, and 7134 viruses at an MOI of 0.1 for 48 hours and total virus quantified via plaque assay on U2OS cells (B). Plaque counts were normalized to Cas9 control cells (A, B). Primary HFFs were transfected with either a non-targeting siRNA pool or a pool targeting TP53BP1. Knockdown cells were infected with 7134 and 7134R at an MOI of 0.1 for 48 hours and total virus quantified by plaque assays on U2OS cells. Protein lysates for knockdown verification were taken at the time of infection (C). Graphed data are averages of three independent experiments with error bars representing the standard error of the mean (SEM). Statistical analyses were performed using unpaired *t* tests. *$p<0.05$, ns – not significant, compared to Cas9 control.

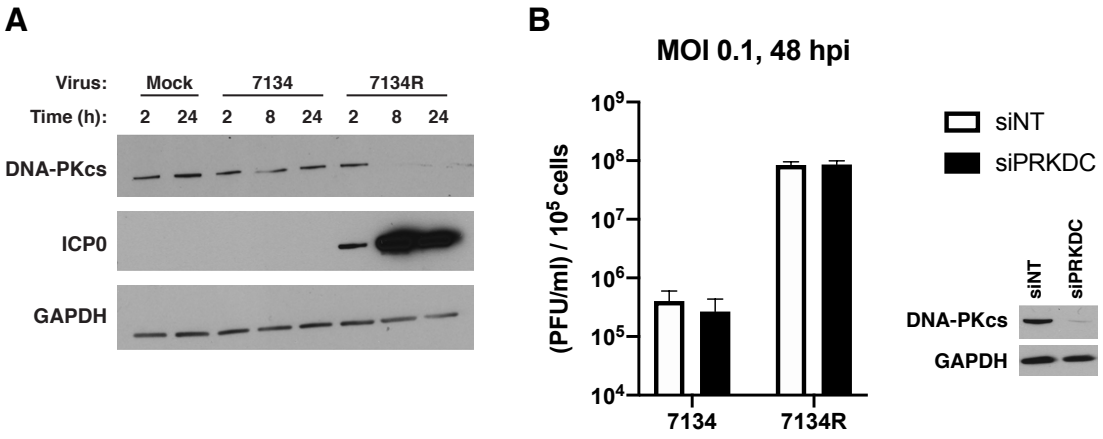

Figure 2.6. Plain HFFs were either mock-infected, or infected with 7134 or 7134R at an MOI of 5, and protein lysates collected at the indicated times post-infection (A). Blot images are representative of two independent experiments. Primary HFFs were transfected with either a non-targeting siRNA or DNA-PKcs-specific siRNA pools for three days. Cells were then infected with either 7134 or 7134R at an MOI of 0.1 and total virus collected after 48 hours and quantified via plaque assay on U2OS cells (B). Data are plotted as the averages with SEM of three independent experiments.

Having observed that DNA-PKcs partially promoted H2AX phosphorylation in response to incoming viral genomes, we next sought to determine its effect on replication. DNA-PKcs is known to be a target of ICP0 and is degraded during infection (Lees-Miller et al., 1996). However, we previously observed co-precipitation of DNA-PKcs with the viral DNA replication protein ICP8 during infection with wild-type virus, suggesting that degradation may not occur in all cell types (Taylor and Knipe, 2004). To test this in our primary fibroblast model system, we infected HFFs with 7134 and 7134R. Over time, DNA-PKcs was degraded with 7134R, but not 7134, infection, indicating that DNA-PKcs is a target of ICP0 in HFFs (Figure 2.6A). Depletion of DNA-PKcs had no effect on the replication of 7134 and 7134R (Figure 2.6B), indicating that DNA-PKcs did not regulate replication in primary fibroblasts. This was surprising as a previous study observed that human gliomal cells deficient in DNA-PK function supported higher levels of viral replication relative to a control cell line (Parkinson et al., 1999). Additionally, we observed previously that murine cells lacking Ku70, a protein necessary for DNA-PKcs localization, also resulted in enhanced replication of the virus (Taylor and Knipe, 2004). Our results may argue that the different subunits of the DNA-PK complex may have different roles in the HSV-1 life cycle in different cell types, the extent of which remains to be determined.

To investigate the effects of Mre11 and H2AX loss on replication, we infected our knockout HFFs with WT, 7134R, and 7134 viruses, and quantified progeny virus by plaque assay. Surprisingly, loss of Mre11 significantly enhanced replication of 7134, and did not affect 7134R or KOS (Figure 2.5B), arguing that Mre11 restricted HSV-1 replication in the absence of ICP0. Mre11 has been reported to be lost over the course

of infection in a manner independent of ICP0 (Gregory and Bachenheimer, 2008). We observed a slight reduction in Mre11 levels at later times during 7134, but not 7134R infection (Figure 2.4C), indicating that ICP0 may target some other protein in the restriction pathway of which Mre11 is a component. Loss of H2AX had no effect on replication of the three viruses (Figure 2.5B), indicating that H2AX was indeed dispensable for replication, as reported previously (Botting et al., 2016).

In the absence of ICP0, the downstream DDR protein 53BP1 localizes to incoming viral genomes (Lilley et al., 2011). However, it is unknown whether this has any role in the regulation of viral replication. To test this, we depleted it in primary HFFs using a pool of siRNAs, and measured the replication of 7134 and 7134R by plaque assay. Despite successful knockdown, replication of both viruses was not affected (Figure 2.5C), arguing that 53BP1 was dispensable for replication. Recruitment of 53BP1 to viral genomes is dependent on H2AX (Lilley et al., 2011). Our results thus far have argued that this H2AX arm of the ATM pathway did not impact the replication cycle of HSV-1, and the actions of ATM were through some other mechanism. Our observations also revealed a novel function of Mre11 in primary fibroblasts, a function in which Mre11 restricted the replication of a virus lacking the expression of ICP0. Furthermore, these contrasting phenotypes between ATM and Mre11 suggested that while Mre11 promoted the partial activation of ATM, these proteins had separate functions in regulating the replication of the virus outside of their roles in propagating the DDR.

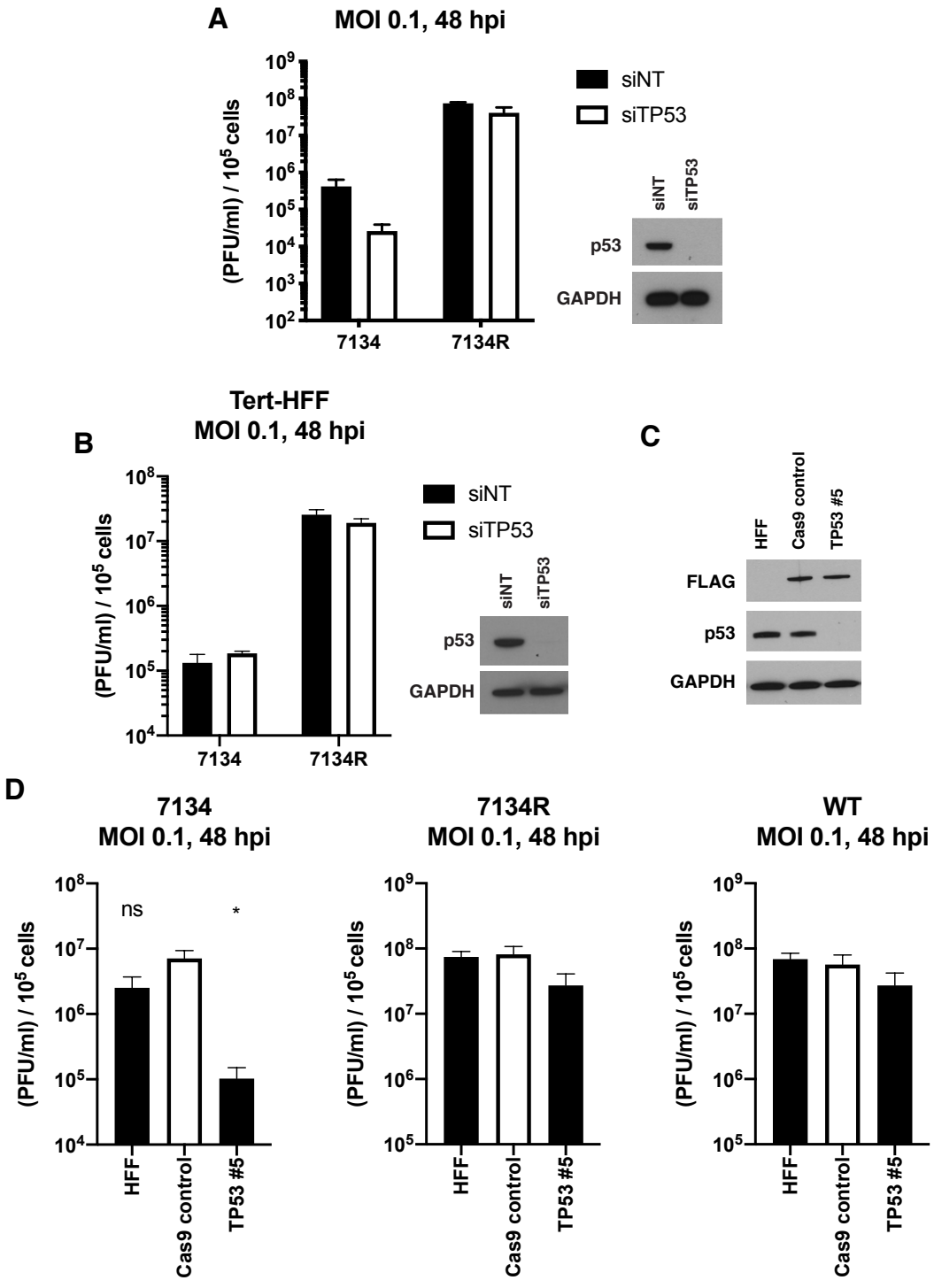
A
MOI 0.1, 48 hpi
(PFU/ml) / 10^5 cells
siNT
siTP53
p53
GAPDH
7134
7134R
B
Tert-HFF
MOI 0.1, 48 hpi
C
HFF
Cas9 control
TP53 #5
FLAG
D
7134
MOI 0.1, 48 hpi
7134R
WT
ns
*

Figure 2.7 (continued)

Figure 2.7. p53 positively regulates the replication of ICP0-null HSV-1. Primary HFFs were transfected with a non-targeting siRNA pool or a pool targeting TP53 and infected with 7134 and 7134R three days later at an MOI of 0.1 for 48 hours and total virus quantified on U2OS cells via plaque assay. Protein lysates were also collected at the time of infection to verify the knockdown (A). Tert-HFFs were infected with 7134 and 7134R at an MOI of 0.1 for 48 hours and total virus was quantified by plaque assay on U2OS cells (B). Primary HFFs were transduced with lentiviruses expressing Cas9 only, or Cas9 along with a guide RNA against TP53. The extent of the knockout was verified via immunoblot after roughly two weeks of puromycin selection. Blots are representative of three passages of cells (C). Normal HFFs, Cas9 control, and TP53 #5 cells were infected with 7134, 7134R, and WT viruses at an MOI of 0.1 for 48 hours and total virus quantified via plaque assay on U2OS cells (D). Graphed data are the averages of three independent experiments (A, B, D). Statistical significance was determined, compared to the Cas9 control cell line, using unpaired *t* tests. *$p<0.05$, ns – not significant. Errors bars represent the SEM.

p53 promotes the replication of ICP0-null HSV-1 in primary fibroblasts

ATM has been shown to be required for p53 phosphorylation on serines 15 and 20 (Boutell and Everett, 2004), and our observations are consistent with that study. Despite being known to promote replication, it is unknown precisely where p53 acts in the viral replication cycle. To determine whether p53 regulates replication in primary HFFs, we knocked it down with siRNA and measured the replication of 7134 and 7134R. Knockdown of p53 reduced replication of 7134 by over ten-fold (Figure 2.7A), but 7134R replication was unaffected. These findings indicated that p53 promoted replication of an ICP0-null virus in primary fibroblasts. To determine whether p53 also promoted replication in another human fibroblast line, we infected telomerase-immortalized human foreskin fibroblasts (tert-HFFs) (Bresnahan et al., 2000). We chose immortalized cells because they would be more amenable to long-term studies. However, knockdown of p53 had no effect on the replication of either virus, indicating that p53 was dispensable for replication in this cell line (Figure 2.7B). Whether this is due to telomerase remains to be determined. For gene knockout studies, we proceeded with primary HFFs. Using CRISPR-Cas9, we generated a gene knockout of *TP53* in HFFs (Figure 2.7C). In agreement with our siRNA results, loss of p53 by CRISPR-Cas9 significantly reduced the replication of 7134, but not 7134R. Furthermore, WT virus was also unaffected by the knockout (Figure 2.7D). Together, our results argued that p53 is a pro-viral protein whose absence can be compensated for by ICP0. In contrast, we observed that an increased abundance of p53 did not enhance replication. We treated HFFs with increasing concentrations of nutlin-3a to increase the levels of p53 (Vassilev et al., 2004), and, despite heightened levels of p53 (Figure 2.8A), replication of all three

viruses was not affected (Figure 2.8B). This indicated that only a loss, and not an over-abundance, of p53 had an effect on replication, indicating that p53 was required but not limiting in the regulation of HSV-1 replication.

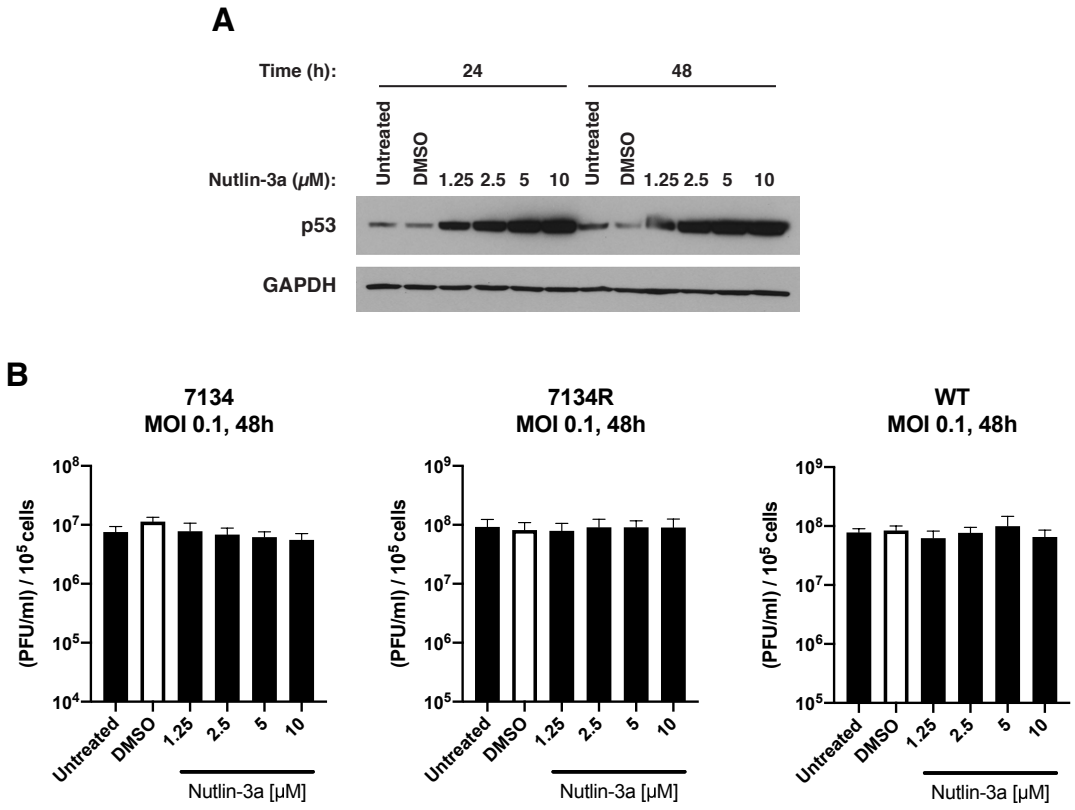

Figure 2.8. HFFs were either untreated, or treated with the indicated concentration of nutlin-3a and protein lysates collected at the indicated times post-treatment. Blots are representative of three independent experiments (A). HFFs were pre-treated with the indicated amount of nutlin-3a for one hour and then infected with 7134, 7134R, or WT viruses at an MOI of 0.1. Cells received nutlin-3a treatment throughout the course of infection. Total virus was harvested at 48 hpi and quantified via plaque assay on U2OS cells (B). The DMSO-only control used the same volume of DMSO as the 10 μM nutlin-3a condition. Data are plotted as the averages of three independent experiments with SEM.

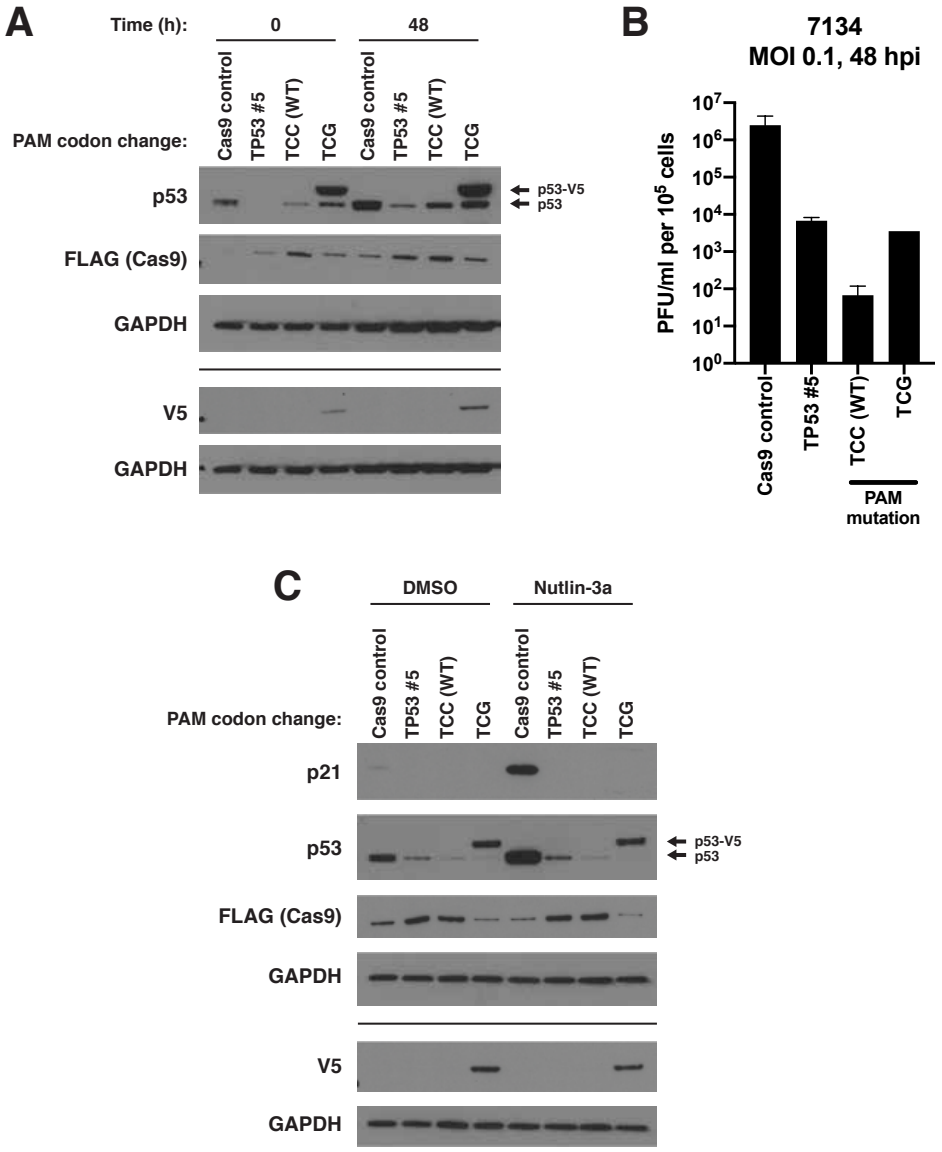

Figure 2.9. Attempted rescue of the *TP53* #5 knockout cell line with a V5-tagged Cas9-resistant p53 lentiviral construct. *TP53* #5 knockout HFFs were transduced with lentiviruses encoding blasticidin resistance along with C-terminally tagged p53 containing either a TCC (WT) or TCG (Cas9-resistant) PAM codon. Transduced cells were selected for roughly two weeks with blasticidin and the expression of V5 and total p53 was compared to the Cas9 control and *TP53* #5 parent cell lines (A). Control, knockout, and rescued HFFs were infected with 7134 at an MOI of 0.1. Total virus was collected 48 hours later and

Figure 2.9 (continued)

titered on U2OS cells (B). Lysates in (A) were taken from parallel wells at the time of infection as well as at the time of collection in (B). Control, knockout, and rescued cells were treated with nutlin-3a for 24 hours and lysates collected for immunoblot (C).

Attempted rescue of p53-deficient HFFs

To validate that the gene knockout was specific to *TP53*, we attempted to re-introduce a Cas9-resistant p53 into our knockout cell line to determine whether this would rescue the replication of 7134. The PAM sequence, that is required for cleavage by Cas9 (Doudna and Charpentier, 2014), of our *TP53* #5 gRNA spans a TCC serine codon. We purchased a lentiviral construct encoding p53 that was C-terminally tagged with a V5 epitope as well as resistance to blasticidin. We sequenced the transgene and compared it to the NCBI sequence for *TP53*. We found a mutation in the coding sequence and corrected it back to the NCBI sequence. There are six possible serine codons, including TCC. We mutated the WT codon to each of the other five codons. Transient expression results showed that the TCG mutant had the highest levels of expression. We then transduced knockout cells with either the WT (TCC) construct or the TCG construct. Following roughly two weeks of selection with blasticidin, we assessed V5 and total p53 expression by immunoblot compared to Cas9 control and parent knockout cell lines. We detected p53-V5 expression in the TCG construct, but not with the WT TCC codon, indicating that the TCG change conferred resistance to Cas9 activity (Figure 2.9A). Next, to determine whether the Cas9-resistant construct rescued replication, we infected Cas9 control, knockout, the TCC WT, and the resistant TCG with 7134 and measured replication by plaque assay. Interestingly, we observed that while knockout reduced the replication of 7134, stable expression of p53-V5 did not rescue (Figure 2.9B). While replication was higher in the Cas9-resistant (TCG) cell line than the Cas9-sensitive (TCC) cell line, these levels were not higher than the original knockout. This suggested that the transgene may not have been functional. To test this,

we treated control, knockout, and transduced cells with nutlin-3a to promote p21 expression in a p53-dependent manner. Nutlin-3a led to a robust induction of p21 expression in Cas9 control cells, but not *TP53* #5 cells, validating our system (Figure 2.9C). However, despite expression of the TCG construct, nutlin-3a treatment did not induce p21, nor did it increase p53-V5 levels like for native p53 in the Cas9 control cell line. This argued that while the construct was indeed Cas9-resistant, it was not functional. We hypothesize that the V5 tag may sterically hinder p53 binding to DNA or otherwise inhibit its function. It would be interesting to remove the tag in the construct and test the effects of nutlin-3a. We still believe that the *TP53* knockout is specific as the *TP53* #5 cell line and siRNA-mediated knockdown have similar effects on viral replication, as well as no p21 induction after nutlin-3a treatment in the knockout cells.

p53 promotes the transcription of an essential viral gene encoding a DNA replication protein

Having demonstrated that p53 promoted progeny virus production, we next sought to determine at which step in the virus replication cycle p53 acted. First, we measured viral DNA replication. Knockout of TP53 significantly reduced DNA replication of 7134 (Figure 2.10A), while DNA replication of 7134R and WT viruses was marginally affected (Figures 2.11A and 2.11C, respectively). This indicated that at least part of the defect in progeny virus production in 7134 virus-infected cells was due to reduced replication of the genome. However, before the initiation of DNA replication, HSV-1 must first express the IE genes, which are required to initiate transcription of the E genes, encoding the DNA replication machinery. Therefore, the reduction in viral DNA

replication could have been due to a defect in either IE or E gene expression. To determine which gene set was regulated by p53, we treated 7134 virus-infected cells with acyclovir (diagrammed in Figure 2.10B). We chose representative genes of each class: *ICP4* and *ICP27* for the IE class, *ICP8* (an essential DNA replication gene) for the E class, and the glycoprotein *gC* for the L class. By using acyclovir, this allowed us to differentiate pre-DNA replication from post-DNA replication gene expression. Without ACV treatment, mRNA levels of the *ICP4*, *ICP27*, *ICP8*, and *gC* genes were significantly reduced in the knockout cells compared to the control line following infection with 7134 (Figure 2.10C). This most likely reflected the transcriptional levels of viral mRNA both before and after DNA replication. However, with acyclovir treatment we observed a significant reduction in *ICP8* gene transcript levels, but not *ICP4* and *ICP27* transcripts, arguing that p53 promoted *ICP8*, but not IE, gene transcription, which then led to decreased DNA replication and progeny virus production. In line with our DNA replication results, viral gene transcript levels were comparable between the control and knockout lines with and without acyclovir treatment for 7134R and WT viruses (Figures 2.11B and 2.11D, respectively). Together, our results indicated that p53 played a pivotal role in promoting the transcription of at lease one essential viral DNA replication protein gene, encoding ICP8.

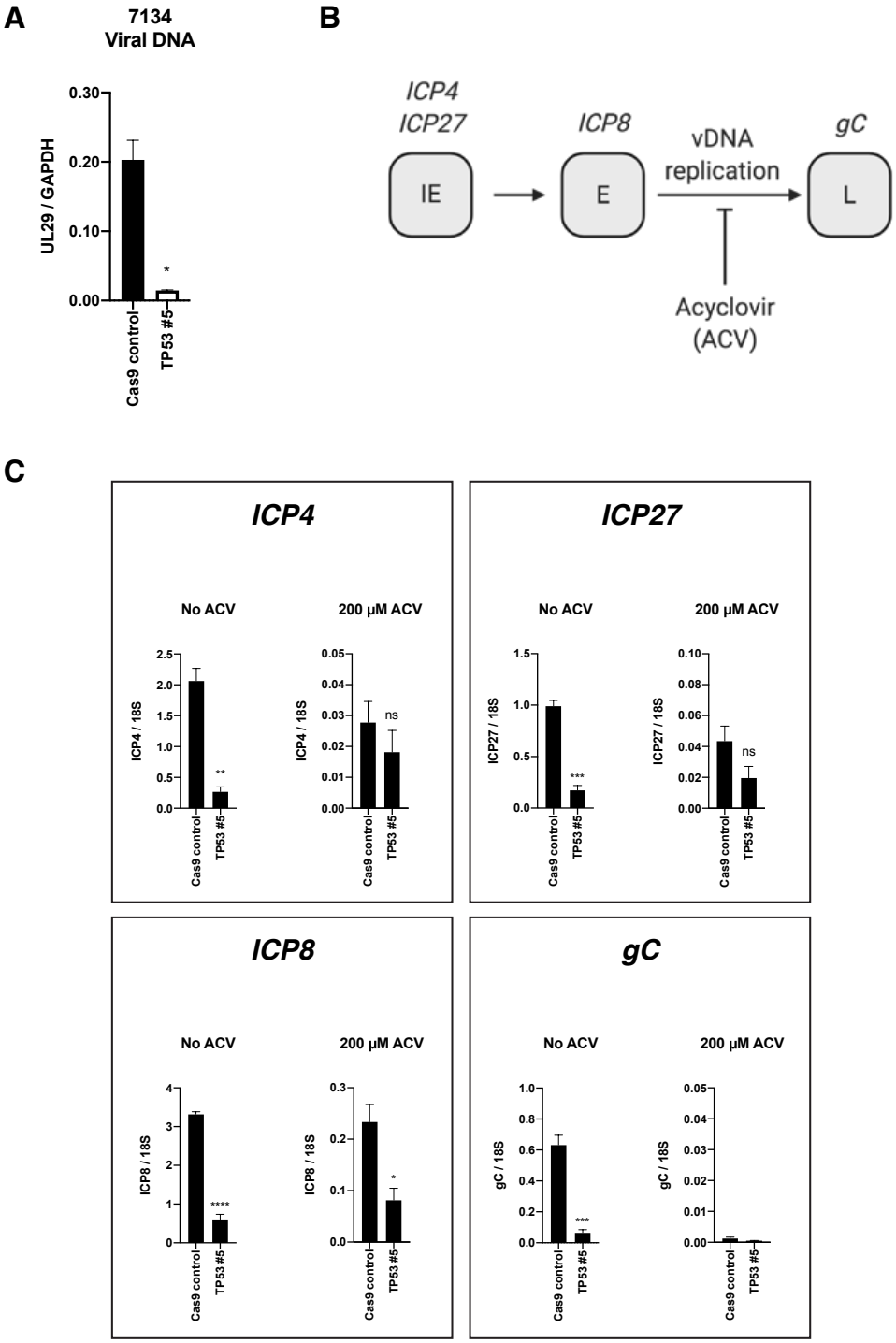

Figure 2.10. p53 promotes pre-replication *ICP8*, but not *ICP4* or *ICP27*, gene transcription. Cas9 and

Figure 2.10 (continued)

TP53 #5 cells were infected with 7134 at an MOI of 1 and nucleic acids collected 24 hours later. Purified DNA was amplified and quantified via real-time PCR with primer pairs for the *UL29* locus of the viral genome and cellular *GAPDH*. The values for *UL29* were normalized to the *GAPDH* values (A). cDNAs of viral genes representative of each viral gene class were quantified. *ICP4* and *ICP27* represented the IE, *ICP8* the E class, and *g*C the L class. Cells were treated with ACV to allow for the quantification of IE and E transcripts before the onset of viral DNA replication (B). Total RNA from the same samples collected in part (A) above was isolated, reverse-transcribed, and the indicated viral transcripts quantified via real-time PCR and normalized to cellular 18S rRNA transcripts (C). Data are plotted as the average with SEM of three independent experiments (A, C). Statistical significance was determined, compared to the Cas9 control cells, via unpaired *t* tests. *p<0.05, **p<0.01, ***p<0.001, ****p<0.0001, ns – not significant.

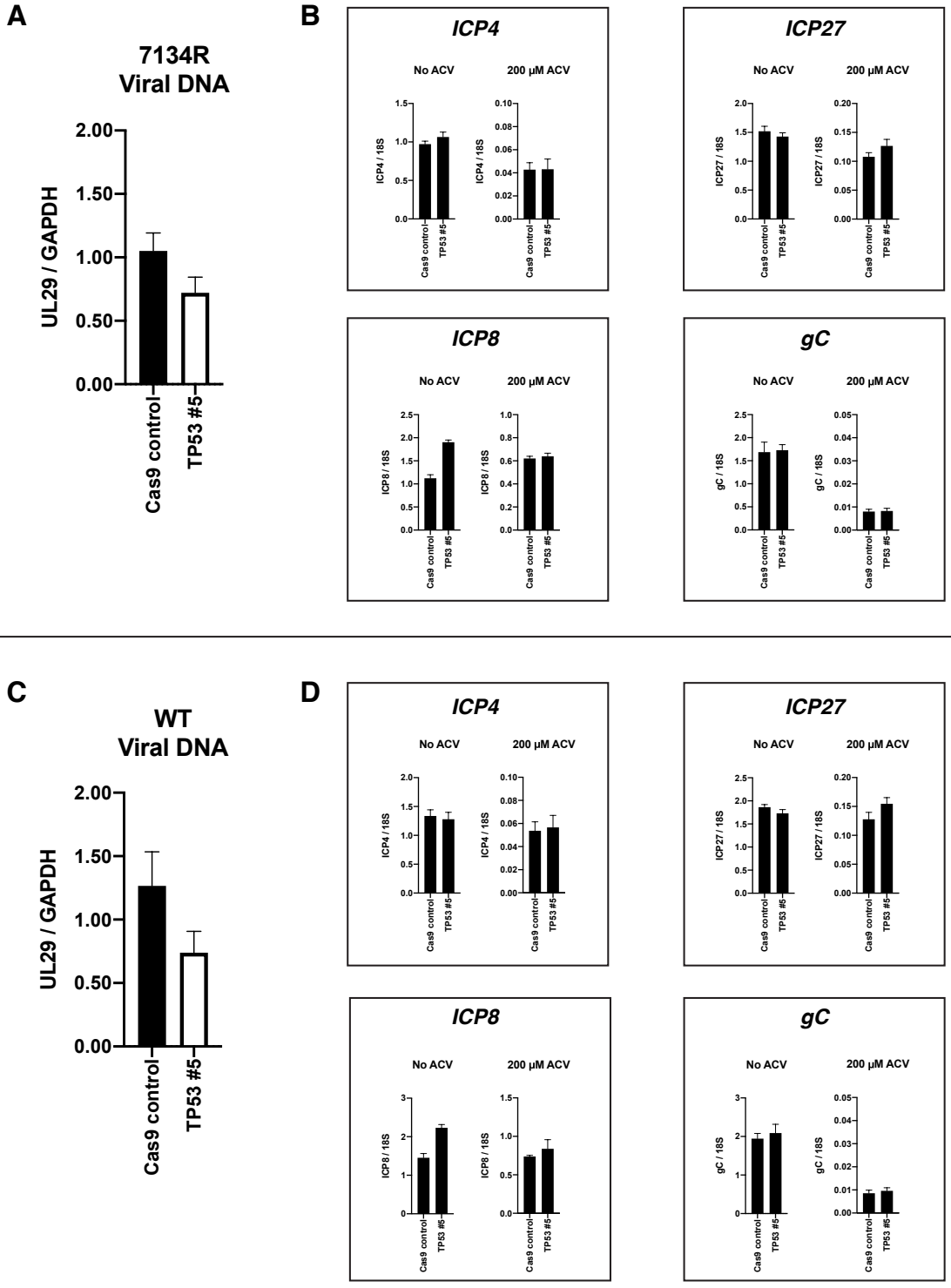
A
7134R
Viral DNA
UL29 / GAPDH
2.00
1.50
1.00
0.50
0.00
Cas9 control
TP53 #5
B
ICP4
ICP27
ICP8
gC
No ACV
200 μM ACV
ICP4 / 18S
ICP27 / 18S
ICP8 / 18S
gC / 18S
Cas9 control
TP53 #5
C
WT
Viral DNA
D

Figure 2.11 (continued)

Figure 2.11. Cas9 control and TP53 #5 cells were infected with 7134R at an MOI 1 and nucleic acids were collected at 24 hpi. Viral DNA (A) and viral gene expression (B) were quantified using the same protocols as figure 6 via real-time PCR. Control and knockout cells were also infected with WT virus at an MOI of 1 and also harvested at 24 hpi. Viral genomes (C) and transcripts (D) were quantified as in (A) and (B). Data are the averages and SEM of three independent experiments.

IFI16 is a cellular protein known to restrict ICP0-null HSV-1 replication (Orzalli et al., 2013). Additionally, IFI16 has been shown to bind to p53 (Johnstone et al., 2000; Liao et al., 2011) and negatively regulate its function (Kwak et al., 2003). This is still a point of contention, however (Fujiuchi et al., 2004; Johnstone et al., 2000; Liao et al., 2011). To determine whether IFI16 had any role with respect to p53, we knocked down p53 in IFI16 knockout HFFs and measured replication of 7134 by plaque assay. We only used 7134 as ICP0 promotes the degradation of IFI16 (Orzalli et al., 2012). Knockdown of p53 resulted in elevated IFI16 protein levels in the Cas9 control cells (Figure 2.12A), indicating that p53 negatively regulated the expression of IFI16. Depletion of p53 in both Cas9 control and IFI16 #1 cells dramatically reduced 7134 replication compared to non-targeting treatment (Figure 2.12B), arguing that IFI16 was not required for p53 function during infection.

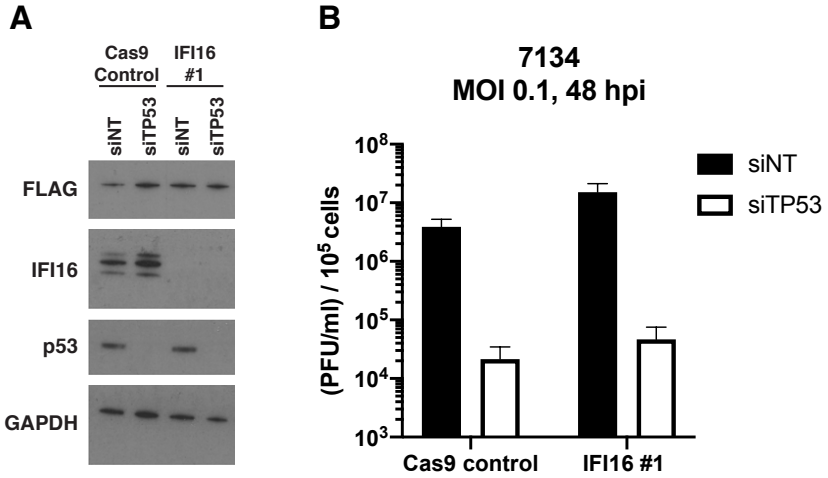

Figure 2.12. Cas9 control and IFI16 #1 knockout cells were transfected with either a non-targeting pool, or a pool targeting TP53 for three days. Protein lysates were collected for immunoblot at the time of the following infections to validate the knockouts and knockdowns (A). Cells were infected with 7134 at an MOI of 0.1. Total virus was collected 48 hours later and quantified on U2OS cells via plaque assay (B). Data are the averages of three independent experiments with SEM. Blots are representative of the three independent experiments.

Discussion

Cells infected with HSV-1 are known to activate proteins in the homologous recombination repair pathway (Lilley et al., 2005). The activation starts at early times post-infection and peaks around times of viral DNA synthesis, but the precise effects of input versus replicated viral DNA had not been defined. Furthermore, the DDR responses to viral infection have not been compared to normal cell responses to DNA damage agents. In this study, we compared the DDR kinase pathways activated in normal human fibroblasts by input HSV-1 genomic DNA, HSV-1 replicating/progeny DNA, and in uninfected cells treated with etoposide. We also defined the cellular gene products needed for each using CRISPR-Cas9 technology to knock out specific cellular genes. We observed unique DDR kinase pathways for each of these of the situations. We observed that etoposide induces strong phosphorylation of both ATM and Chk2, while input HSV-1 DNA activates a strong Chk2 phosphorylation response and replicating/progeny HSV-1 DNA activated a strong ATM phosphorylation response. Furthermore, we observed that key DDR proteins act to regulate HSV-1 infection in that ATM and p53 promote replication of ICP0-null HSV-1 while Mre11 acts to restrict ICP0-null HSV-1. Individual DDR components can be pro-viral or anti-viral; thus, these results argue that HSV-1 manipulates the host cell DDR response to utilize specific components for its optimal replication while inactivating the antiviral aspects of the DDR.

The DDR to HSV-1 infection is biphasic

HSV-1 lytic infection involves two states of the viral genome, the incoming parental genome, and the replicating and replicated progeny genomes. Using mutant

viruses and acyclovir to inhibit viral DNA replication, we were able to document the responses to both states and present a model (Figure 2.13). The viral genome enters the nucleus as a linear molecule containing not only two free double-stranded ends, but also nicks and gaps of various lengths that can activate the DDR (Smith et al., 2014). We used the *d*109 virus to interrogate the response to the parental genome without any potential effects caused by viral gene transcription. We observed that while ATM was responsible for p53 and Chk2 phosphorylation during this phase of the viral replication cycle, γH2AX accumulation was not dependent on ATM. It is conceivable that DNA-PK, ATR, or a redundancy between them and ATM is responsible for γH2AX accumulation. In any case, we observed that H2AX was dispensable for replication, indicating that whichever kinase(s) is responsible, the mechanism by which ATM functions does not involve H2AX. With regards to ATM-dependent Chk2 activation following infection with *d*109, compared to more robust ATM activation discussed in the next paragraph, this would suggest that ATM specificity may change over the course of infection, or perhaps is manipulated by viral gene products. This is exemplified in the transition from ATM-independent to ATM-dependent γH2AX formation during viral genome replication.

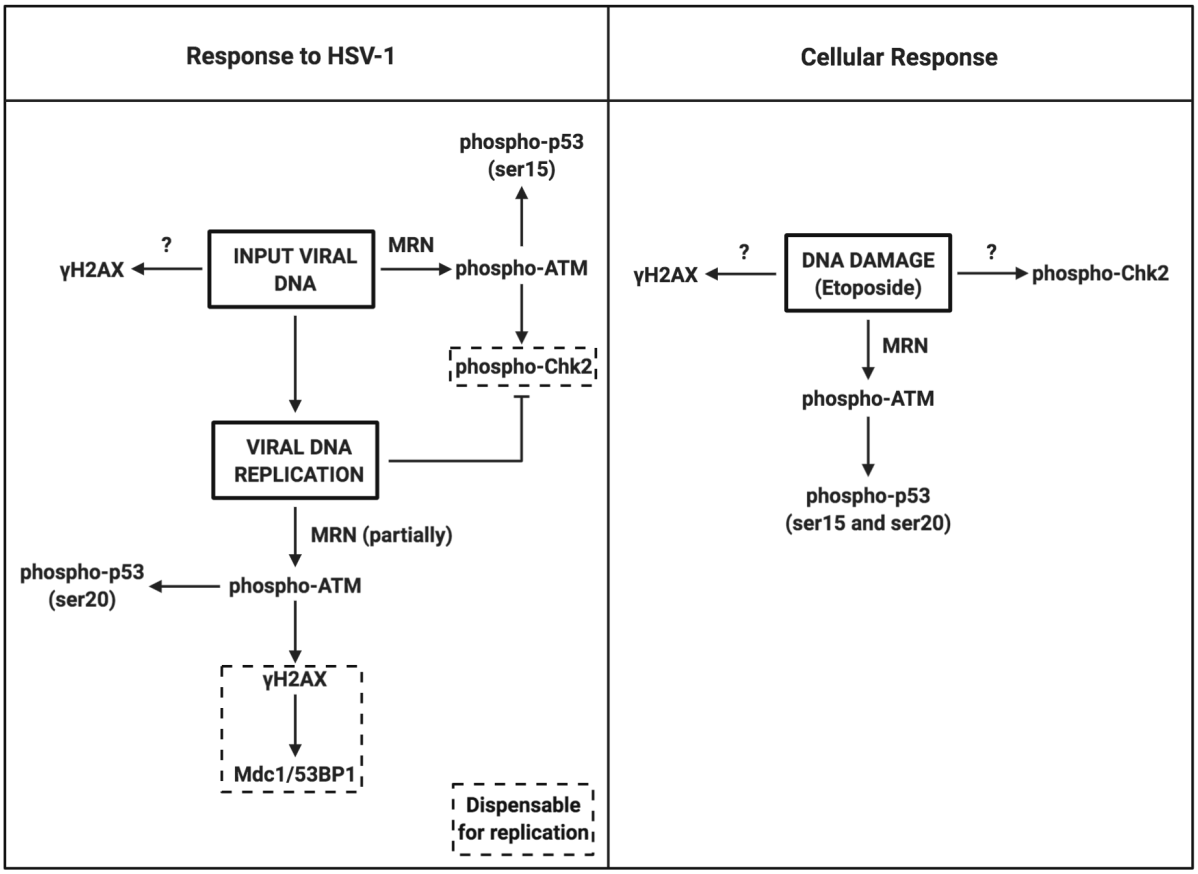

Figure 2.13. A comparison between the DDR to HSV-1 infection and the DDR to the cellular genome following etoposide treatment.

Viral genome replication led to further ATM activation, p53 phosphorylation, γH2AX formation, and suppression of Chk2 phosphorylation. At this stage, H2AX phosphorylation was dependent on ATM, indicating that as viral lytic replication progresses, ATM becomes the dominant kinase active, shifting away from Chk2, exhibiting a biphasic modality. Mdc1 and 53BP1 are downstream of ATM, recruited by γH2AX. Interestingly, depletion of these proteins had no effect on replication of the virus, indicating that this arm of the ATM pathway was irrelevant for infection. This may be due, in part, to the relatively small size of the viral genome compared to the cellular genome as cellular H2AX DDRs span millions of base pairs (Rogakou et al., 1999). Histones are loaded onto the viral genome within an hour from initial infection (Lee et al., 2016). While H2AX associates with the viral genome by two hours following infection (Dembowski and DeLuca, 2018) and with newly synthesized genomes (Dembowski et al., 2017), γH2AX appears to be excluded from viral replication compartments (Wilkinson and Weller, 2006). Therefore, the γH2AX signal we observed during the viral DNA replication phase may be phosphorylation of H2AX present on the cellular genome by ATM that was activated by viral DNA replication. However, we cannot discount that HSV-1 replication may induce damage to the cellular genome. Further investigation of ATM substrates is necessary to determine how ATM regulates replication. With regards to Chk2 phosphorylation, while it was ATM-dependent in the context of HSV-1 replication, it was ATM-independent when cells were treated with etoposide. This indicates some specificity in ATM substrates between infection and cellular DNA damage responses. Moreover, we hypothesize these differences in substrate

phosphorylation may be due to active manipulation by the virus to optimize the replication process.

The viral UL12 nuclease binds to the MRN complex and has been proposed, in tandem with ICP8, to facilitate efficient packaging of daughter viral genomes into new capsids (Balasubramanian et al., 2010). One hypothesis is that a UL12/ICP8 complex may localize MRN to viral DNA to activate ATM, at least in part. This manipulation would activate the MRN complex to allow for full activation of ATM, which then exerts its pro-viral role, possibly through p53, while ICP0 inhibits the anti-viral effects of Mre11 via degradation of a target protein, or multiple proteins, in the Mre11 pathway. The effect on Mre11 may be through direct interaction with ICP0 as we have described this interaction previously (Conwell et al., 2015). This hypothesis is supported as we observed replication-dependent ATM activation. Because ICP8 is required for viral DNA replication (Conley et al., 1981), an ICP8$^-$ virus should phenocopy acyclovir treatment. It would be interesting to determine whether viruses lacking UL12 and ICP8 elicit similar DDR responses to acyclovir-inhibited WT virus infection.

Cellular DNA damage and HSV-1 infection are treated differently by the host DDR machinery

Our observations for the cellular response to DNA damage in the absence of infection are also diagrammed in Figure 2.13 as a comparison with HSV-1 infection. We observed that etoposide induces a DDR in HFFs characterized by MRN-dependent ATM activation and p53 phosphorylation. What was interesting, however, was that both Chk2 and H2AX phosphorylation were not dependent on either Mre11 or ATM,

suggesting to us that more than just the canonical MRN-ATM response was activated by etoposide-generated DNA damage. There is precedence for ATM-independent Chk2 phosphorylation (Theard et al., 2001). The caveat, however, was that this required prolonged DDR activation, whereas we observed the same phenotype by two hours. ATR has been shown to phosphorylate Chk2 in response to DNA damage (Pabla et al., 2008), leading us to hypothesize that ATR may have also been activated by etoposide treatment, which, in turn, led to the phosphorylation of Chk2. This idea can be extended to H2AX phosphorylation. Because ATR can also phosphorylate this histone variant (Ward and Chen, 2001), it is conceivable that this was the underlying mechanism for the apparent ATM-independent phosphorylation of H2AX. DNA-PK is also known to promote the phosphorylation of H2AX (An et al., 2010; Mukherjee et al., 2006) and even Chk2 (Li and Stern, 2005), so we may be observing the effects of all three (ATM, ATR, and DNA-PKcs) kinases simultaneously with etoposide treatment. Future work will focus on individual and combinatorial depletions of these kinases to further explore this hypothesis. HSV-1 encodes two major proteins kinases: U_S3 and U_L13. It is possible that these viral kinases may phosphorylate DDR proteins. The caveat, however, is that both of these kinases are encoded by late genes, which are sensitive to acyclovir treatment. Therefore, these kinases may be responsible for the phosphorylation of ATM, H2AX, and/or serine 20 of p53, but most likely not Chk2 as its phosphorylation was reduced following viral DNA replication. These two kinases are also present in the tegument of the viral particle which is introduced into the cytosol upon initial infection (Kelly et al., 2009). It is possible that enough of these kinases are present in the particle to phosphorylate Chk2. Both of these kinases are not essential for the replication of the

virus, so generating viral particles missing both of these proteins should be a relatively simple process. There is the possibility that the amounts of these kinases in the tegument may be sufficient to phosphorylate Chk2 and H2AX as we observed increased input gB from *d*109 particles. Given this etoposide-driven DDR profile, HSV-1 infection appears to elicit a modified, or perhaps targeted, DDR different to that of normal cellular DDR. The different DDR responses may be due to effects of viral gene products or differences in the characteristics of the viral and cellular genomes.

Viral DNA is not associated with histones inside the capsid (Gibson and Roizman, 1971). Instead, the viral genome enters as a naked linear molecule that is loaded with histones within one hour (Kent et al., 2004; Lee et al., 2016). Compared to cellular DNA breaks, the incoming viral genome may not be a sufficient stimulus for full ATM activation, leaving only Chk2 efficiently activated. There is evidence that, as viral DNA replication progresses, the daughter DNA molecules are associated with fewer histone complexes (Oh and Fraser, 2008). This exposed DNA may be the key feature that leads to ATM activation, and the stimulus from the parental viral genome that was activating Chk2 is no longer present, leading to the observed DNA replication-dependent reduction in Chk2 phosphorylation.

Mre11 restricts and ATM promotes viral replication

We observed that Mre11 restricted replication of an ICP0$^-$ virus, indicating that ICP0 is responsible for attenuating a different portion of the pathway as we did not observe changes in Mre11 levels in the presence of ICP0, in contrast to what has been previously described (Gregory and Bachenheimer, 2008). We also observed that ATM

promoted replication of the virus. In the canonical DDR pathway, Mre11 promotes ATM activation, which is in apparent opposition to our findings as Mre11 and ATM depletion gave opposing effects on progeny virus production. Mre11 depletion did not totally abolish ATM activation, indicating a redundant mechanism for ATM activation in response to infection. The Tip60 histone acetyltransferase is known to promote ATM activation (Sun et al., 2005). While it interacts with the MRN complex and its knockdown decreases γH2AX and Rad50 foci formation (Chailleux et al., 2010), it remains undetermined whether Tip60 alone is sufficient for ATM activation. This could explain the partial Mre11-independence of ATM activation during HSV-1 infection. The HSV-1 UL13 kinase has been shown to interact with and phosphorylate Tip60 (Li et al., 2011). This would provide an elegant mechanism to circumvent Mre11 restriction to promote the pro-viral functions of ATM: i.e., UL13 phosphorylates Tip60, which in turn acetylates ATM, leading to its phosphorylation and activation. Future experiments will focus on testing this hypothesis. With regards to a mechanism, ATM appears to be the determinant kinase of p53 phosphorylation and we hypothesize that this phosphorylation is what promotes efficient replication of this virus. We explore this hypothesis further later on in this discussion.

Concerning the restriction phenotype of Mre11, formation of protein complexes known to restrict HSV-1 replication, termed PML nuclear bodies (PML-NBs) or nuclear domain 10 bodies (Saffert and Kalejta, 2008), is sensitive to Mre11 depletion. Cells harboring non-functional Mre11 accumulated fewer PML-NBs after the cellular genome was damaged by etoposide (Dellaire et al., 2006). This could be a potential mechanism-of-action for Mre11-mediated restriction of ICP0-null HSV-1 replication: association of

Mre11 with the viral genome recruits PML-NB proteins to silence viral gene expression and subsequent replication. Our results are consistent with the hypothesis that Mre11 recruits other PML-NB proteins and ICP0 targeting these PML-NB proteins for degradation (Roizman, 2013) to attenuate this Mre11 pathway.

Our observations also indicate that the mechanism by which Mre11 affects HSV-1 replication may not necessarily be tied to homologous recombination. Viral DNA can undergo HR catalyzed by Rad51/Rad52 (Tang et al., 2014), and depletion of Rad51 and Rad52 reduces replication when the virus was pre-treated with UV radiation (Muylaert and Elias, 2010). Canonically, Mre11 initiates the sensing pathway that leads to HR. Our observations imply a mechanism of Mre11 action that does not involve Rad51/Rad52 as they yield opposing phenotypes. Collectively, our results reveal a novel, or otherwise non-canonical, function of Mre11 outside of HR in suppressing the replication of ICP0-null HSV-1.

Others have found that a modified DDR restricts adenovirus replication (Shah and O'Shea, 2015). In that study, both the MRN complex and ATM restricted an adenovirus not expressing E1B-55K/E4-ORF3 through a mechanism where both Mre11 and ATM associated with the viral genome. The MRN complex and ATM also associates with the HSV-1 genome at various points in the replication cycle (Dembowski and DeLuca, 2015, 2018; Dembowski et al., 2017), so it is possible that a similar pathway targets HSV-1. However, in our study, ATM did not restrict HSV-1, indicating that the restriction by Mre11 is not through ATM.

A role for p53 in the HSV-1 lytic replication cycle

Previous studies have observed that p53 localizes to sites of viral DNA replication (Wilcock and Lane, 1991) and enhances the production of progeny viruses (Maruzuru et al., 2013). We also observed this in our HFF model. Knockout of p53 significantly reduced *ICP8*, but not *ICP4* or *ICP27*, gene transcription before the onset of viral DNA replication. ICP8 is an essential viral DNA replication protein, so a reduction would lead to a decrease in both viral DNA replication and progeny viral production, both of which we observed. The mechanism by which p53 exerts this function is not well understood. We and others (Boutell and Everett, 2004) have observed that p53 is phosphorylated by ATM during HSV-1 infection. Phosphorylation of serine 15 is crucial for the activity of p53 in regulating gene expression (Loughery et al., 2014) and we hypothesize that this may be the mechanism by which ATM exerts its pro-viral function. Concerning the lack of phenotype in the presence of ICP0, p53 is ubiquitinated by ICP0 (Boutell and Everett, 2003), and this modification may serve to inhibit the function of p53, but this has yet to be demonstrated. While this would block any potential apoptosis to prolong progeny virus production, this would come at the expense of its effects on viral gene expression. Because ICP0 is such a potent transactivator of HSV-1 gene expression, this inhibition of p53 may be inconsequential.

p53 binds to the viral genome both *in vitro* and during productive infection, adjacent to the origins of replication (Hsieh et al., 2014). The *ICP8* and *ICP4* open reading frames are adjacent to *oriL* and *oriS*, respectively. Therefore, one possible mechanism is that the binding of p53 to the viral genome promotes the transcription of essential viral genes. We observed an effect only on pre-replication *ICP8* transcription, indicating that p53 function may be restricted to the instances where it binds to *oriL*. The

association dynamics between p53 and the viral genome have not been thoroughly explored. Time-course genome-wide p53 association studies would inform not only whether there is a bias for binding to the origins, but also if there are other binding sites not previously described. Coupled with RNA deep sequencing analysis, this would provide a powerful system to investigate where and when p53 binds, and whether this also correlates with altered viral gene transcription surrounding these sites.

In summary, our study has revealed novel roles for key proteins in the cellular DNA damage response to HSV-1 infection. Early recognition of damaged DNA by Mre11 has a restrictive effect on replication, while downstream ATM and p53 activation promotes replication. Our observations not only provide new insight into the relationship between the virus and the host, but also may inform studies of viral reactivation from latency, which is known to be intimately tied to the DDR (Brown, 2017; Hu et al., 2019).

Materials and Methods

Cells, viruses, and infections

HFF, U2OS, Vero, and HEK293T cells were obtained from the American Type Culture Collection (ATCC) (CRL-1634, HTB-96, CCL-81, CRL-3216, respectively) and were cultured in Dulbecco's Modified Eagle's medium (DMEM; Corning) containing 10% (v/v) fetal bovine serum (FBS) and pen/strep. All HSV-1 infections were carried out as described previously (Merkl et al., 2018). Henceforth, the DMEM 1% BCS medium will be referred to as "low serum medium". The HSV-1 wild-type KOS strain (Schaffer et al., 1970) was propagated on Vero cells. The derivative viruses 7134 and 7134R (Cai and Schaffer, 1989) were propagated on U2OS cells. Prior to use, all three viruses were

titered in parallel on U2OS cells. The *d*109 virus (Samaniego et al., 1998) was grown on U2OS ICP4/ICP27 cells and titered on the Vero FO6 cell line as described previously (Oh et al., 2019).

Viral yield experiments

Equal numbers of control, knockout, or plain HFFs were seeded (1 x 10^5 per well in 12-well plates) and infected with the indicated HSV-1 viruses at a multiplicity of infection (MOI) of 0.1 PFU/cell. After 48 hours, total virus was collected by adding an equivalent volume of sterile 10% non-fat milk followed by three freeze-thaw cycles at -80°C. Lysates were titered via ten-fold serial dilution on confluent U2OS cells. Following the one hour absorption period, cells were overlaid with low serum medium containing 0.16% (v/v) human IgG. After 72 hours, the cells were fixed with methanol chilled to -20°C. Cells were stained with Giemsa stain (Sigma) and plaques counted.

Drug treatments

The viral DNA replication inhibitor acyclovir (Sigma) was supplemented to the post-infection low serum medium to a final concentration of 200 μM. Nutlin-3a (Sigma) was supplemented to low serum medium to the indicated concentrations. Control treatments contained only medium (“Untreated”), or an equivalent volume of DMSO as the highest concentration of nutlin-3a used. HFFs were pre-treated with the indicated concentrations of nutlin-3a for one hour. Infections were carried out normally, without the addition of nutlin-3a. Following removal of the inoculum after absorption, the low serum medium added back contained the same concentration of nutlin-3a used in the

pre-treatment step. Cells were incubated in low serum medium supplemented with etoposide (Sigma) at a final concentration of 20 μM for the indicated periods of time.

Immunoblots

Immunoblots were performed as described previously (Orzalli et al., 2013) with minor modifications. Briefly, cells were lysed in 1xNuPAGE LDS sample buffer (Invitrogen) containing 5% (v/v) 2-mercaptoethanol and a protease/phosphatase inhibitor cocktail (HALT, ThermoFisher Scientific). Lysates were separated through 4-12% gradient NuPAGE Bis-Tris gels (Invitrogen) and transferred to nitrocellulose membranes (Bio-Rad). Transfer quality was determined via staining with a solution consisting of 0.5% Ponceau S (w/v) (Sigma) and 1% (v/v) acetic acid. Stain was removed by washing with phosphate-buffered saline (PBS) containing 0.1% (v/v) Tween (PBST). De-stained membranes were blocked with a solution of 5% (w/v) non-fat milk in PBST for one hour at room temperature. Membranes were cut horizontally above and below each protein investigated and incubated with the respective antibody. Primary antibodies were used in 5% milk and blots were incubated overnight at 4°C and then washed three times with PBST. Secondary antibodies were also used in 5% milk for one hour at room temperature. Following three washes in PBST, proteins were detected by exposure to film (Denville).

Table 2.1 Antibodies used

Antibody (dilution)	Vendor/Source	Catalog information
Anti-GAPDH (1:5000)	Abcam	ab8245
Anti-gB (1:5000)	Abcam	ab6506
Anti-H2AX (1:1000)	Cell Signaling	7631S
Anti-ATM (1:2000)	Abcam	ab78
Anti-Chk2 (1:1000)	Cell Signaling	3440S
Anti-p53 (DO-1) (1:1000)	Santa Cruz Biotech	sc-126
Anti-γH2AX (Ser139) (1:1000)	Abcam	ab2893
Anti-phospho-ATM (Ser1981) (1:1000)	Cell Signaling	4526S
Anti-phospho-Chk2 (Thr68) (1:1000)	Cell Signaling	2197S
Anti-phospho-p53 (Ser15) (1:1000)	Cell Signaling	9284S
Anti-phospho-p53 (Ser20) (1:1000)	Invitrogen	PA5-17894
Anti-ICP0 (1:2000)	East Coast Bio	H1A027
Anti-Mdc1 (1:2000)	Abcam	ab11171
Anti-ICP8 (3-83) (1:5000)	(Knipe et al., 1987)	
Anti-FLAG (1:2000)	Sigma	F1804
Anti-Mre11 (1:2000)	Novus Biologicals	NB100-142
Anti-ICP4 (58S) (1:2000)	(Showalter et al., 1981)	
Anti-53BP1 (1:1000)	Abcam	ab21083
Anti-DNA-PKcs (1:2000)	Abcam	ab70250
Anti-IFI16 (1:1000)	Abcam	ab55328
Anti-Rabbit-HRP conjugated (secondary antibody) (1:5000)	Cell Signaling	7074S
Anti-Mouse-HRP conjugated (secondary antibody) (1:5000)	Cell Signaling	7076S

siRNA knockdowns

siRNA RNA transfections were carried out as described previously (Cabral et al., 2018) with minor modifications. Briefly, 1 x 10^5 HFFs per well in 12-well plates were transfected with 10 picomoles of siRNA per well using Lipofectamine RNAiMAX (Invitrogen) according to the manufacturer's protocol. Two days later, cells were trypsinized, diluted 1:2 in fresh culture medium, and used the next day.

Table 2.2 siRNA pools used

siRNA	Vendor	Catalog information
ON-TARGETplus non-targeting pool	Dharmacon	D-001810-10-50
ON-TARGETplus TP53 SMARTpool	Dharmacon	L-003329-00-0005
ON-TARGETplus TP53BP1 SMARTpool	Dharmacon	L-003548-00-0005
ON-TARGETplus PRKDC SMARTpool	Dharmacon	L-005030-00-0005

CRISPR/Cas9 gene knockouts

Knockout cells were generated as described previously (Cabral et al., 2018) with minor modifications. Briefly, oligonucleotides were purchased from IDT and were cloned into the lentiCRISPR v2 backbone plasmid (Sanjana et al., 2014). HEK293T cells were transfected with the lentiCRISPR plasmid along with psPAX2 and pVSVG packaging plasmids using high molecular weight PEI. Cell supernatants were collected two days later and filtered though a 0.45 μm filter. Low-passage HFFs (passages 3-4) were overlaid with the filtered supernatant. Polybrene (Santa Cruz Biotechnology) was added to a final concentration of 5 μg/ml. After 24 hours, virus was removed and replaced with fresh medium containing 1 μg/ml puromycin (Santa Cruz Biotechnology). Cells were trypsinized and transferred to larger flasks when they reached confluency in their current flask. Knockout efficiency was validated via immunoblot roughly two weeks later when they had grown to confluency in T150 flasks. Cells were used until passage 15.

Table 2.3 DDR guide RNA sequences used

Target / gRNA number	Sequence (DNA form in oligo) (5' -> 3')	Reference
ATM gRNA #2	TGATAGAGCTACAGAACGAA	(Sanjana et al., 2014)
CHEK2 gRNA #1	AAGAAGCCTTAAGACACCCG	(Sanjana et al., 2014)
MDC1 gRNA #1	CCGAATGCCTGACTGCTCTG	(Sanjana et al., 2014)
MRE11 gRNA #3	GTTTGCTGCGTATTAAAGGG	(Doench et al., 2016)
MRE11 gRNA #4	GCAATCATGACGATCCCACA	(Doench et al., 2016)
H2AFX gRNA #3	CCGCGGCAAGACTGGCGGCA	(Doench et al., 2016)
TP53 gRNA #5	CCATTGTTCAATATCGTCCG	(Doench et al., 2016)
IFI16 gRNA #1	GTTCCGAGGTGATGCTGGTT	(Merkl et al., 2018)

p53-V5 mutagenesis, lentivirus particle production, and transduction

pLenti6/V5-p53 was purchased from Addgene (#22945). All mutageneses were conducted with the QuikChange II XL site-directed mutagenesis kit (Agilent Technologies) according to the manufacturer's protocol. Lentivirus particles were prepared, and cells transduced, using the same protocol as for the CRISPR/Cas9 particles. Transduced TP53 #5 cells were doubly selected with 1 μg/ml puromycin and 5 μg/ml blasticidin.

Nucleic acid extraction, reverse transcription, and quantitative PCR

Both RNA and DNA were extracted and processed for qPCR as described previously (Raja et al., 2016) with modifications. Briefly, the medium was removed and the cells lysed in 0.35 ml of buffer RLT containing 1% (v/v) 2-mercaptoethanol. DNA and RNA were prepared using the AllPrep kit (Qiagen) according to the manufacturer's protocol. DNA was used directly for qPCR and RNA was DNase-treated (Invitrogen DNA-*free* kit) and subsequently reverse transcribed (Agilent Technologies high-capacity reverse transcription kit), both according to the manufacturer's suggested protocols, and then used for qPCR. Transcripts were quantified using a standard curve generated by

using a ten-fold dilution series of DNA/cDNA prepared from HFFs infected with WT virus. All qPCRs were performed using an Applied Biosystems 7500 Fast Real-Time PCR System. Fast SYBR Green Master Mix (Applied Biosystems) was used for all qPCRs.

Table 2.4 qPCR primer sequences used

Oligo	Sequence (5' -> 3')	Reference
UL29 forward (DNA)	GAGACCGGGGTTGGGGAATGAATC	(Lee et al., 2016)
UL29 reverse (DNA)	CCCGGGGGTTGTCTGTGAAGG	(Lee et al., 2016)
GAPDH forward (DNA)	CAGGCGCCCAATACGACCAAATC	(Merkl et al., 2018)
GAPDH reverse (DNA)	TTCGACAGTCAGCCGCATCTTCTT	(Merkl et al., 2018)
18S forward (cDNA)	GCATTCGTATTGCGCCGCTA	(Lee et al., 2016)
18S reverse (cDNA)	AGCTGCCCGGCGGGTC	(Lee et al., 2016)
ICP4 forward (cDNA)	CGGTGATGAAGGAGCTGCTGTTGC	(Garvey et al., 2014)
ICP4 reverse (cDNA)	CTGATCACGCGGCTGCTGTACA	(Garvey et al., 2014)
ICP27 forward (cDNA)	AGACGCCTCGTCCGACGGA	(Garvey et al., 2014)
ICP27 reverse (cDNA)	GAGGCGCGACCACACACTGT	(Garvey et al., 2014)
ICP8 forward (cDNA)	CATCAGCTGCTCCACCTCGCG	(Garvey et al., 2014)
ICP8 reverse (cDNA)	GCAGTACGTGGACCAGGCGGT	(Garvey et al., 2014)
gC forward (cDNA)	GAGGAGGTCCTGACGAACATCACC	(Garvey et al., 2014)
gC reverse (cDNA)	CCGGTGACAGAATACAACGGAGG	(Garvey et al., 2014)

Software for figure graphs and diagrams

Graphs and statistical analyses were generated using GraphPad Prism. Figure 2.10B and 2.13 diagrams were created with Biorender.com.

Acknowledgments

We thank Jeho Shin and Patrick T. Waters for technical and manuscript assistance, respectively. This work was supported by NIH pre-doctoral fellowship F31 AI129207 to M.E.M., and research grant AI106934 to D.M.K.

Chapter 3: General discussion

3.1 Summary of results

Activation of the DDR upon HSV-1 infection

In chapter 2, we explored the DDR to HSV-1 infection and documented distinct responses to parental and progeny viral genomes. Incoming viral genomes robustly activated the Chk2 kinase, while minimally activating ATM. The H2AX histone variant was also up-regulated and phosphorylated early in infection. Chk2 and ATM activation were dependent on MRN, but γH2AX formation was not, indicating that most likely some other DDR pathway was concurrently activated. The loss of ATM also did not affect γH2AX formation in response to the incoming genomes, further supporting our hypothesis. Once viral genome replication commenced, ATM was robustly activated while Chk2 activation was suppressed. γH2AX formation, as well as p53 phosphorylation, was dependent on ATM. The MRN complex appeared to promote p53 phosphorylation, but only partial ATM and H2AX phosphorylation, indicating that redundant DDR pathways were activated. Our results collectively revealed a biphasic kinase response to parental and daughter viral genomes characterized by an initial Chk2 response followed by robust ATM activation.

Regulation of HSV-1 replication by DDR proteins and p53

We also observed that some of these DDR proteins regulated replication of the virus. Arguably, the most surprising finding was that Mre11 and ATM had opposing phenotypes. Mre11, and possibly the MRN complex as a whole, restricted replication while ATM promoted efficient replication. Moreover, both of these phenotypes required

the absence of ICP0, indicating that, in the case of Mre11, ICP0 inhibited this pathway, while also being able to compensate for the loss of ATM. Intriguingly, DDR proteins downstream of MRN and ATM, i.e. H2AX, 53BP1, and Mdc1, did not have a detectable role in the viral replication cycle. This indicated that while Mre11 and ATM are DDR proteins, they exert their roles possibly outside of the context of the DDR. However, more investigation is needed. The p53 protein also served a positive role in the replication cycle. Both siRNA-mediated and CRISPR-Cas9-mediated depletions of p53 reduced the replication of an ICP0$^-$ virus. Furthermore, we found that p53 promoted transcription of the gene of an essential viral DNA replication protein, ICP8, before viral DNA replication commenced. This appeared specific to ICP8, and most likely other E genes as well, because IE genes were not affected by this loss of p53. We also hypothesize that ATM activation promotes this activity of p53.

The LINC complex and the type-I interferon response to HSV-1 infection (Appendix)

In the appendix of this dissertation, we explore the role of protein components of the linker of the nucleoskeleton and cytoskeleton (LINC) complex with respect to the cellular responses to HSV-1 infection and potential effects on viral gene expression. Primary HFFs mount a robust type-I interferon (IFN) response to HSV-1 *d*109 infection (Orzalli et al., 2012). In HFFs, we depleted via siRNA pools two primary proteins of the LINC complex: Sun1 and Sun2, as well the transiently associated TorsinA protein. Initially, we observed that depletion of Sun1 by siRNA led to a decrease in STING, TBK1, and IRF3 phosphorylation, all markers of the IFN response, as well as a

decrease in IFNβ mRNA transcripts following infection with *d*109. These results appeared to indicate that Sun1 facilitates nuclear sensing of HSV-1 genomes, at least when depleted by siRNA. Interestingly, when we disrupted the *SUN1* gene by CRISPR-Cas9 editing, there were no effects on the IFN response to not only *d*109, but also HCMV, infection, indicating that, in this system, Sun1 is dispensable and does not facilitate innate sensing of viral DNA. We next tested each of the siRNAs in the *SUN1* pool individually. We found that our observed phenotype was a combination of effects from different siRNAs. While all of the siRNAs depleted Sun1 to varying degrees compared to a non-targeting pool, some siRNAs reduced IFN signaling, while others had minimal effects. We therefore conclude that the initially apparent role of Sun1 in innate sensing of HSV-1 infection was due to an off-target effect of the siRNA pool and Sun1, in fact, has no role in the IFN pathway.

The LINC complex and intrinsic immunity to HSV-1 infection (Appendix)

In addition to the effects of siRNA depletion of Sun1 on the IFN pathway, depletion of Sun1 also had negative effects on viral gene transcription, viral protein accumulation, and progeny virus production. siRNA-mediated depletion of Sun1 reduced IE gene expression and those effects resonated throughout the rest of kinetic classes of viral genes. Interestingly, this was only the case for a virus lacking ICP0 expression, indicating that ICP0 was able to compensate for the absence of Sun1. As with the IFN response, disruption of *SUN1* by CRISPR/Cas9 had no effect on viral replication, arguing that Sun1 also had no function in the HSV-1 replication cycle. Sun2 was also not able to compensate for the loss of Sun1. We determined that this

discrepancy in phenotypes again was due to an off-target effect in the siRNA pool. Sun1 protein levels were reduced by each of the siRNAs individually, but only one reduced viral ICP4 levels.

3.2 General discussion and future directions

The DDR to different stages of the viral replication cycle

In chapter 2, we observed the phosphorylation and activation of several proteins in the HR pathway. Previous studies using proteomics analyses have observed that some DDR proteins associate with the viral DNA (Dembowski and DeLuca, 2015, 2018; Dembowski et al., 2017), but the interdependencies between these proteins remains poorly defined. We have developed a method for detecting and visualizing proteins that associate with the viral genome as soon as it enters the nucleus (Cabral et al., 2018). This involves chemically labeling viral DNA with a nucleoside analog within the capsid, which can be covalently linked to a fluorescent molecule via click chemistry, and a protein in question can be visualized with a specific antibody. Another study described a highly similar method for similar applications (Dembowski and DeLuca, 2018). The free ends of the linear viral genome could serve as attractive targets for the Ku and/or MRN complexes. It would be especially informative to determine whether the MRN complex associates immediately as Mre11 was necessary for the optimal DDR response to parental viral genomes. Moreover, we observed that Mre11 restricted viral gene expression beginning as early as 2 hours post-infection. One possibility is that binding of the MRN complex to the DNA ends decreases the efficiency of the circularization of

the genome, and possibly could therefore impair transcription of the IE genes. It would be very informative to assess the circularization kinetics of the viral genome in our MRE11A knockout HFFs. With regards to Ku, it is just as likely that this complex also binds to the ends of the viral genome. The LigIV/XRCC4 complex is required for optimal replication of the virus and is thought to facilitate the circularization of the viral genome (Muylaert and Elias, 2007). However, loss of Ku70 increases HSV-1 replication (Taylor and Knipe, 2004); therefore, this observation needs to be reconciled with what was observed for LigIV/XRCC4. Circularization of the viral genome also plays a role in the persistence of the viral genome during latent infection in neuronal cells (Wilson and Mohr, 2012). There may exist a vital role for LigIV/XRCC4 in promoting latency of the genome via facilitating circularization in the infected neuron.

The DDR to replicating viral DNA is distinct from the response to input genomes, characterized by ATM activation. However, we found that ATM activation was not entirely dependent on MRN. As discussed in the previous chapter, we hypothesize that the Tip60 acetyltransferase may contribute to the activation of ATM following infection. Loss of Tip60 increases HSV-1 replication in the brains of mice, but this appears to be through the regulation of cGAS (Song et al., 2020). A potential role for Tip60 in regulating HSV-1 replication through ATM may be masked by the effects on the innate immune response to infection. The type-I interferon response does not significantly inhibit ICP0^{-} virus replication in primary fibroblasts (Orzalli et al., 2013), so an effect of Tip60 on ATM resulting in decreased viral replication could possibly be observed in cell culture. We also hypothesized that phosphorylation of Tip60 by the viral US3 kinase (Li et al., 2011) stimulates the activation of ATM to aid in the viral replication cycle. This

hypothesis follows the theme of this dissertation on the manipulation of host cell pathways, in this case the DDR, by the virus to efficiently replicate the viral genome and assemble new particles.

Our observations and conclusions of replication-stimulated DDR protein phosphorylation are predicated on the effects of acyclovir treatment. Acyclovir, being a nucleoside analog, is initially phosphorylated by the viral thymidine kinase to the monophosphate form, and, once converted to the triphosphate form by cellular kinases, is incorporated by the viral DNA polymerase into the replicating viral DNA molecule (Elion, 1982). However, another nucleotide cannot be covalently joined to this analog, and thus acyclovir acts as a chain terminator (Elion, 1982). It is not lost on us that chain termination caused by acyclovir could elicit a DDR, akin to the response to replication fork collapse, to this terminated strand, and that we are in fact observing an effect of this phenomenon instead of a response to otherwise normal DNA damage formed during the replication process. It is important to note, however, that we are observing a loss of activation upon treatment, not a gain, arguing that the effects of acyclovir are more likely representative of the DDR to the entire replication process, of which a potential acyclovir-driven response is most likely minimal. Currently, however, we cannot discount the possibility that a response triggered by chain termination may dampen or otherwise hinder ATM activation. There are many orthogonal methods to test these arguments. Many of the viral DNA replication proteins are essential for synthesizing new viral genomes (Roizman, 2013), so a virus lacking any one of them would mimic the effects of acyclovir treatment. We have shown previously that different HSV-1 viruses missing individual components of the viral DNA replication machinery all yield the same

phenotype, one wherein replication compartment formation, a marker of robust genome replication, is impaired, indicating a defect in the replication process (Liptak et al., 1996). It is possible that any of these viral proteins themselves may shape the DDR, so chemical inhibition of DNA polymerization may be preferred. Phosphonoacetic acid, usually supplied as sodium phosphonoacetate, is a direct inhibitor of the viral DNA polymerase (Mao et al., 1975; Purifoy and Powell, 1977), instead of inhibition by incorporation into the DNA, in the case of acyclovir. We predict that this inhibition of replication by either gene deletion or phosphonoacetic acid treatment will yield the same DDR phenotype as acyclovir-mediated inhibition.

It has been reported that HSV-1 infection increases the instances of double-stranded breaks as measured by a comet assay (Kanai et al., 2012). While HSV-1 DNA may experience breaks during the replication process, this finding indicates that the cellular genome may be experiencing damage as well. This is supported by the observation that γH2AX forms around, but not within, viral replication compartments (Wilkinson and Weller, 2006). This suggests that while ATM is activated by infection, this kinase may phosphorylate H2AX present on the cellular genome. The extent of which could be determined via chromatin immunoprecipitation coupled with deep sequencing analysis.

Opposing roles for Mre11 and ATM in HSV-1 replication

Our results also revealed a surprising phenomenon where Mre11 and ATM seemingly had opposing effects on the replication of the virus. Furthermore, this suggests that these proteins may have roles outside of the canonical DDR. What is

unknown, however, is at which point in the viral lifecycle these proteins act. Mre11 promoted the early DDR to infection, while ATM was activated by viral DNA replication. As mentioned in the previous section, we hypothesize that Mre11 or MRN may bind to the ends of incoming linear viral genome and that this is a potential mechanism of restriction. This could be tested in a manner akin to our investigation of p53 function: to measure IE, E, and L gene expression in the presence of acyclovir/phosphonoacetic acid, or E gene deletions for that matter. If Mre11 indeed restricts initial viral gene transcription, then IE gene expression should be enhanced upon the loss of Mre11, despite the inhibition of viral DNA replication.

Concerning ATM, if it promotes progeny virus production after the onset of genome replication, then the loss of ATM should not affect pre-replicative IE and E gene transcription, i.e., with replication inhibitor treatment. To narrow down a potential mechanism for ATM, a good indicator would be the effect on L gene transcription by loss of the kinase. This would need to be performed without inhibitor treatment, as viral DNA replication is required for L gene expression (Holland et al., 1980; Honess and Roizman, 1975; Jones and Roizman, 1979). If L gene transcription is reduced by ATM knockout, then ATM most likely functions in promoting L gene expression, but if L gene transcription is not affected, then this would suggest that ATM is involved in packaging of the nascent genomes into new capsids. We referenced in the previous chapter the viral UL12 protein at how it associates with MRN (Balasubramanian et al., 2010). It is unknown whether UL12 is required for full ATM activation, and given that UL12 is not a part of the core DNA replication machinery (Roizman, 2013), it may be that viral DNA replication is required for UL12-mediated activation of ATM. This activation of ATM may

serve the purpose to promote efficient packaging of viral genomes by an unknown mechanism. UL12 is thought to facilitate the packaging of replicated genomes (Grady et al., 2017; Porter and Stow, 2004) and to promote recombination in concert with ICP8 (Reuven et al., 2004). It may be that UL12 coordinates efficient packaging of replicated genomes by activating ATM to prime the cellular recombination machinery. One place to start would be to examine the DDR to a UL12-deficient virus. Under our hypothesis, we would predict that the loss of UL12 would phenocopy acyclovir treatment of a WT virus infection.

The regulation of HSV-1 replication by p53

Another potential mechanism for ATM is in promoting the transcriptional activity of p53. Phosphorylation of serine 15 is essential for its activity (Loughery et al., 2014), and we observed that HSV-1-induced phosphorylation was dependent on ATM. However, we are assuming that the phosphorylation of this residue is what confers the pro-viral effect. One method to test this would be to re-introduce mutant p53 into our knockout cells that contains a mutation of this serine residue to an alanine (S15A). S15A p53 would be unable to be phosphorylated, and, furthermore, we predict that this mutant would not support efficient viral replication compared to the WT protein.

Another important observation is that p53 directly binds to the viral genome at specific sequences (Hsieh et al., 2014). It would be interesting to see whether mutation or deletion of these sequences has a profound effect on replication. Furthermore, to solidify that the binding of p53 to the viral genome is indeed the relevant mechanism, we would predict that substitution of a binding sequence from the cellular genome, e.g.,

from p21, would still support efficient replication. The caveat to this idea is that any changes in these viral sequences could cause a loss of fitness, independent of p53. To rule out this possibility, replication of mutant viruses would need to be compared to the WT and rescued viruses in a cell line where p53 is not required for replication. Our tert-HFFs could serve this purpose because HSV-1 replication was not dependent on p53 in these cells.

An off-target effect regulates both the innate and intrinsic responses to HSV-1 infection

In the appendix, our aim was to investigate relationship between a resident protein complex of the inner and outer nuclear membranes and both innate and intrinsic cellular antiviral responses to HSV-1 infection. We initially hypothesized that the LINC complex facilitated both of these responses as various components of this complex interact with IFI16 following HSV-1 infection (Diner et al., 2015). We initially observed that loss of the integral inner nuclear membrane protein Sun1 reduced the type-I interferon response stimulated by HSV-1 infection, but surprisingly reduced replication of the virus, suggesting that Sun1 has a pro-viral function in replication. Following further investigation of the phenotype, we discovered that an off-target effect was present in the SUN1 siRNA pool, and Sun1 did not have an obvious role in the cellular antiviral responses to HSV-1 infection. However, although our results refuted our hypothesis, some value was still gained. siRNA #5 appears to promote STING, TBK1, and IRF3 phosphorylation as well as the expression of at least ICP4. Identification of the target(s) of this siRNA has the potential to uncover novel regulatory factors of innate

sensing of HSV-1 infection and viral replication. This could be accomplished by RNA deep sequencing (RNA-seq) or by mass spectrometry.

3.3 Concluding remarks

The collective cellular response to HSV-1 infection is complex and involves multiple pathways. In this dissertation, we investigated the relationship between HSV-1 and the cellular DDR, with surprising results. Our observations underscore the concept that viruses manipulate the host to their benefit, be it repurposing cellular machinery, or inactivating cellular pathways all together. The understanding of these pathways in the context of infection is critical for the development of therapeutic interventions. In our case, it may be to inhibit the functions of ATM, or maybe to promote the antiviral effects of Mre11. However, the dogma of preferentially targeting viral proteins over host proteins is especially important in the context of the DDR as these proteins play a vital role in protecting the integrity of the cellular genome. If we can determine which viral proteins shape the DDR, we will have identified valuable targets for antiviral therapies. We believe our work only scratches the surface of what there is to learn about the DDR and herpes simplex viruses.

Appendix

The LINC Complex Does Not Regulate the Innate and Intrinsic Responses to Herpes Simplex Virus 1 Infection

Abstract

Cells have evolved complex sets of pathways to sense viral infections and mount an antiviral response to suppress replication of the pathogen. Herpes simplex virus 1 infection triggers the transcription of type-I interferon genes and it has been shown that the viral genomic DNA is sensed in the nucleus by the IFI16 protein, aided by cGAS, to elicit this interferon response. STING is the major adapter protein for the DNA sensing pathway; however, STING is present on the membranes of the endoplasmic reticulum, outside of the nucleus. Sun1 and Sun2, two proteins of the inner nuclear membrane and members of the linker of the nucleoskeleton and cytoskeleton (LINC) complex, were reported to interact with IFI16 following HSV-1 infection. We hypothesized that they help relay this signal from IFI16, through the nuclear envelope, culminating in the activation of STING. Our initial results implicated Sun1, and not Sun2, in promoting STING activation. Moreover, we observed a pro-viral role for Sun1, seemingly independent of the antiviral response. However, upon further investigation, we found that Sun1 was actually dispensable for STING activation and for HSV-1 replication. We determined that an off-target effect in the siRNA pool was responsible for the initial phenotype.

Introduction

In response to infection by DNA viruses, cells up-regulate their type-I interferon (IFN) pathways in order to suppress replication of the pathogen. Foreign DNA is primarily sensed by cyclic GMP-AMP synthase (cGAS) (Sun et al., 2013). Binding of cGAS to double-stranded DNA, aided by the G3BP1 protein (Liu et al., 2019), activates its catalytic activity (Li et al., 2013) to synthesize the cyclic GMP-AMP (cGAMP)

dinucleotide (Wu et al., 2013), which then binds STING, an essential adapter protein (Ishikawa and Barber, 2008), in the cytosol. Binding of cGAMP to STING triggers a conformational change in the protein to its active form (Shang et al., 2019). Activated STING recruits both the TBK1 kinase and the IRF3 transcription factor and TBK1 phosphorylates IRF3 (Liu et al., 2015). Activated IRF3 then dimerizes and moves to the nucleus where is promotes the transcription of IFNs as well as other gene targets (Au et al., 1995). Interferon-inducible protein 16 (IFI16) is another sensor of foreign DNA, also using STING as its adapter (Unterholzner et al., 2010). An additional role for cGAS has been described where it stabilizes IFI16 to help facilitate IFN pathway activation (Orzalli et al., 2015). Other studies found that IFI16 was required for optimal cGAMP production and activation of STING (Almine et al., 2017; Jønsson et al., 2017).

Herpes simplex virus 1 (HSV-1) infection activates the IFN pathway through both IFI16 and cGAS (Orzalli et al., 2015; Orzalli et al., 2012; Sun et al., 2013; Unterholzner et al., 2010). IFI16 associates with the viral DNA soon after infection (Cabral et al., 2018) and oligomerizes on the genome (Lum et al., 2019). While STING is required for the IFN response to HSV-1 infection (Ishikawa and Barber, 2008; Orzalli et al., 2015), it is unknown the precise mechanism by which STING becomes activated. A proteomics study identified the resident nuclear envelope proteins Sun1 and Sun2 as interaction partners of IFI16 following infection (Diner et al., 2015). We hypothesize that these proteins may be the missing link for STING activation. Sun1 and Sun2 are members of the linker of the nucleoskeleton and cytoskeleton (LINC) complex that spans the inner and outer nuclear membranes (Meinke and Schirmer, 2015). Sun1 and Sun2 interact together (Lu et al., 2008), with the large Nesprin family of proteins (Meinke and

Schirmer, 2015), as well as with the TorsinA ATPase (Nery et al., 2008). While TorsinA was not observed to associate with IFI16, its interaction partner TOR1AIP1 (LAP1) (Goodchild and Dauer, 2005) was detected (Diner et al., 2015). Interaction of viral DNA with IFI16 may lead to association with Sun1 and Sun2 to initiate a signaling cascade that culminates in the activation of STING. IFI16 is also involved in the restriction of HSV-1 gene expression (Orzalli et al., 2013), so there is an additional possibility that Sun1 and Sun2 may facilitate this as well.

In this section of the appendix, we explore the potential role of Sun1, Sun2, and TorsinA in both the innate and intrinsic responses to HSV-1 infection. We report that depletion of Sun1, but not Sun2 or TorsinA, by siRNA knockdown, reduces the IFN response to replication-defective HSV-1 infection as well as reduces the replication of ICP0$^-$ HSV-1. However, when the *SUN1* gene was disrupted by CRISPR-Cas9, there was no effect on either the IFN response or on viral replication, contradicting the siRNA results. We demonstrate that this was due to an off-target effect present in the siRNA pool. Our results collectively argue that the LINC complex, at least with respect to Sun1, Sun2, and TorsinA, has no role in the HSV-1 lytic replication cycle or in the cellular response to infection. The mechanisms of action of IFI16 remain to be determined.

Results

siRNA-mediated depletion of Sun1 reduces the type-I interferon response to both HSV-1 and Sendai virus infection

To determine whether the LINC complex facilitated in the innate sensing of HSV-1 infection, we transfected HFFs with either a non-targeting siRNA pool, or pools

targeting Sun1, Sun2, and TorsinA, and STING as a positive control, and infected with *d*109 three days later. *d*109 was used as we previously observed that it stimulates a type-I interferon response in HFFs (Orzalli et al., 2012). Both RNA and protein were collected 6 hours post-infection (hpi). Compared to non-targeting siRNA treatment, knockdown of Sun1 reduced *IFNB* transcripts roughly 5-fold, indicating that Sun1 appeared to promote the type-I interferon response to HSV-1 infection (Figure A.1A). Depletion of Sun2 and TorsinA did not affect *IFNB* mRNA accumulation, arguing that they are dispensable for the innate response to infection. This was interesting as it suggested that the activated pathway was specific to Sun1 and not Sun2, despite the previous report of their interaction (Lu et al., 2008). STING depletion also reduced the innate response to infection, in agreement with our previous observations (Orzalli et al., 2012).

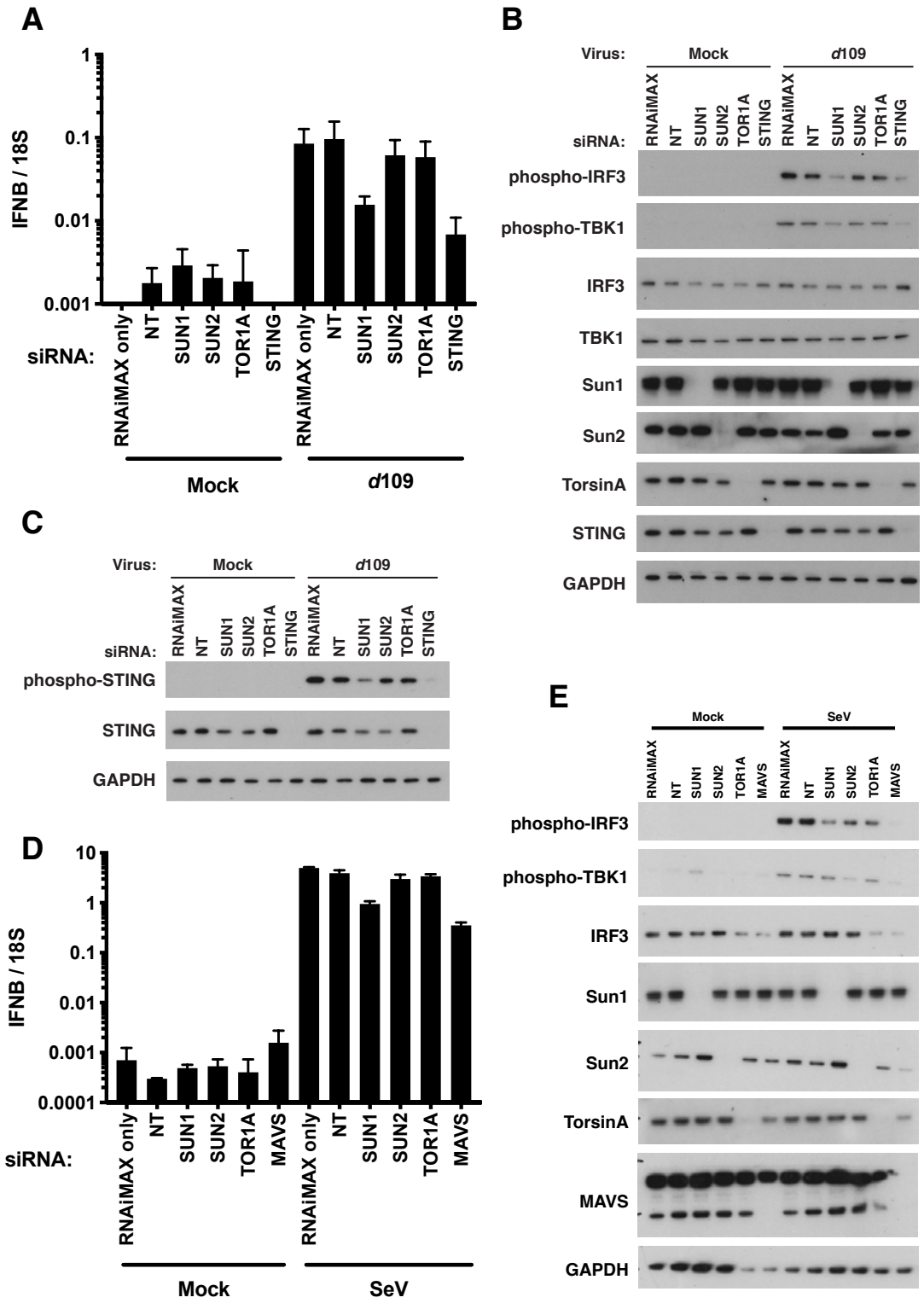
A
IFNB / 18S
1
0.1
0.01
0.001
siRNA:
RNAiMAX only
NT
SUN1
SUN2
TOR1A
STING
RNAiMAX only
NT
SUN1
SUN2
TOR1A
STING
Mock
d109
B
Virus:
Mock
d109
siRNA:
RNAiMAX
NT
SUN1
SUN2
TOR1A
STING
RNAiMAX
NT
SUN1
SUN2
TOR1A
STING
phospho-IRF3
phospho-TBK1
IRF3
TBK1
Sun1
Sun2
TorsinA
STING
GAPDH
C
Virus:
Mock
d109
siRNA:
RNAiMAX
NT
SUN1
SUN2
TOR1A
STING
RNAiMAX
NT
SUN1
SUN2
TOR1A
STING
phospho-STING
STING
GAPDH
D
IFNB / 18S
10
1
0.1
0.01
0.001
0.0001
siRNA:
RNAiMAX only
NT
SUN1
SUN2
TOR1A
MAVS
RNAiMAX only
NT
SUN1
SUN2
TOR1A
MAVS
Mock
SeV
E
Mock
SeV
RNAiMAX
NT
SUN1
SUN2
TOR1A
MAVS
RNAiMAX
NT
SUN1
SUN2
TOR1A
MAVS
phospho-IRF3
phospho-TBK1
IRF3
Sun1
Sun2
TorsinA
MAVS
GAPDH

Figure A.1 (continued)

Figure A.1. Sun1 promotes the type-I interferon response to HSV-1 *d*109 and Sendai virus (SeV) infection.

(A) Primary HFFs were treated with transfection reagent only (RNAiMAX), or transfected with a non-targeting siRNA pool, or a pool targeting Sun1, Sun2, TorsinA, or STING. 72 hours later, cells were infected with *d*109 at an MOI of 5 for 6 hours and RNA collected for RT-qPCR using *IFNB*-specific primers.

(B) Protein lysates were collected from parallel wells from (A) and IRF3 and TBK1 phosphorylation were measured by immunoblot.

(C) STING phosphorylation in the protein lysates from (B) was determined by immunoblot.

(D) HFFs were treated as in (A) and infected with Sendai virus for 6 hours. RNA was collected and analyzed by RT-qPCR for *IFNB* transcripts.

(E) Protein was collected from parallel wells from (D) and IRF3 and TBK1 phosphorylation was determined by immunoblot.

Upstream of *IFNB* transcription, TBK1, IRF3, and STING become phosphorylated, an indication of their activation (Liu et al., 2015). To determine whether Sun1 depletion affected the phosphorylation of these proteins, HFFs were again transfected and infected as above, except this time protein was collected. Mirroring our mRNA results, depletion of Sun1, but not Sun2 or TorsinA, reduced IRF3 and TBK1 phosphorylation (Figure A.1B), as well as STING phosphorylation (Figure A.1C). Our observations indicated that the effects on *IFNB* mRNA accumulation were due to reduced phosphorylation of STING, as STING phosphorylation is required for both TBK1 and IRF3 phosphorylation (Liu et al., 2015).

Because of the localization of Sun1 to the inner nuclear membrane, we reasoned that its depletion should not affect the innate response to a cytosolic stimulus. We chose to use an RNA virus, Sendai virus, as it replicates exclusively in the cytosol (Blair and Robinson, 1970), spatially separated from Sun1. We transfected HFFs with the same siRNA pools used above, but this time substituted a pool targeting MAVS in place of STING, as a positive control. MAVS is a protein present on the mitochondrion that facilitates the innate response to cytosolic RNA also using TBK1 and IRF3 (Seth et al., 2005). Three days post-knockdown, we infected the cells with Sendai virus and collected total RNA and protein 6 hpi. Interestingly, Sun1 knockdown reduced *IFNB* mRNA levels compared to non-targeting treatment (Figure A.1D). This argued that Sun1 has a role not only in facilitating the innate response to nuclear DNA, but also the response to cytosolic RNA. Like with *d*109 infection, depletion of Sun2 and TorsinA had no effect on *IFNB* mRNA levels. Knockdown of MAVS drastically reduced *IFNB* mRNA levels as expected. In agreement with our mRNA results, knockdown of Sun1 reduced

IRF3, but minimally TBK1, phosphorylation (Figure A.1E). This argued that the effects on *IFNB* transcription were an effect of dysregulated IRF3 and not TBK1. Taken together, our results indicated that Sun1 played a role in promoting the cellular type-I interferon response to both DNA and RNA stimuli.

Telomerase-immortalized human fibroblasts mount an innate immune response to foreign RNA, but not foreign DNA

Having described the phenotype in primary fibroblasts, we next sought to determine whether the same phenotype would occur in another human fibroblast cell line. We chose to investigate telomerase-immortalized human fibroblasts (tert-HFFs) (Bresnahan et al., 2000), as they are more amenable for longer studies due to their immortalization. First, we needed to determine whether tert-HFFs mounted an innate immune response to DNA and RNA stimuli in a similar manner to HFFs. We treated both HFFs and tert-HFFs with various stimuli. For DNA, we transfected cells with double-stranded DNA or infected cells with HSV-1 *d*109. For RNA stimuli, we either transfected cells with poly(I:C) as a mimic of double-stranded RNA, or infected with Sendai virus. We also treated cells with cGAMP to activate STING directly. We monitored cells for innate immune activation via immunoblotting for phosphorylated IRF3 and TBK1.

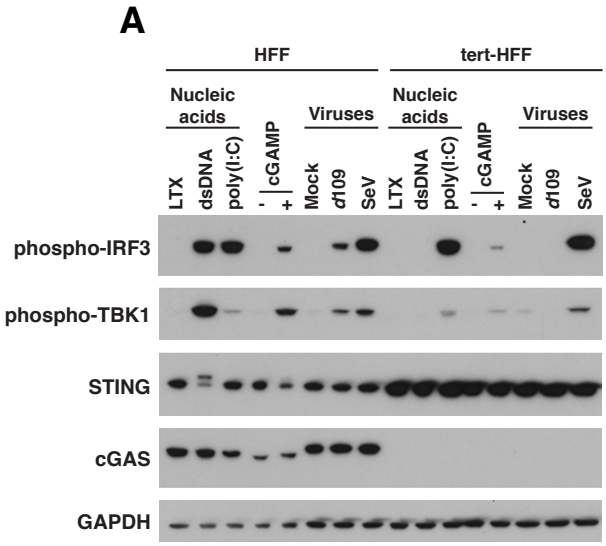

Figure A.2. Tert-HFFs mount an innate immune response to foreign RNA, but not foreign DNA. (A) Primary HFFs and tert-HFFs were transfected with salmon sperm DNA (dsDNA), poly(I:C), permeabilized and treated with cGAMP, or infected with *d*109 (MOI 5) or Sendai virus for 6 hours. Activation of the type-I interferon pathway was assessed by immunoblot. LTX – Lipofectamine transfection reagent.

In HFFs, both DNA stimuli, as well as cGAMP, promoted IRF3 and TBK1 phosphorylation relative to each of their respective controls (Figure A.2A). Both RNA stimuli led to robust IRF3 phosphorylation, but only Sendai virus infection caused appreciable TBK1 phosphorylation. Interestingly, in tert-HFFs, both IRF3 and TBK1 were phosphorylated with both RNA stimuli, but not following treatment with the DNA stimuli. cGAMP treatment only led to modest TBK1 and IRF3 phosphorylation. An immuoblot for cGAS revealed that it was expressed in HFFs, but not tert-HFFs, indicating this as the underlying reason for the lack of innate response to DNA in the immortalized cells. Whether this was due to telomerase activity remains to be determined. Together, our results indicated that, for innate immune studies of HSV-1 infection, tert-HFF was not a suitable cell line. Future type-I interferon experiments will be performed exclusively with HFFs.

Sun1 promotes HSV-1 gene expression and progeny virus production in HFFs

In addition to its role in sensing foreign DNA, IFI16 also restricts HSV-1 gene expression and replication (Merkl et al., 2018; Orzalli et al., 2013). We next sought to determine whether Sun1 had any role in regulating the replication of HSV-1 with the hypothesis that this may be part of the mechanism by which IFI16 restricts the virus. We transfected HFFs with either a non-targeting pool or a pool against Sun1, and measured the replication of the ICP0-null virus 7134 and the repaired virus, 7134R (Cai and Schaffer, 1989), by plaque assay. We used an ICP0-null virus as ICP0 promotes the degradation of IFI16 (Orzalli et al., 2012), which would therefore abolish any potential Sun1 phenotype if the mechanism was dependent on IFI16. Depletion of Sun1

drastically reduced the replication of 7134, but not 7134R (Figure A.3A), indicating that, in the absence of ICP0, Sun1 promoted replication. This was in contrast to our initial hypothesis of Sun1 promoting the restrictive activity of IFI16. If this were the case, then we would have expected Sun1 depletion to have a similar phenotype as IFI16 depletion. Instead, our results suggested that the association of IFI16 with Sun1 inhibited IFI16 function, and the depletion Sun1 made more IFI16 available to restrict replication.

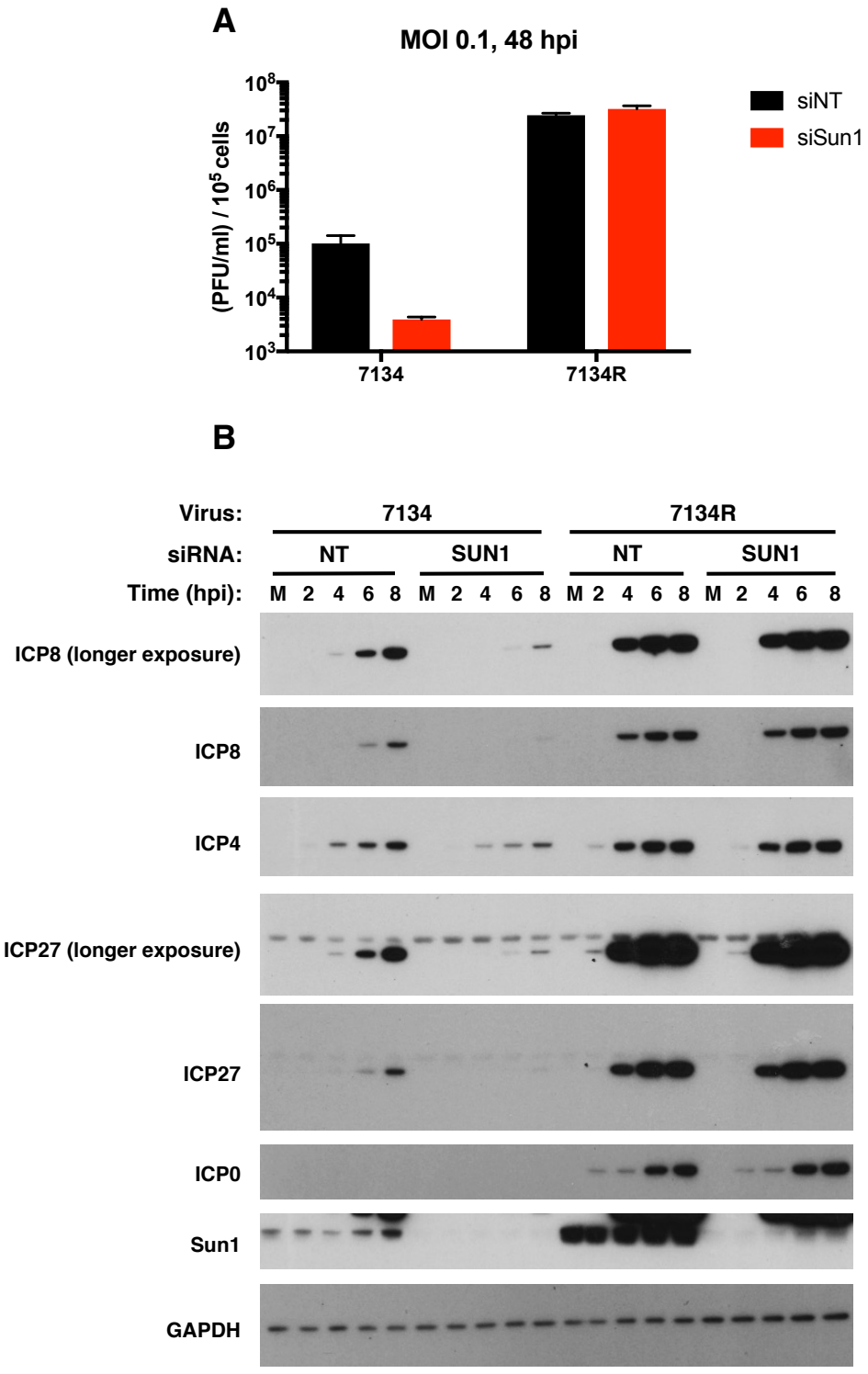
A
MOI 0.1, 48 hpi
(PFU/ml) / 10^5 cells
10^8
10^7
10^6
10^5
10^4
10^3
7134
7134R
siNT
siSun1
B
Virus:
7134
7134R
siRNA:
NT
SUN1
NT
SUN1
Time (hpi):
M 2 4 6 8 M 2 4 6 8 M 2 4 6 8 M 2 4 6 8
ICP8 (longer exposure)
ICP8
ICP4
ICP27 (longer exposure)
ICP27
ICP0
Sun1
GAPDH

Figure A.3 (continued)

Figure A.3. Knockdown of Sun1 reduces the replication and gene expression of HSV-1.

(A) HFFs were transfected with non-targeting or Sun1-specific siRNA pools. 72 hours later, cells were infected with 7134 or 7134R at an MOI of 0.1. 48 hours later, total virus was collected and quantified by plaque assay on U2OS cells.

(B) Knockdown cells were infected with 7134 or 7134R at an MOI of 5 and protein lysates were collected 2, 4, 6, and 8 hpi for immunoblotting.

In order to determine whether this reduction in replication was caused by a reduction in viral gene expression, we infected knockdown cells with the same viruses and measured viral protein translation by immunoblot. In agreement with our replication results, compared to non-targeting siRNA, depletion of Sun1 reduced ICP4, ICP27, and ICP8 protein accumulation over the course of 7134, but not 7134R, infection (Figure A.3B). ICP8 expression requires ICP4 (Roizman, 2013), so the reduction in ICP8 levels was due to a reduction in ICP4 translation. This reduction in ICP4 and ICP27 can be seen as early as 4 hpi, indicating that Sun1 affected gene expression soon after infection. Together, our results argued that Sun1 promoted IE and E gene expression in primary HFFs, but only in the absence of ICP0.

Sun1 promotes viral gene expression in tert-HFFs

Although the tert-HFFs did not mount an innate immune response to foreign DNA, we wanted to determine whether Sun1 also promoted replication in the immortalized fibroblasts. We knocked down Sun1 and infected with 7134. We observed decreased ICP4, ICP27, ICP8, and gD accumulation over the course of infection (Figure A.4A), indicating that, like in HFFs, Sun1 promoted viral protein accumulation in tert-HFFs. Furthermore, *ICP4*, *ICP8*, and *gB* transcript levels were reduced (Figure A.4B), indicating that the reduction in protein levels stemmed from reduced gene transcription. Lastly, when we measured produced virus by plaque assay, depletion of Sun1 resulted in fewer infectious particles present at later time points (Figure A.4C). These results argued that the loss of Sun1 reduced *ICP4* and *ICP27* gene transcription, leading to decreased protein levels, which culminated in fewer progeny viruses.

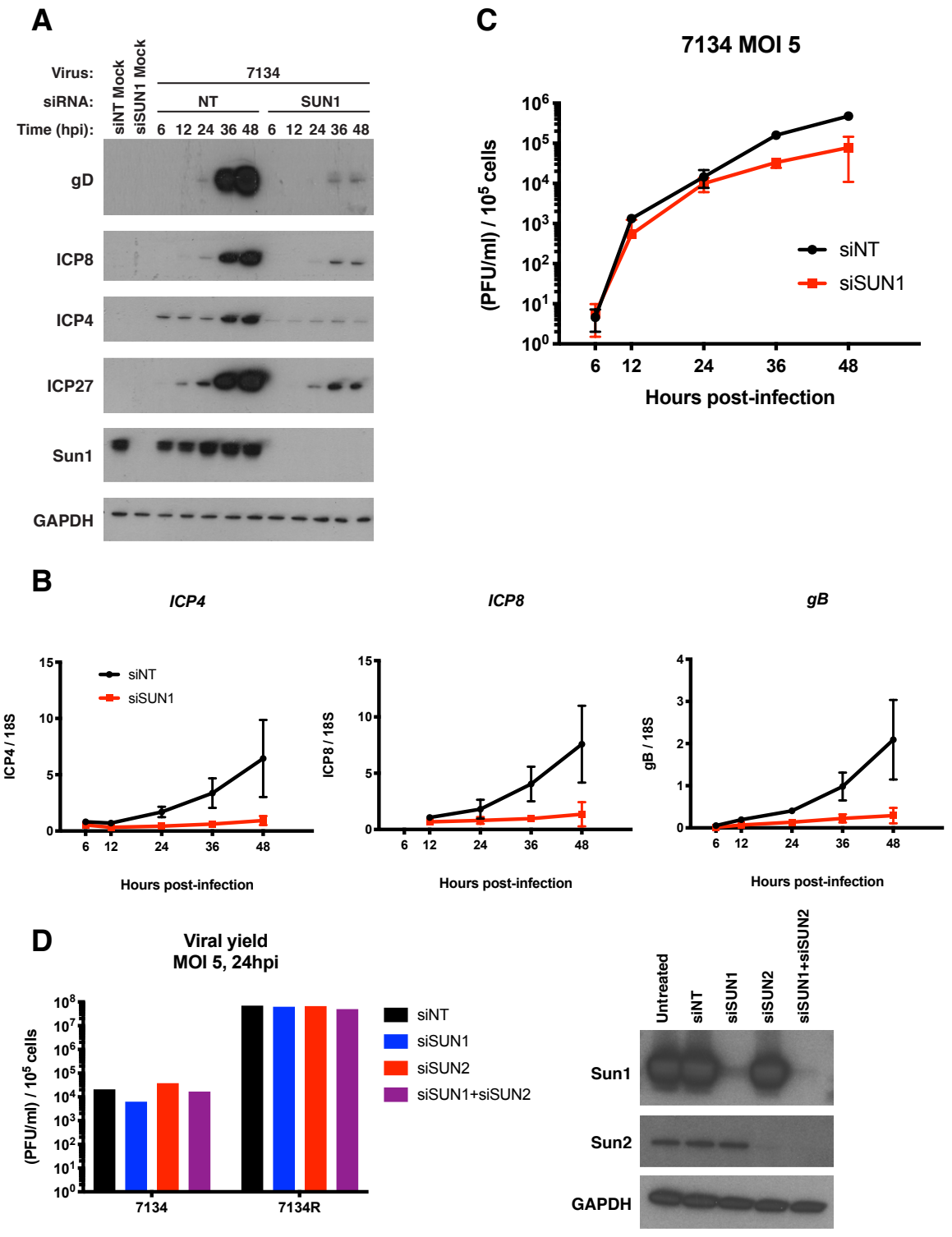
A
Virus:
siRNA:
Time (hpi):
siNT Mock
siSUN1 Mock
7134
NT
SUN1
6 12 24 36 48 6 12 24 36 48
gD
ICP8
ICP4
ICP27
Sun1
GAPDH
C
7134 MOI 5
(PFU/ml) / 10^5 cells
Hours post-infection
siNT
siSUN1
B
ICP4
ICP8
gB
ICP4 / 18S
ICP8 / 18S
gB / 18S
Hours post-infection
D
Viral yield
MOI 5, 24hpi
(PFU/ml) / 10^5 cells
7134
7134R
siNT
siSUN1
siSUN2
siSUN1+siSUN2
Untreated
Sun1
Sun2
GAPDH

Figure A.4 (continued)

Figure A.4. Knockdown of Sun1 in tert-HFFs reduces 7134 gene expression and replication.

(A) Tert-HFFs were transfected with non-targeting and Sun1 siRNA pools and infected with 7134 at an MOI of 5 and protein lysates harvested 6, 12, 24, 36, 48 hpi for immunoblot analysis.

(B) RNA was collected from parallel wells from (A) and analyzed for the indicated viral transcripts by RT-qPCR.

(C) Total virus was collected from parallel wells from (A) and (B) and quantified by plaque assay on U2OS cells.

(D) Tert-HFFs were transfected with a non-targeting pool, the Sun1 pool, the Sun2 pool, or the Sun1 and Sun2 pools together. 72 hours later, the cells were infected with 7134 and 7134R at an MOI of 5. Total virus was collected 24 hours later and quantified by plaque assay on U2OS cells. Protein lysates were collected from parallel wells at the time of infection and knockdowns verified by immunoblotting.

Because Sun1 and Sun2 have been suggested to function redundantly (Lei et al., 2009), we hypothesized that Sun2 could have compensated for the loss of Sun1. To test this, we transfected tert-HFFs with non-targeting siRNA, a Sun1 pool, a Sun2 pool, or a combination of both Sun pools, and measured the replication of 7134 and 7134R. Interestingly, despite successful and specific knockdown, all transfection conditions gave comparable amounts of progeny with respect to each virus (Figure A.4D), indicating that Sun2 did not function redundantly with Sun1, and that Sun2 itself did not promote replication within this initial window of the viral life cycle. Taken together, our results indicated that, in two distinct human fibroblast cell lines, Sun1 promoted the replication of an ICP0-null virus beginning as early as the expression of the essential IE genes *ICP4* and *ICP27*.

Construction of CRISPR-Cas9 gene knockouts in primary HFFs

Having initially described the roles of Sun1 in the innate response to, and replication kinetics of, HSV-1 infection using siRNA knockdown, we next sought to generate gene deletions in primary HFFs via CRISPR-Cas9. We constructed knockouts in HFFs only as tert-HFFs did not harbor an intact DNA sensing pathway, and the defect in replication was observed in both cell types. HFFs were transduced with lentiviruses encoding Cas9 only, or Cas9 along with a single guide RNA (gRNA) and two gRNAs per gene were tested. We targeted the *SUN1*, *SUN2*, *IFI16*, and *STING* genes. The *STING* and *IFI16* knockouts serve as positive controls for the innate response and restriction phenotypes, respectively. After two weeks of transduction, the extents of the knockouts were determined by immunoblot. Each of the gRNAs yielded knockouts of

varying efficiencies, and we chose the gRNAs for future experiments with the largest reductions in protein levels for their respective genes: SUN1 #2, SUN2 #1, IFI16 #1, and STING #1 (Figure A.5A).

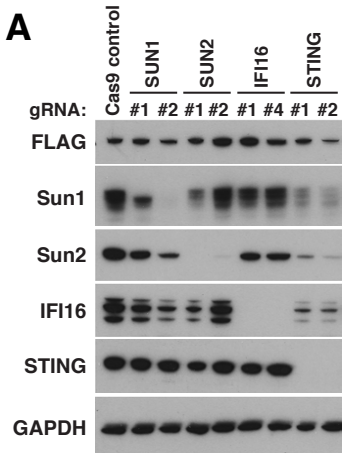

Figure A.5. Construction of gene knockouts in primary HFFs.

(A) Primary HFFs were transduced with lentiviruses constructed to express puromycin resistance and Cas9, or both along with an individual gRNA against the *SUN1*, *SUN2*, *IFI16*, and *STING* genes, as outlined in the materials and methods section. After two weeks of selection, protein lysates were sampled from cells during passage and the knockouts verified by immunoblot.

Knockout of Sun1 does not affect the innate response to HSV-1 infection

First, we set out to determine whether knockout of Sun1 reduced the type-I interferon response to infection. We infected control and knockout fibroblasts with *d*109 for 6, 12, and 24 hours, and measured STING, TBK1, and IRF3 phosphorylation by immunoblot. Interestingly, at all time points, relative to control cells, knockout of Sun1 had no effect on phosphorylation of all three proteins, arguing that Sun1 was dispensable (Figure A.6A). Similarly, knockout of Sun2 and IFI16 had no effect. The knockout of STING abolished TBK1 and IRF3 phosphorylation, indicating canonical function of the DNA sensing pathway. Together, our results indicated that depletion of Sun1 by siRNA, and not CRISPR-Cas9, reduced the innate response to infection. The reason for this will be addressed later in this appendix.

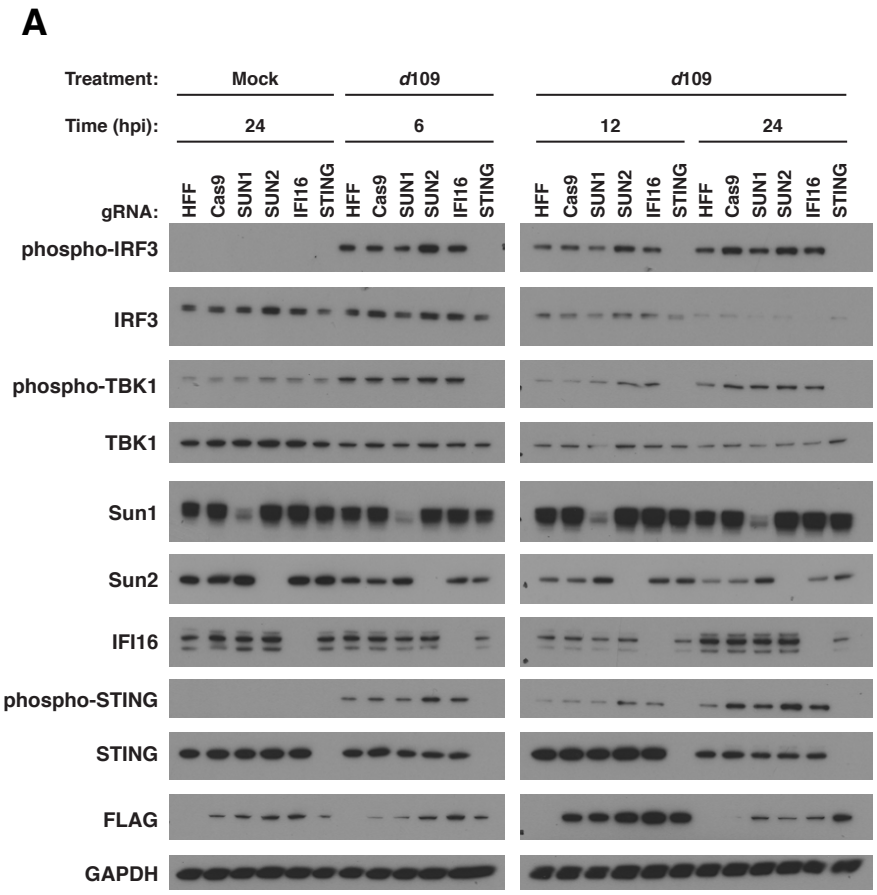

Figure A.6. LINC complex gene knockouts do not affect the innate response to *d*109 infection.

(A) Non-transduced HFFs, Cas9 control, and the knockout cells were infected with *d*109 at an MOI of 5 and protein lysates were taken at 6, 12, and 24 hpi and activation of the type-I interferon pathway was assessed by immunoblot.

Sun1 is dispensable for the innate response to HCMV infection

Having observed that Sun1 depletion via knockout had no effect on the innate response to HSV-1 infection, we wondered if this was also the case for a different DNA virus. We infected control and knockout cells with another herpesvirus, human cytomegalovirus (HCMV), for 6, 12, and 24 hours, and assessed pathway activation by immunoblot. Like with *d*109 infection, loss of Sun1 had no effect on STING, TBK1, and IRF3 phosphorylation at 6 and 12 hpi (Figure A.7A), indicating that the dispensability of Sun1 in the sensing of foreign DNA was not limited to HSV-1 infection. Knockout of Sun2 and IFI16 also had no effect on phosphorylation, and the knockout of STING abolished TBK1 and IRF3 phosphorylation, as expected. We observed a substantial reduction in pathway activation 24 hpi as well as reduced STING levels. This most likely reflects exhaustion of the pathway as STING is degraded after prolonged activation (Xia et al., 2019). Together, our results indicated that differential methods of Sun1 depletion did not yield similar phenotypes. We hypothesized that the combination of the four siRNAs in the pool may be to blame, compared to the single gRNA of the CRISPR-Cas9 knockout.

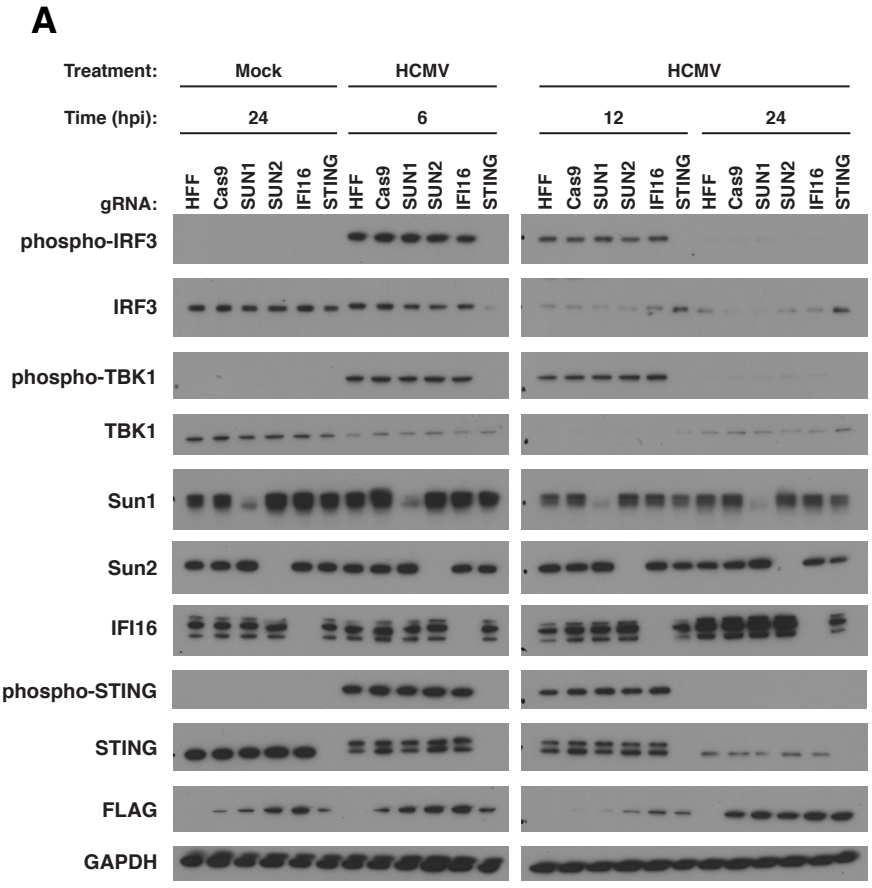

Figure A.7. LINC complex knockout does not affect the innate response to HCMV infection.

(A) Control and knockout HFFs we infected with HCMV strain Ad169 at an MOI of 1 and protein lysates were harvested for immunoblot at 6, 12, and 24 hpi.

Knockout of Sun1 does not affect the replication of HSV-1

Although, Sun1 knockout did not appear to affect the innate response to infection, we wanted to investigate whether the knockout would affect replication of the virus in a similar manner as siRNA knockdown. We infected control and knockout HFFs with 7134 (Figure A.8A) and 7134R (Figure A.8B) and measured produced virus by plaque assay. Surprisingly, knockout of Sun1 and Sun2 did not affect the replication of 7134, indicating that Sun1 also had no role in the lytic replication cycle. Knockout of IFI16 increased the replication of 7134 by roughly ten-fold, validating our knockout system. The replication of 7134R was not affected by any of the knockouts, as expected. Our results argued that, like with the innate response, replication of HSV-1 was independent of Sun1. Taken together, we observed additional phenotypic differences between siRNA knockdown and CRISPR-Cas9 knockout of Sun1.

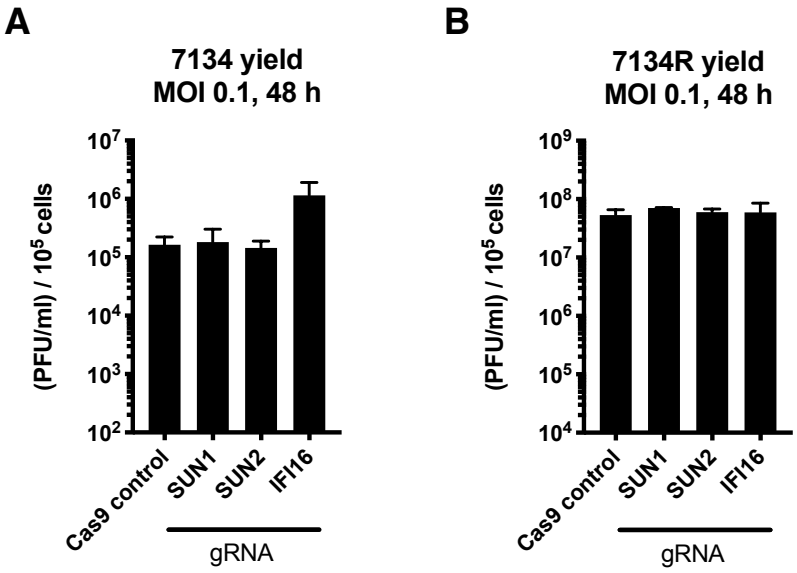

Figure A.8. LINC complex knockout does not affect the replication of HSV-1.

(A) Control and knockout HFFs were infected with 7134 at an MOI of 0.1. Total virus was collected at 48 hpi and quantified by plaque assay on U2OS cells.

(B) Control and knockout HFFs were infected with 7134R at an MOI of 0.1 for 48 hours and total virus was quantified by plaque assay on U2OS cells.

Sun1 is not redundant with Sun2 in CRISPR-Cas9 knockout cells

We observed that Sun2 could not compensate for the absence of Sun1, with respect to HSV-1 replication, in tert-HFFs. We were curious as to whether this was the case in HFFs as well, and this would explain why the knockout of Sun1 had no effect on replication. To test this, we treated control and Sun1 knockout cells with non-targeting or Sun2 siRNA pools and measured 7134 (Figure A.9A) and 7134R (Figure A.9B) replication by plaque assay. Despite specific and successful knockdown of Sun2 (Figure A.9C), double depletion had no effect on the replication of either virus, indicating that Sun2 did not compensate for the absence of Sun1. Our results argued that, not only did CRISPR-Cas9 knockout of Sun1 have no effect on viral replication, further depletion of Sun2 had no added effect.

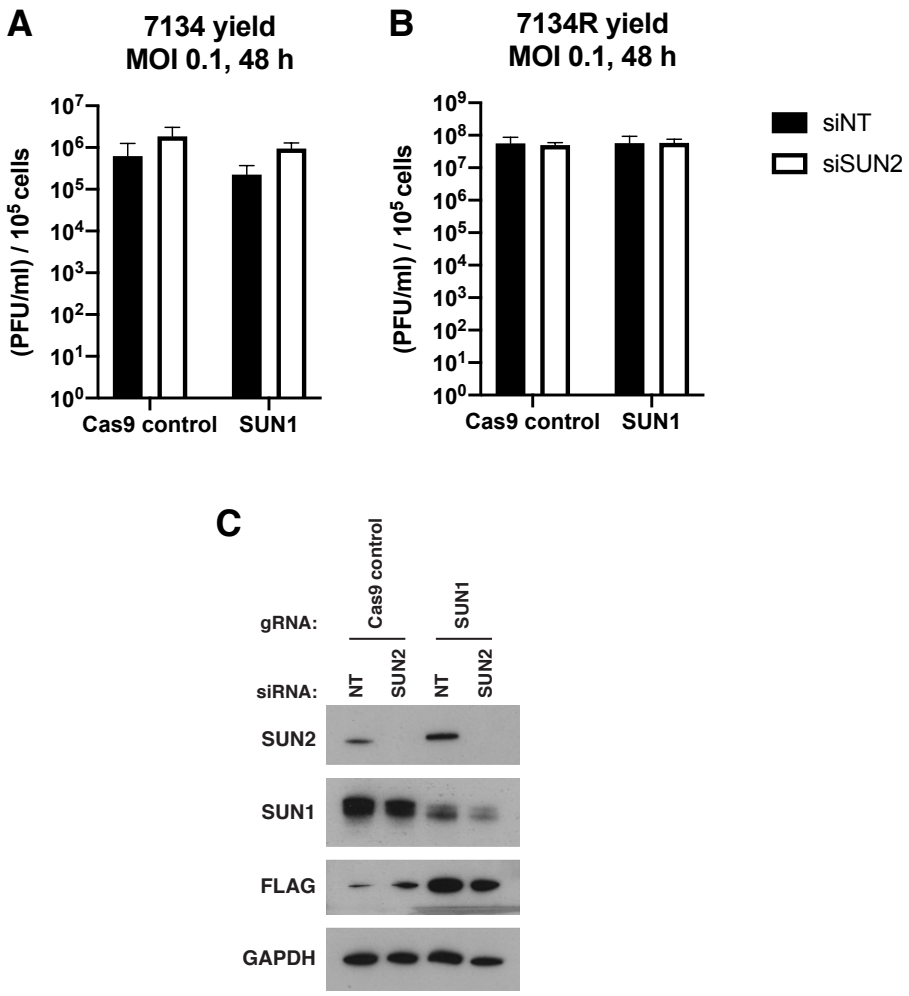

Figure A.9. Sun1 and Sun2 do not function redundantly in HFFs.

(A) Cas9 control and Sun1 knockout HFFs were transfected with either a non-targeting siRNA pool or one targeting Sun2 and infected with 7134 at an MOI of 0.1. 48 hours later, total virus was collected and quantified by plaque assay.

(B) Parallel wells of treated cells from (A) were infected with 7134R at an MOI of 0.1 for 48 hours and produced virus quantified by plaque assay.

(C) Protein lysates were collected from parallel wells from (A) and (B) and analyzed by immunoblot.

An off-target effect of the Sun1 siRNA pool is responsible for regulating the innate response to, and replication kinetics of, HSV-1 infection

Our results thus far have been inconsistent between siRNA and CRISPR-Cas9 depletions of Sun1 and the effects on the type-I interferon response to HSV-1 infection and on the replication kinetics of the virus. We hypothesized that possibly one or more of the siRNAs in the pool were giving an off-target effect. To test this, we transfected HFFs with the non-targeting pool, the complete Sun1 pool, or each of the four individual siRNAs comprising the pool (#5-#8). To test the type-I interferon response, we infected transfected cells with *d*109 and measured IRF3 phosphorylation. As seen before, compared to the non-targeting pool, the pool of Sun1 siRNAs reduced IRF3 phosphorylation (Figure A.10A). Interestingly, while all of the individual siRNAs reduced Sun1 protein levels to varying degrees, they had different effects on IRF3 phosphorylation. #5 drastically reduced phosphorylation, #7 had no effect compared to non-targeting treatment, and #8 was comparable to the pool. Surprisingly, #6 actually enhanced phosphorylation. These results indicated that there indeed was an off-target effect of the siRNA pool, cause by #5. #5 reduced Sun1 levels to a similar extent as #7, but #7 had minimal effects on IRF3 phosphorylation.

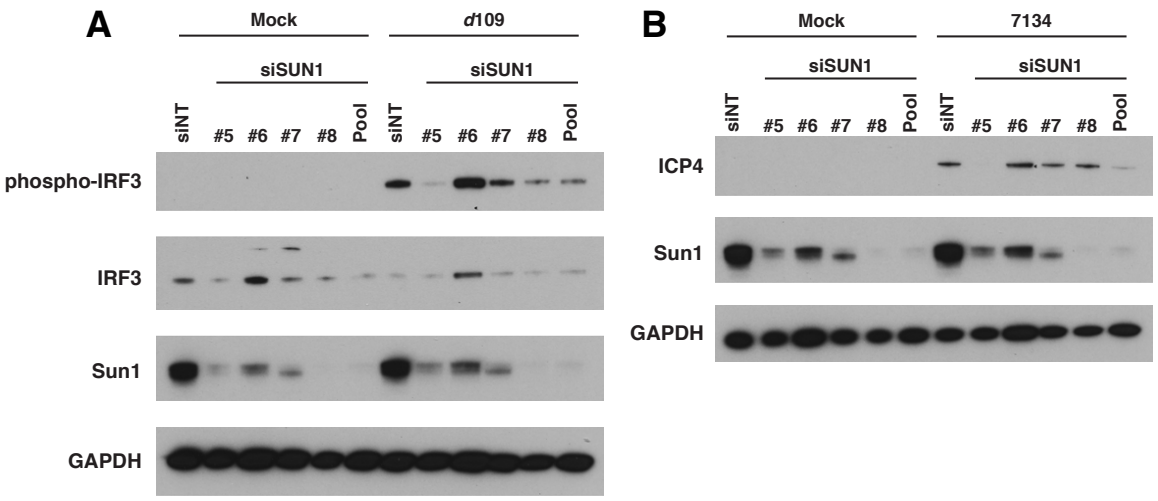

Figure A.10. An off-target effect of the Sun1 pool misleads the phenotype of *d*109 and 7134 infections.

(A) HFFs were transfected with the non-targeting pool, the Sun1 pool, or each of the individual siRNAs comprising the Sun1 pool (#5-#8). 72 hours later, cells were infected with *d*109 at an MOI of 5 and protein lysates were collected at 6 hpi. IRF3 phosphorylation was determined by immunoblot.

(B) Parallel wells were infected with 7134 at an MOI of 5 and protein lysates were collected at 8 hpi for immunoblot.

Next, to determine whether the effect on replication of the virus was due to an off-target effect, we infected treated cells with 7134 and measured the accumulation of ICP4. We observed a similar trend as for IRF3 phosphorylation. Both the pool and #5 reduced ICP4 levels, but #6, #7, and #8 had minimal effects (Figure A.10B). These results argued that #5 was also responsible for the reduction in viral replication by an off-target mechanism. Taken together, our initial siRNA studies of Sun1 were misguided by the #5 siRNA in the pool, and the phenotypes of the other siRNAs, along with the CRISPR-Cas9 knockout, indicated that Sun1 was actually dispensable for both the cellular innate response to infection as well as the genetic regulation of the virus.

Discussion

In this section of the appendix, we investigated two members, and one accessory member, of the LINC complex as to their involvement with the IFN response to HSV-1 infection. When depleted by and siRNA pool, Sun1 appears to promote STING activation following HSV-1 *d*109 infection. However, disruption of the *SUN1* gene by CRISPR-Cas9 has no effect on the response to infection to not only *d*109, but also HCMV. This is also true for the regulation of HSV-1 gene expression. Depletion of Sun1 by siRNA reduces the replication of 7134, but knockout of *SUN1* has no effect. After deconvoluting the siRNA pool, we found that one of the siRNAs gave an off-target effect that was responsible for the phenotypes.

It still largely remains elusive how STING becomes activated when viral DNA is sensed in the nucleus. IFI16 was reported to associate with STING after viral infection (Ansari et al., 2015), but we did not observe this, however (Orzalli et al., 2012). It may

be due to possible differences between cell types. There is increasing evidence for direct interaction between IFI16 and STING as the TRIM21 protein was recently reported to promote the degradation of IFI16 following association with STING (Li et al., 2019). Because Sun1 is intimately tied to the nuclear pore (Liu et al., 2007), a reasonable hypothesis would have been that Sun1 facilitates the export of IFI16 from the nucleus. However, we demonstrated that this was not the case. The details of the IFI16-STING pathway remain to be determined. With regards to the pro-viral effects of Sun1 on viral gene expression, initial viral IE gene transcription is initiated by the viral VP16 protein at the periphery of the nucleus in a manner dependent on the nuclear lamina (Silva et al., 2008; Silva et al., 2012), so our initial hypothesis was that Sun1 was also required for the proper localization of VP16 to IE gene promoters. Indeed, like for the IFN response, we found Sun1 to be dispensable for this process as well, and that the off-target effect responsible for the initial phenotype was siRNA #5 of the pool.

Although Sun1 itself proved dispensable for the innate and intrinsic responses to HSV-1 infection, we cannot rule out that siRNA #5 may have targeted additional Sun proteins. The Sun domain-containing protein family includes Sun1, Sun2, Sun3, Spag5, and Sun5 (Meinke and Schirmer, 2015). While Sun2 levels were not affected by the Sun1 siRNA pool, the effects on the other Sun proteins remains to be determined. It is possible that the depletion of these proteins is what is responsible for our observed phenotypes. The silver lining of our findings is that even though there was an unanticipated off-target effect of the Sun1 siRNA pool, the target of siRNA #5 promotes both the IFN response to infection as well as IE gene expression. Identification of this target may yield a novel regulator of these two processes.

Materials and methods

Cells and viruses

The HFF, U2OS, and HEK293T cell lines were purchased from ATCC. The tert-HFF (Bresnahan et al., 2000) and the FO6 (Samaniego et al., 1997) cell lines have been described previously. The 7134 and 7134R viruses (Cai and Schaffer, 1989) were grown and titered on U2OS cells. The *d*109 virus (Samaniego et al., 1998) was grown and titered on FO6 cells. Sendai virus was purchased from ATCC. The HCMV strain Ad169 was grown and titered on HFFs.

Infections and viral yield assays

Cells were overlaid with the given virus in phosphate-buffered saline (PBS) containing 0.1% glucose and 1% bovine calf serum (BCS) ("infection medium"). After a one hour incubation step at 37°C with agitation, the inoculum was removed and replaced with DMEM containing 1% BCS ("low serum medium"). For viral yield experiments, following the indicated amounts of incubation time, an equal volume of sterile 10% non-fat milk was added to the well and subjected to three freeze-thaw cycles at -80°C. These lysates were then serially diluted in ten-fold increments in infection medium. Confluent U2OS cells were infected with the dilutions using the infection protocol above. After the one hour incubation, cells were overlaid with low serum medium containing 0.16% human IgG. Three days later, cells were fixed with 100% methanol chilled to -20°C for 15 minutes, and then stained with Giemsa stain for one hour. Plaque counts were plotted as plaque-forming units (PFU) per milliliter of lysate, per 1 x 10^5 initially infected cells (i.e. HFFs, tert-HFFs).

Reverse transcription and quantitative PCR

Lysates were collected and processed (Qiagen RNeasy kit) according to the manufacturer's specifications. Purified RNA was DNase-treated (Invitrogen DNA-*free* kit) and then reverse transcribed (Agilent Technologies high-capacity reverse transcription kit). cDNA was quantified by qPCR using primer pairs for a given gene along with Fast SYBR Green Master Mix (Applied Biosystems). cDNA quantities were determined by generating a standard curve using cDNA from Sendai virus-infected HFFs or WT HSV-1-infected HFFs. Quantities for viral and interferon transcripts were normalized to cellular 18S rRNA transcripts.

Table A.1 qPCR primer sequences used

Oligo	Sequence (5' -> 3')	Reference
IFNB forward (cDNA)	AAACTCATGAGCAGTCTGCA	(Orzalli et al., 2015)
IFNB reverse (cDNA)	AGGAGATCTTCAGTTTCGGAGG	(Orzalli et al., 2015)
18S forward (cDNA)	GCATTCGTATTGCGCCGCTA	(Orzalli et al., 2015)
18S reverse (cDNA)	AGCTGCCCGGCGGGTC	(Orzalli et al., 2015)
ICP4 forward (cDNA)	GCGTCGTCGAGGTCGT	(Merkl et al., 2018)
ICP4 reverse (cDNA)	CGCGGAGACGGAGGAG	(Merkl et al., 2018)
ICP8 forward (cDNA)	GGAGGTGCACCGGATACC	(Merkl et al., 2018)
ICP8 reverse (cDNA)	GGCTAACCGGCATGAAC	(Merkl et al., 2018)
gB forward (cDNA)	TGTGTACATGTCCCCGTTTTACG	(Merkl et al., 2018)
gB reverse (cDNA)	GCGTAGAAGCCGTCAACCT	(Merkl et al., 2018)

Immunoblots

Cells were lysed in NuPAGE LDS sample buffer (Invitrogen) containing 5% 2-mercaptoethanol and a protease/phosphatase inhibitor cocktail (HALT, ThermoFisher Scientific). Proteins were separated though 4-12% NuPAGE bis-tris gels (Invitrogen) and were transferred to PVDF membranes (Millipore). Membranes were blocked in 5% non-fat milk in PBS containing 0.1% Tween (PBST) for one hour at room temperature

and then incubated with a given primary antibody in 5% milk overnight at 4°C. Secondary antibodies were used in 5% milk for one hour at room temperature. Blots were developed using film (Denville).

Table A.2 Antibodies used

Antibody (dilution)	**Vendor / Source**	**Catalog Info**
Anti-GAPDH (1:5000)	Abcam	ab8245
Anti-STING (1:2000)	Cell Signaling	13647
Anti-TorsinA (1:1000)	Cell Signaling	2150
Anti-Sun2 (1:2000)	Millipore	ABT272
Anti-Sun1 (1:1000)	Abcam	ab124770
Anti-TBK1 (1:1000)	Cell Signaling	3504
Anti-IRF3 (1:1000)	Cell Signaling	4302
Anti-MAVS (1:2000)	Enzo	ALX-210-929-C100
Anti-cGAS (1:1000)	Cell Signaling	15102
Anti-ICP8 (3-83) (1:5000)	(Knipe et al., 1987)	
Anti-ICP4 (58S) (1:2000)	(Showalter et al., 1981)	
Anti-ICP27 (1:2000)	Abcam	ab31631
Anti-ICP0 (1:2000)	East Coast Bio	H1A027
Anti-gD (1:5000)	Gary Cohen/Roselyn Eisenberg	
Anti-FLAG (1:2000)	Sigma	F1804
Anti-IFI16 (1:2000)	Abcam	ab55328
Anti-phospho-IRF3 (Ser386) (1:1000)	Abcam	ab76493
Anti-phospho-TBK1 (Ser172) (1:1000)	Cell Signaling	5483
Anti-phospho-STING (Ser366) (1:1000)	Cell Signaling	85735
Anti-Rabbit HRP conjugated (1:5000)	Cell Signaling	7074S
Anti-Mouse HRP conjugated (1:5000)	Cell Signaling	7076S

siRNA knockdowns

All single and pool siRNAs were purchased from Dharmacon. The MAVS pool was a gift from Dr. Michaela U. Gack. HFFs were transfected with 10 picomoles of a given siRNA using Lipofectamine RNAiMAX (ThermoFisher Scientific) according to the

manufacturer's specifications. Two days later, cells were trypsinized, diluted 1:2, re-seeded, and used the following day.

Table A.3 siRNA pools used

siRNA	Vendor / Source	Catalog Info
siNT	Dharmacon	D-001810-10-50
siSUN1 (Pool)	Dharmacon	L-025277-00-0005
siSUN1 #5	Dharmacon	J-025277-05-0002
siSUN1 #6	Dharmacon	J-025277-06-0002
siSUN1 #7	Dharmacon	J-025277-07-0002
siSUN1 #8	Dharmacon	J-025277-08-0002
siSUN2	Dharmacon	L-009959-01-0005
siTOR1A	Dharmacon	L-011023-01-0005
siSTING	(Orzalli et al., 2012)	
siMAVS	Dr. Michaela U. Gack	

CRISPR/Cas9 gene knockouts

Guide RNAs were cloned into the pLentiCRISPR V2 backbone (Sanjana et al., 2014) as described previously (Cabral et al., 2018). HEK293T were transfected with this plasmid, psPAX2, and pVSVG using high molecular weight PEI. The Cas9 control construct received a non-cloned plasmid. After 48 hours, culture supernatants were filtered through a 0.45 μm filter and added to fresh, low passage (passages 3-4) HFFs with 5 μg/ml polybrene (Santa Cruz Biotechnology). The next day, the medium was changed to DMEM containing 10% FBS and 1 μg/ml puromycin (Santa Cruz Biotechnology). After roughly two weeks of selection and passaging, knockouts were verified by immunoblot.

Table A.4 Guide RNA sequences used

gRNA	Sequence (DNA form) (5' -> 3')	Reference
SUN1 #1	TACGTGTAGCCCGTGTTCTC	(Schaller et al., 2017)
SUN1 #2	TCGTGGCCAGGCGCAAACTA	(Schaller et al., 2017)
SUN2 #1	CGCCTCACGCGCTACTCCCA	(Schaller et al., 2017)
SUN2 #2	AACTGCATGGTGACGCCAAC	(Schaller et al., 2017)
IFI16 #1	GTTCCGAGGTGATGCTGGTT	(Merkl et al., 2018)
IFI16 #4	TTGATGGAAGAAAAGTTCCG	(Merkl et al., 2018)
STING #1	AGAGCACACTCTCCGGTACC	(Stabell et al., 2018)
STING #2	TCCATCCATCCCGTGTCCCA	Dharmacon online tool

Nucleic acid treatments

Cells were transfected with salmon sperm DNA (dsDNA; Invitrogen) or high molecular weight poly(I:C) using Lipofectamine LTX (ThermoFisher Scientific). Cells were treated with cGAMP (Invivogen) as described previously (Orzalli et al., 2015).

Acknowledgments

We thank Jeho Shin for technical assistance.

References

Alekseev, O., Donovan, K., and Azizkhan-Clifford, J. (2014). Inhibition of ataxia telangiectasia mutated (ATM) kinase suppresses herpes simplex virus type 1 (HSV-1) keratitis. Invest Ophthalmol Vis Sci *55*, 706-715.

Almine, J.F., O'Hare, C.A., Dunphy, G., Haga, I.R., Naik, R.J., Atrih, A., Connolly, D.J., Taylor, J., Kelsall, I.R., Bowie, A.G.*, et al.* (2017). IFI16 and cGAS cooperate in the activation of STING during DNA sensing in human keratinocytes. Nat Commun *8*, 14392.

An, J., Huang, Y.C., Xu, Q.Z., Zhou, L.J., Shang, Z.F., Huang, B., Wang, Y., Liu, X.D., Wu, D.C., and Zhou, P.K. (2010). DNA-PKcs plays a dominant role in the regulation of H2AX phosphorylation in response to DNA damage and cell cycle progression. BMC Mol Biol *11*, 18.

Anacker, D.C., Gautam, D., Gillespie, K.A., Chappell, W.H., and Moody, C.A. (2014). Productive replication of human papillomavirus 31 requires DNA repair factor Nbs1. J Virol *88*, 8528-8544.

Ansari, M.A., Dutta, S., Veettil, M.V., Dutta, D., Iqbal, J., Kumar, B., Roy, A., Chikoti, L., Singh, V.V., and Chandran, B. (2015). Herpesvirus Genome Recognition Induced Acetylation of Nuclear IFI16 Is Essential for Its Cytoplasmic Translocation, Inflammasome and IFN-β Responses. PLoS Pathog *11*, e1005019.

Au, W.C., Moore, P.A., Lowther, W., Juang, Y.T., and Pitha, P.M. (1995). Identification of a member of the interferon regulatory factor family that binds to the interferon-stimulated response element and activates expression of interferon-induced genes. Proc Natl Acad Sci U S A *92*, 11657-11661.

Balasubramanian, N., Bai, P., Buchek, G., Korza, G., and Weller, S.K. (2010). Physical interaction between the herpes simplex virus type 1 exonuclease, UL12, and the DNA double-strand break-sensing MRN complex. J Virol *84*, 12504-12514.

Blackford, A.N., and Jackson, S.P. (2017). ATM, ATR, and DNA-PK: The Trinity at the Heart of the DNA Damage Response. Mol Cell *66*, 801-817.

Blackford, A.N., Nieminuszczy, J., Schwab, R.A., Galanty, Y., Jackson, S.P., and Niedzwiedz, W. (2015). TopBP1 interacts with BLM to maintain genome stability but is dispensable for preventing BLM degradation. Mol Cell *57*, 1133-1141.

Blair, C.D., and Robinson, W.S. (1970). Replication of Sendai virus. II. Steps in virus assembly. J Virol *5*, 639-650.

Bonilla, B., Hengel, S.R., Grundy, M.K., and Bernstein, K.A. (2020). RAD51 Gene Family Structure and Function. Annual review of genetics.

Botting, C., Lu, X., and Triezenberg, S.J. (2016). H2AX phosphorylation and DNA damage kinase activity are dispensable for herpes simplex virus replication. Virol J *13*, 15.

Boutell, C., and Everett, R.D. (2003). The herpes simplex virus type 1 (HSV-1) regulatory protein ICP0 interacts with and Ubiquitinates p53. J Biol Chem *278*, 36596-36602.

Boutell, C., and Everett, R.D. (2004). Herpes simplex virus type 1 infection induces the stabilization of p53 in a USP7- and ATM-independent manner. J Virol *78*, 8068-8077.

Bresnahan, W.A., Hultman, G.E., and Shenk, T. (2000). Replication of wild-type and mutant human cytomegalovirus in life-extended human diploid fibroblasts. J Virol *74*, 10816-10818.

Brouwer, I., Sitters, G., Candelli, A., Heerema, S.J., Heller, I., de Melo, A.J., Zhang, H., Normanno, D., Modesti, M., Peterman, E.J.*, et al.* (2016). Sliding sleeves of XRCC4-XLF bridge DNA and connect fragments of broken DNA. Nature *535*, 566-569.

Brown, J.C. (2017). Herpes Simplex Virus Latency: The DNA Repair-Centered Pathway. Adv Virol *2017*, 7028194.

Burma, S., Chen, B.P., Murphy, M., Kurimasa, A., and Chen, D.J. (2001). ATM phosphorylates histone H2AX in response to DNA double-strand breaks. J Biol Chem *276*, 42462-42467.

Cabral, J.M., Oh, H.S., and Knipe, D.M. (2018). ATRX promotes maintenance of herpes simplex virus heterochromatin during chromatin stress. Elife *7*.

Cai, W.Z., and Schaffer, P.A. (1989). Herpes simplex virus type 1 ICP0 plays a critical role in the de novo synthesis of infectious virus following transfection of viral DNA. J Virol *63*, 4579-4589.

Canman, C.E., Lim, D.S., Cimprich, K.A., Taya, Y., Tamai, K., Sakaguchi, K., Appella, E., Kastan, M.B., and Siliciano, J.D. (1998). Activation of the ATM kinase by ionizing radiation and phosphorylation of p53. Science *281*, 1677-1679.

Chailleux, C., Tyteca, S., Papin, C., Boudsocq, F., Puget, N., Courilleau, C., Grigoriev, M., Canitrot, Y., and Trouche, D. (2010). Physical interaction between the histone acetyl transferase Tip60 and the DNA double-strand breaks sensor MRN complex. Biochem J *426*, 365-371.

Chakraborty, S., Veettil, M.V., and Chandran, B. (2012). Kaposi's Sarcoma Associated Herpesvirus Entry into Target Cells. Frontiers in microbiology *3*, 6.

Chang, H.H., Watanabe, G., Gerodimos, C.A., Ochi, T., Blundell, T.L., Jackson, S.P., and Lieber, M.R. (2016). Different DNA End Configurations Dictate Which NHEJ Components Are Most Important for Joining Efficiency. J Biol Chem *291*, 24377-24389.

Chang, H.H.Y., Pannunzio, N.R., Adachi, N., and Lieber, M.R. (2017). Non-homologous DNA end joining and alternative pathways to double-strand break repair. Nat Rev Mol Cell Biol *18*, 495-506.

Chehab, N.H., Malikzay, A., Appel, M., and Halazonetis, T.D. (2000). Chk2/hCds1 functions as a DNA damage checkpoint in G(1) by stabilizing p53. Genes Dev *14*, 278-288.

Chelbi-Alix, M.K., and de Thé, H. (1999). Herpes virus induced proteasome-dependent degradation of the nuclear bodies-associated PML and Sp100 proteins. Oncogene *18*, 935-941.

Chiang, J.J., Sparrer, K.M.J., van Gent, M., Lässig, C., Huang, T., Osterrieder, N., Hopfner, K.P., and Gack, M.U. (2018). Viral unmasking of cellular 5S rRNA pseudogene transcripts induces RIG-I-mediated immunity. Nat Immunol *19*, 53-62.

Christensen, M.H., Jensen, S.B., Miettinen, J.J., Luecke, S., Prabakaran, T., Reinert, L.S., Mettenleiter, T., Chen, Z.J., Knipe, D.M., Sandri-Goldin, R.M.*, et al.* (2016). HSV-1 ICP27 targets the TBK1-activated STING signalsome to inhibit virus-induced type I IFN expression. Embo j *35*, 1385-1399.

Cliffe, A.R., Arbuckle, J.H., Vogel, J.L., Geden, M.J., Rothbart, S.B., Cusack, C.L., Strahl, B.D., Kristie, T.M., and Deshmukh, M. (2015). Neuronal Stress Pathway Mediating a Histone Methyl/Phospho Switch Is Required for Herpes Simplex Virus Reactivation. Cell Host Microbe *18*, 649-658.

Cliffe, A.R., and Knipe, D.M. (2008). Herpes simplex virus ICP0 promotes both histone removal and acetylation on viral DNA during lytic infection. J Virol *82*, 12030-12038.

Conley, A.J., Knipe, D.M., Jones, P.C., and Roizman, B. (1981). Molecular genetics of herpes simplex virus. VII. Characterization of a temperature-sensitive mutant produced by in vitro mutagenesis and defective in DNA synthesis and accumulation of gamma polypeptides. J Virol *37*, 191-206.

Conwell, S.E., White, A.E., Harper, J.W., and Knipe, D.M. (2015). Identification of TRIM27 as a novel degradation target of herpes simplex virus 1 ICP0. J Virol *89*, 220-229.

Critchlow, S.E., Bowater, R.P., and Jackson, S.P. (1997). Mammalian DNA double-strand break repair protein XRCC4 interacts with DNA ligase IV. Curr Biol *7*, 588-598.

Davison, A.J., Eberle, R., Ehlers, B., Hayward, G.S., McGeoch, D.J., Minson, A.C., Pellett, P.E., Roizman, B., Studdert, M.J., and Thiry, E. (2009). The order Herpesvirales. Archives of virology *154*, 171-177.

Dellaire, G., Ching, R.W., Ahmed, K., Jalali, F., Tse, K.C., Bristow, R.G., and Bazett-Jones, D.P. (2006). Promyelocytic leukemia nuclear bodies behave as DNA damage sensors whose response to DNA double-strand breaks is regulated by NBS1 and the kinases ATM, Chk2, and ATR. J Cell Biol *175*, 55-66.

Dembowski, J.A., and DeLuca, N.A. (2015). Selective recruitment of nuclear factors to productively replicating herpes simplex virus genomes. PLoS Pathog *11*, e1004939.

Dembowski, J.A., and DeLuca, N.A. (2018). Temporal Viral Genome-Protein Interactions Define Distinct Stages of Productive Herpesviral Infection. mBio *9*.

Dembowski, J.A., Dremel, S.E., and DeLuca, N.A. (2017). Replication-Coupled Recruitment of Viral and Cellular Factors to Herpes Simplex Virus Type 1 Replication Forks for the Maintenance and Expression of Viral Genomes. PLoS Pathog *13*, e1006166.

Diner, B.A., Lum, K.K., Javitt, A., and Cristea, I.M. (2015). Interactions of the Antiviral Factor Interferon Gamma-Inducible Protein 16 (IFI16) Mediate Immune Signaling and Herpes Simplex Virus-1 Immunosuppression. Mol Cell Proteomics *14*, 2341-2356.

Doench, J.G., Fusi, N., Sullender, M., Hegde, M., Vaimberg, E.W., Donovan, K.F., Smith, I., Tothova, Z., Wilen, C., Orchard, R.*, et al.* (2016). Optimized sgRNA design to maximize activity and minimize off-target effects of CRISPR-Cas9. Nat Biotechnol *34*, 184-191.

Döhner, K., Wolfstein, A., Prank, U., Echeverri, C., Dujardin, D., Vallee, R., and Sodeik, B. (2002). Function of dynein and dynactin in herpes simplex virus capsid transport. Molecular biology of the cell *13*, 2795-2809.

Doil, C., Mailand, N., Bekker-Jensen, S., Menard, P., Larsen, D.H., Pepperkok, R., Ellenberg, J., Panier, S., Durocher, D., Bartek, J.*, et al.* (2009). RNF168 binds and amplifies ubiquitin conjugates on damaged chromosomes to allow accumulation of repair proteins. Cell *136*, 435-446.

Doudna, J.A., and Charpentier, E. (2014). Genome editing. The new frontier of genome engineering with CRISPR-Cas9. Science *346*, 1258096.

Dumaz, N., Milne, D.M., Jardine, L.J., and Meek, D.W. (2001). Critical roles for the serine 20, but not the serine 15, phosphorylation site and for the polyproline domain in regulating p53 turnover. Biochem J *359*, 459-464.

Duursma, A.M., Driscoll, R., Elias, J.E., and Cimprich, K.A. (2013). A role for the MRN complex in ATR activation via TOPBP1 recruitment. Mol Cell *50*, 116-122.

E, X., Pickering, M.T., Debatis, M., Castillo, J., Lagadinos, A., Wang, S., Lu, S., and Kowalik, T.F. (2011). An E2F1-mediated DNA damage response contributes to the replication of human cytomegalovirus. PLoS Pathog *7*, e1001342.

Edwards, T.G., Bloom, D.C., and Fisher, C. (2018). The ATM and Rad3-Related (ATR) Protein Kinase Pathway Is Activated by Herpes Simplex Virus 1 and Required for Efficient Viral Replication. J Virol *92*.

el-Deiry, W.S., Kern, S.E., Pietenpol, J.A., Kinzler, K.W., and Vogelstein, B. (1992). Definition of a consensus binding site for p53. Nat Genet *1*, 45-49.

Elion, G.B. (1982). Mechanism of action and selectivity of acyclovir. The American journal of medicine *73*, 7-13.

Everett, R.D., Freemont, P., Saitoh, H., Dasso, M., Orr, A., Kathoria, M., and Parkinson, J. (1998). The disruption of ND10 during herpes simplex virus infection correlates with the Vmw110- and proteasome-dependent loss of several PML isoforms. J Virol *72*, 6581-6591.

Everett, R.D., Parada, C., Gripon, P., Sirma, H., and Orr, A. (2008). Replication of ICP0-null mutant herpes simplex virus type 1 is restricted by both PML and Sp100. J Virol *82*, 2661-2672.

Fujiuchi, N., Aglipay, J.A., Ohtsuka, T., Maehara, N., Sahin, F., Su, G.H., Lee, S.W., and Ouchi, T. (2004). Requirement of IFI16 for the maximal activation of p53 induced by ionizing radiation. J Biol Chem *279*, 20339-20344.

Garber, D.A., Beverley, S.M., and Coen, D.M. (1993). Demonstration of circularization of herpes simplex virus DNA following infection using pulsed field gel electrophoresis. Virology *197*, 459-462.

Garvey, C.E., McGowin, C.L., and Foster, T.P. (2014). Development and evaluation of SYBR Green-I based quantitative PCR assays for herpes simplex virus type 1 whole transcriptome analysis. J Virol Methods *201*, 101-111.

Germond, J.E., Hirt, B., Oudet, P., Gross-Bellark, M., and Chambon, P. (1975). Folding of the DNA double helix in chromatin-like structures from simian virus 40. Proc Natl Acad Sci U S A *72*, 1843-1847.

Gibson, W., and Roizman, B. (1971). Compartmentalization of spermine and spermidine in the herpes simplex virion. Proc Natl Acad Sci U S A *68*, 2818-2821.

Goodarzi, A.A., Yu, Y., Riballo, E., Douglas, P., Walker, S.A., Ye, R., Härer, C., Marchetti, C., Morrice, N., Jeggo, P.A*., et al.* (2006). DNA-PK autophosphorylation facilitates Artemis endonuclease activity. Embo j *25*, 3880-3889.

Goodchild, R.E., and Dauer, W.T. (2005). The AAA+ protein torsinA interacts with a conserved domain present in LAP1 and a novel ER protein. J Cell Biol *168*, 855-862.

Gottlieb, T.M., and Jackson, S.P. (1993). The DNA-dependent protein kinase: requirement for DNA ends and association with Ku antigen. Cell *72*, 131-142.

Grady, L.M., Szczepaniak, R., Murelli, R.P., Masaoka, T., Le Grice, S.F.J., Wright, D.L., and Weller, S.K. (2017). The Exonuclease Activity of Herpes Simplex Virus 1 UL12 Is Required for Production of Viral DNA That Can Be Packaged To Produce Infectious Virus. J Virol *91*.

Graham, T.G., Walter, J.C., and Loparo, J.J. (2016). Two-Stage Synapsis of DNA Ends during Non-homologous End Joining. Mol Cell *61*, 850-858.

Gravel, S., Chapman, J.R., Magill, C., and Jackson, S.P. (2008). DNA helicases Sgs1 and BLM promote DNA double-strand break resection. Genes Dev *22*, 2767-2772.

Grawunder, U., Wilm, M., Wu, X., Kulesza, P., Wilson, T.E., Mann, M., and Lieber, M.R. (1997). Activity of DNA ligase IV stimulated by complex formation with XRCC4 protein in mammalian cells. Nature *388*, 492-495.

Gregory, D.A., and Bachenheimer, S.L. (2008). Characterization of mre11 loss following HSV-1 infection. Virology *373*, 124-136.

Gu, H., and Roizman, B. (2003). The degradation of promyelocytic leukemia and Sp100 proteins by herpes simplex virus 1 is mediated by the ubiquitin-conjugating enzyme UbcH5a. Proc Natl Acad Sci U S A *100*, 8963-8968.

Hafner, A., Bulyk, M.L., Jambhekar, A., and Lahav, G. (2019). The multiple mechanisms that regulate p53 activity and cell fate. Nat Rev Mol Cell Biol *20*, 199-210.

Hau, P.M., and Tsao, S.W. (2017). Epstein-Barr Virus Hijacks DNA Damage Response Transducers to Orchestrate Its Life Cycle. Viruses *9*.

Haupt, Y., Maya, R., Kazaz, A., and Oren, M. (1997). Mdm2 promotes the rapid degradation of p53. Nature *387*, 296-299.

Herrera, F.J., and Triezenberg, S.J. (2004). VP16-dependent association of chromatin-modifying coactivators and underrepresentation of histones at immediate-early gene promoters during herpes simplex virus infection. J Virol *78*, 9689-9696.

Hirao, A., Kong, Y.Y., Matsuoka, S., Wakeham, A., Ruland, J., Yoshida, H., Liu, D., Elledge, S.J., and Mak, T.W. (2000). DNA damage-induced activation of p53 by the checkpoint kinase Chk2. Science *287*, 1824-1827.

Holland, L.E., Anderson, K.P., Shipman, C., Jr., and Wagner, E.K. (1980). Viral DNA synthesis is required for the efficient expression of specific herpes simplex virus type 1 mRNA species. Virology *101*, 10-24.

Hollingworth, R., Horniblow, R.D., Forrest, C., Stewart, G.S., and Grand, R.J. (2017). Localization of Double-Strand Break Repair Proteins to Viral Replication Compartments following Lytic Reactivation of Kaposi's Sarcoma-Associated Herpesvirus. J Virol *91*.

Honda, R., Tanaka, H., and Yasuda, H. (1997). Oncoprotein MDM2 is a ubiquitin ligase E3 for tumor suppressor p53. FEBS Lett *420*, 25-27.

Honess, R.W., and Roizman, B. (1974). Regulation of herpesvirus macromolecular synthesis. I. Cascade regulation of the synthesis of three groups of viral proteins. J Virol *14*, 8-19.

Honess, R.W., and Roizman, B. (1975). Regulation of herpesvirus macromolecular synthesis: sequential transition of polypeptide synthesis requires functional viral polypeptides. Proc Natl Acad Sci U S A *72*, 1276-1280.

Hsieh, J.C., Kuta, R., Armour, C.R., and Boehmer, P.E. (2014). Identification of two novel functional p53 responsive elements in the herpes simplex virus-1 genome. Virology *460-461*, 45-54.

Hu, H.L., Shiflett, L.A., Kobayashi, M., Chao, M.V., Wilson, A.C., Mohr, I., and Huang, T.T. (2019). TOP2beta-Dependent Nuclear DNA Damage Shapes Extracellular Growth Factor Responses via Dynamic AKT Phosphorylation to Control Virus Latency. Mol Cell *74*, 466-480 e464.

Huertas, P., and Jackson, S.P. (2009). Human CtIP mediates cell cycle control of DNA end resection and double strand break repair. J Biol Chem *284*, 9558-9565.

Ishikawa, H., and Barber, G.N. (2008). STING is an endoplasmic reticulum adaptor that facilitates innate immune signalling. Nature *455*, 674-678.

Johnstone, R.W., Wei, W., Greenway, A., and Trapani, J.A. (2000). Functional interaction between p53 and the interferon-inducible nucleoprotein IFI 16. Oncogene *19*, 6033-6042.

Jones, P.C., and Roizman, B. (1979). Regulation of herpesvirus macromolecular synthesis. VIII. The transcription program consists of three phases during which both extent of transcription and accumulation of RNA in the cytoplasm are regulated. J Virol *31*, 299-314.

Jønsson, K.L., Laustsen, A., Krapp, C., Skipper, K.A., Thavachelvam, K., Hotter, D., Egedal, J.H., Kjolby, M., Mohammadi, P., Prabakaran, T.*, et al.* (2017). IFI16 is required for DNA sensing in human macrophages by promoting production and function of cGAMP. Nat Commun *8*, 14391.

Jurak, I., Silverstein, L.B., Sharma, M., and Coen, D.M. (2012). Herpes simplex virus is equipped with RNA- and protein-based mechanisms to repress expression of ATRX, an effector of intrinsic immunity. J Virol *86*, 10093-10102.

Kanai, R., Rabkin, S.D., Yip, S., Sgubin, D., Zaupa, C.M., Hirose, Y., Louis, D.N., Wakimoto, H., and Martuza, R.L. (2012). Oncolytic virus-mediated manipulation of DNA damage responses: synergy with chemotherapy in killing glioblastoma stem cells. Journal of the National Cancer Institute *104*, 42-55.

Kang, M.A., So, E.Y., Simons, A.L., Spitz, D.R., and Ouchi, T. (2012). DNA damage induces reactive oxygen species generation through the H2AX-Nox1/Rac1 pathway. Cell death & disease *3*, e249.

Kelly, B.J., Fraefel, C., Cunningham, A.L., and Diefenbach, R.J. (2009). Functional roles of the tegument proteins of herpes simplex virus type 1. Virus research *145*, 173-186.

Kent, J.R., Zeng, P.Y., Atanasiu, D., Gardner, J., Fraser, N.W., and Berger, S.L. (2004). During lytic infection herpes simplex virus type 1 is associated with histones bearing modifications that correlate with active transcription. J Virol *78*, 10178-10186.

Kimberlin, D.W.a.W., R. , and J. (2007). Chapter 64: Antiviral therapy of HSV-1 and -2. In Human Herpesviruses: Biology, Therapy, and Immunoprophylaxis, A. Arvin, G. Campadelli-Fiume, E. Mocarski, P.S. Moore, B. Roizman, R. Whitley, and K. Yamanishi, eds. (Cambridge: Cambridge University Press
Copyright © Cambridge University Press 2007.).

Knipe, D.M., Senechek, D., Rice, S.A., and Smith, J.L. (1987). Stages in the nuclear association of the herpes simplex virus transcriptional activator protein ICP4. J Virol *61*, 276-284.

Kolas, N.K., Chapman, J.R., Nakada, S., Ylanko, J., Chahwan, R., Sweeney, F.D., Panier, S., Mendez, M., Wildenhain, J., Thomson, T.M.*, et al.* (2007). Orchestration of the DNA-damage response by the RNF8 ubiquitin ligase. Science *318*, 1637-1640.

Kouwaki, T., Okamoto, M., Tsukamoto, H., Fukushima, Y., Matsumoto, M., Seya, T., and Oshiumi, H. (2017). Zyxin stabilizes RIG-I and MAVS interactions and promotes type I interferon response. Scientific reports *7*, 11905.

Kubbutat, M.H., Jones, S.N., and Vousden, K.H. (1997). Regulation of p53 stability by Mdm2. Nature *387*, 299-303.

Kumagai, A., Lee, J., Yoo, H.Y., and Dunphy, W.G. (2006). TopBP1 activates the ATR-ATRIP complex. Cell *124*, 943-955.

Kutluay, S.B., DeVos, S.L., Klomp, J.E., and Triezenberg, S.J. (2009). Transcriptional coactivators are not required for herpes simplex virus type 1 immediate-early gene expression in vitro. J Virol *83*, 3436-3449.

Kwak, J.C., Ongusaha, P.P., Ouchi, T., and Lee, S.W. (2003). IFI16 as a negative regulator in the regulation of p53 and p21(Waf1). J Biol Chem *278*, 40899-40904.

Lacasse, J.J., and Schang, L.M. (2012). Herpes simplex virus 1 DNA is in unstable nucleosomes throughout the lytic infection cycle, and the instability of the nucleosomes is independent of DNA replication. J Virol *86*, 11287-11300.

Lamarche, B.J., Orazio, N.I., and Weitzman, M.D. (2010). The MRN complex in double-strand break repair and telomere maintenance. FEBS Lett *584*, 3682-3695.

Lambert, P.F., Kashanchi, F., Radonovich, M.F., Shiekhattar, R., and Brady, J.N. (1998). Phosphorylation of p53 serine 15 increases interaction with CBP. J Biol Chem *273*, 33048-33053.

Lee, J.H., and Paull, T.T. (2005). ATM activation by DNA double-strand breaks through the Mre11-Rad50-Nbs1 complex. Science *308*, 551-554.

Lee, J.S., Raja, P., and Knipe, D.M. (2016). Herpesviral ICP0 Protein Promotes Two Waves of Heterochromatin Removal on an Early Viral Promoter during Lytic Infection. MBio *7*, e02007-02015.

Lee, J.S., Raja, P., Pan, D., Pesola, J.M., Coen, D.M., and Knipe, D.M. (2018). CCCTC-Binding Factor Acts as a Heterochromatin Barrier on Herpes Simplex Viral Latent Chromatin and Contributes to Poised Latent Infection. mBio *9*.

Lees-Miller, S.P., Long, M.C., Kilvert, M.A., Lam, V., Rice, S.A., and Spencer, C.A. (1996). Attenuation of DNA-dependent protein kinase activity and its catalytic subunit by the herpes simplex virus type 1 transactivator ICP0. J Virol *70*, 7471-7477.

Lei, K., Zhang, X., Ding, X., Guo, X., Chen, M., Zhu, B., Xu, T., Zhuang, Y., Xu, R., and Han, M. (2009). SUN1 and SUN2 play critical but partially redundant roles in anchoring nuclei in skeletal muscle cells in mice. Proc Natl Acad Sci U S A *106*, 10207-10212.

Li, D., Wu, R., Guo, W., Xie, L., Qiao, Z., Chen, S., Zhu, J., Huang, C., Huang, J., Chen, B.*, et al.* (2019). STING-Mediated IFI16 Degradation Negatively Controls Type I Interferon Production. Cell Rep *29*, 1249-1260.e1244.

Li, H., Baskaran, R., Krisky, D.M., Bein, K., Grandi, P., Cohen, J.B., and Glorioso, J.C. (2008). Chk2 is required for HSV-1 ICP0-mediated G2/M arrest and enhancement of virus growth. Virology *375*, 13-23.

Li, J., and Stern, D.F. (2005). Regulation of CHK2 by DNA-dependent protein kinase. J Biol Chem *280*, 12041-12050.

Li, R., Zhu, J., Xie, Z., Liao, G., Liu, J., Chen, M.R., Hu, S., Woodard, C., Lin, J., Taverna, S.D.*, et al.* (2011). Conserved herpesvirus kinases target the DNA damage

response pathway and TIP60 histone acetyltransferase to promote virus replication. Cell Host Microbe *10*, 390-400.

Li, X., Shu, C., Yi, G., Chaton, C.T., Shelton, C.L., Diao, J., Zuo, X., Kao, C.C., Herr, A.B., and Li, P. (2013). Cyclic GMP-AMP synthase is activated by double-stranded DNA-induced oligomerization. Immunity *39*, 1019-1031.

Liao, J.C., Lam, R., Brazda, V., Duan, S., Ravichandran, M., Ma, J., Xiao, T., Tempel, W., Zuo, X., Wang, Y.X.*, et al.* (2011). Interferon-inducible protein 16: insight into the interaction with tumor suppressor p53. Structure *19*, 418-429.

Lilley, C.E., Carson, C.T., Muotri, A.R., Gage, F.H., and Weitzman, M.D. (2005). DNA repair proteins affect the lifecycle of herpes simplex virus 1. Proc Natl Acad Sci U S A *102*, 5844-5849.

Lilley, C.E., Chaurushiya, M.S., Boutell, C., Everett, R.D., and Weitzman, M.D. (2011). The intrinsic antiviral defense to incoming HSV-1 genomes includes specific DNA repair proteins and is counteracted by the viral protein ICP0. PLoS Pathog *7*, e1002084.

Lin, R., Noyce, R.S., Collins, S.E., Everett, R.D., and Mossman, K.L. (2004). The herpes simplex virus ICP0 RING finger domain inhibits IRF3- and IRF7-mediated activation of interferon-stimulated genes. J Virol *78*, 1675-1684.

Liptak, L.M., Uprichard, S.L., and Knipe, D.M. (1996). Functional order of assembly of herpes simplex virus DNA replication proteins into prereplicative site structures. J Virol *70*, 1759-1767.

Liu, L., Scolnick, D.M., Trievel, R.C., Zhang, H.B., Marmorstein, R., Halazonetis, T.D., and Berger, S.L. (1999). p53 sites acetylated in vitro by PCAF and p300 are acetylated in vivo in response to DNA damage. Mol Cell Biol *19*, 1202-1209.

Liu, Q., Pante, N., Misteli, T., Elsagga, M., Crisp, M., Hodzic, D., Burke, B., and Roux, K.J. (2007). Functional association of Sun1 with nuclear pore complexes. J Cell Biol *178*, 785-798.

Liu, S., Cai, X., Wu, J., Cong, Q., Chen, X., Li, T., Du, F., Ren, J., Wu, Y.T., Grishin, N.V.*, et al.* (2015). Phosphorylation of innate immune adaptor proteins MAVS, STING, and TRIF induces IRF3 activation. Science *347*, aaa2630.

Liu, Z.S., Cai, H., Xue, W., Wang, M., Xia, T., Li, W.J., Xing, J.Q., Zhao, M., Huang, Y.J., Chen, S.*, et al.* (2019). G3BP1 promotes DNA binding and activation of cGAS. Nat Immunol *20*, 18-28.

Loughery, J., Cox, M., Smith, L.M., and Meek, D.W. (2014). Critical role for p53-serine 15 phosphorylation in stimulating transactivation at p53-responsive promoters. Nucleic Acids Res *42*, 7666-7680.

Lu, W., Gotzmann, J., Sironi, L., Jaeger, V.M., Schneider, M., Luke, Y., Uhlen, M., Szigyarto, C.A., Brachner, A., Ellenberg, J.*, et al.* (2008). Sun1 forms immobile macromolecular assemblies at the nuclear envelope. Biochim Biophys Acta *1783*, 2415-2426.

Lukashchuk, V., and Everett, R.D. (2010). Regulation of ICP0-null mutant herpes simplex virus type 1 infection by ND10 components ATRX and hDaxx. J Virol *84*, 4026-4040.

Lum, K.K., Howard, T.R., Pan, C., and Cristea, I.M. (2019). Charge-Mediated Pyrin Oligomerization Nucleates Antiviral IFI16 Sensing of Herpesvirus DNA. mBio *10*.

Ma, Y., Lu, H., Tippin, B., Goodman, M.F., Shimazaki, N., Koiwai, O., Hsieh, C.L., Schwarz, K., and Lieber, M.R. (2004). A biochemically defined system for mammalian nonhomologous DNA end joining. Mol Cell *16*, 701-713.

Ma, Y., Pannicke, U., Lu, H., Niewolik, D., Schwarz, K., and Lieber, M.R. (2005). The DNA-dependent protein kinase catalytic subunit phosphorylation sites in human Artemis. J Biol Chem *280*, 33839-33846.

Ma, Y., Pannicke, U., Schwarz, K., and Lieber, M.R. (2002). Hairpin opening and overhang processing by an Artemis/DNA-dependent protein kinase complex in nonhomologous end joining and V(D)J recombination. Cell *108*, 781-794.

Mao, J.C., Robishaw, E.E., and Overby, L.R. (1975). Inhibition of DNA polymerase from herpes simplex virus-infected wi-38 cells by phosphonoacetic Acid. J Virol *15*, 1281-1283.

Maréchal, A., and Zou, L. (2013). DNA damage sensing by the ATM and ATR kinases. Cold Spring Harbor perspectives in biology *5*.

Maruzuru, Y., Fujii, H., Oyama, M., Kozuka-Hata, H., Kato, A., and Kawaguchi, Y. (2013). Roles of p53 in herpes simplex virus 1 replication. J Virol *87*, 9323-9332.

Maruzuru, Y., Koyanagi, N., Takemura, N., Uematsu, S., Matsubara, D., Suzuki, Y., Arii, J., Kato, A., and Kawaguchi, Y. (2016). p53 Is a Host Cell Regulator during Herpes Simplex Encephalitis. J Virol *90*, 6738-6745.

Maul, G.G., Guldner, H.H., and Spivack, J.G. (1993). Modification of discrete nuclear domains induced by herpes simplex virus type 1 immediate early gene 1 product (ICP0). The Journal of general virology *74 (Pt 12)*, 2679-2690.

McQuillan, G., Kruszon-Moran, D., Flagg, E.W., and Paulose-Ram, R. (2018). Prevalence of Herpes Simplex Virus Type 1 and Type 2 in Persons Aged 14-49: United States, 2015-2016. NCHS data brief, 1-8.

Meinke, P., and Schirmer, E.C. (2015). LINC'ing form and function at the nuclear envelope. FEBS Lett *589*, 2514-2521.

Merkl, P.E., Orzalli, M.H., and Knipe, D.M. (2018). Mechanisms of Host IFI16, PML, and Daxx Protein Restriction of Herpes Simplex Virus 1 Replication. J Virol *92*.

Mimori, T., and Hardin, J.A. (1986). Mechanism of interaction between Ku protein and DNA. J Biol Chem *261*, 10375-10379.

Mirza, A., Wu, Q., Wang, L., McClanahan, T., Bishop, W.R., Gheyas, F., Ding, W., Hutchins, B., Hockenberry, T., Kirschmeier, P*., et al.* (2003). Global transcriptional program of p53 target genes during the process of apoptosis and cell cycle progression. Oncogene *22*, 3645-3654.

Möhl, B.S., Chen, J., Sathiyamoorthy, K., Jardetzky, T.S., and Longnecker, R. (2016). Structural and Mechanistic Insights into the Tropism of Epstein-Barr Virus. Molecules and cells *39*, 286-291.

Mohni, K.N., Livingston, C.M., Cortez, D., and Weller, S.K. (2010). ATR and ATRIP are recruited to herpes simplex virus type 1 replication compartments even though ATR signaling is disabled. J Virol *84*, 12152-12164.

Moody, C.A., and Laimins, L.A. (2009). Human papillomaviruses activate the ATM DNA damage pathway for viral genome amplification upon differentiation. PLoS Pathog *5*, e1000605.

Mukherjee, B., Kessinger, C., Kobayashi, J., Chen, B.P., Chen, D.J., Chatterjee, A., and Burma, S. (2006). DNA-PK phosphorylates histone H2AX during apoptotic DNA fragmentation in mammalian cells. DNA Repair (Amst) *5*, 575-590.

Muylaert, I., and Elias, P. (2007). Knockdown of DNA ligase IV/XRCC4 by RNA interference inhibits herpes simplex virus type I DNA replication. J Biol Chem *282*, 10865-10872.

Muylaert, I., and Elias, P. (2010). Contributions of nucleotide excision repair, DNA polymerase eta, and homologous recombination to replication of UV-irradiated herpes simplex virus type 1. J Biol Chem *285*, 13761-13768.

Nery, F.C., Zeng, J., Niland, B.P., Hewett, J., Farley, J., Irimia, D., Li, Y., Wiche, G., Sonnenberg, A., and Breakefield, X.O. (2008). TorsinA binds the KASH domain of nesprins and participates in linkage between nuclear envelope and cytoskeleton. J Cell Sci *121*, 3476-3486.

Nimonkar, A.V., Genschel, J., Kinoshita, E., Polaczek, P., Campbell, J.L., Wyman, C., Modrich, P., and Kowalczykowski, S.C. (2011). BLM-DNA2-RPA-MRN and EXO1-BLM-RPA-MRN constitute two DNA end resection machineries for human DNA break repair. Genes Dev *25*, 350-362.

Nimonkar, A.V., Ozsoy, A.Z., Genschel, J., Modrich, P., and Kowalczykowski, S.C. (2008). Human exonuclease 1 and BLM helicase interact to resect DNA and initiate DNA repair. Proc Natl Acad Sci U S A *105*, 16906-16911.

Oh, H.S., Neuhausser, W.M., Eggan, P., Angelova, M., Kirchner, R., Eggan, K.C., and Knipe, D.M. (2019). Herpesviral lytic gene functions render the viral genome susceptible to novel editing by CRISPR/Cas9. Elife *8*.

Oh, J., and Fraser, N.W. (2008). Temporal association of the herpes simplex virus genome with histone proteins during a lytic infection. J Virol *82*, 3530-3537.

Orzalli, M.H., Broekema, N.M., Diner, B.A., Hancks, D.C., Elde, N.C., Cristea, I.M., and Knipe, D.M. (2015). cGAS-mediated stabilization of IFI16 promotes innate signaling during herpes simplex virus infection. Proc Natl Acad Sci U S A *112*, E1773-1781.

Orzalli, M.H., Conwell, S.E., Berrios, C., DeCaprio, J.A., and Knipe, D.M. (2013). Nuclear interferon-inducible protein 16 promotes silencing of herpesviral and transfected DNA. Proc Natl Acad Sci U S A *110*, E4492-4501.

Orzalli, M.H., DeLuca, N.A., and Knipe, D.M. (2012). Nuclear IFI16 induction of IRF-3 signaling during herpesviral infection and degradation of IFI16 by the viral ICP0 protein. Proc Natl Acad Sci U S A *109*, E3008-3017.

Pabla, N., Huang, S., Mi, Q.S., Daniel, R., and Dong, Z. (2008). ATR-Chk2 signaling in p53 activation and DNA damage response during cisplatin-induced apoptosis. J Biol Chem *283*, 6572-6583.

Parkinson, J., Lees-Miller, S.P., and Everett, R.D. (1999). Herpes simplex virus type 1 immediate-early protein vmw110 induces the proteasome-dependent degradation of the catalytic subunit of DNA-dependent protein kinase. J Virol *73*, 650-657.

Peri, P., Mattila, R.K., Kantola, H., Broberg, E., Karttunen, H.S., Waris, M., Vuorinen, T., and Hukkanen, V. (2008). Herpes simplex virus type 1 Us3 gene deletion influences toll-like receptor responses in cultured monocytic cells. Virol J *5*, 140.

Porter, I.M., and Stow, N.D. (2004). Replication, recombination and packaging of amplicon DNA in cells infected with the herpes simplex virus type 1 alkaline nuclease null mutant ambUL12. The Journal of general virology *85*, 3501-3510.

Purifoy, D.J., and Powell, K.L. (1977). Herpes simplex virus DNA polymerase as the site of phosphonoacetate sensitivity: temperature-sensitive mutants. J Virol *24*, 470-477.

Raja, P., Lee, J.S., Pan, D., Pesola, J.M., Coen, D.M., and Knipe, D.M. (2016). A Herpesviral Lytic Protein Regulates the Structure of Latent Viral Chromatin. mBio *7*.

Reuven, N.B., Willcox, S., Griffith, J.D., and Weller, S.K. (2004). Catalysis of strand exchange by the HSV-1 UL12 and ICP8 proteins: potent ICP8 recombinase activity is

revealed upon resection of dsDNA substrate by nuclease. Journal of molecular biology *342*, 57-71.

Rodgers, K., and McVey, M. (2016). Error-Prone Repair of DNA Double-Strand Breaks. Journal of cellular physiology *231*, 15-24.

Rogakou, E.P., Boon, C., Redon, C., and Bonner, W.M. (1999). Megabase chromatin domains involved in DNA double-strand breaks in vivo. J Cell Biol *146*, 905-916.

Roizman, B., Knipe, D.M., and Whitley, R.J. (2013). Herpes simplex viruses. In Fields Virology (Philadelphia, PA: Lippincott Williams & Wilkins), pp. 1823-1897.

Saffert, R.T., and Kalejta, R.F. (2008). Promyelocytic leukemia-nuclear body proteins: herpesvirus enemies, accomplices, or both? Future Virol *3*, 265-277.

Samaniego, L.A., Neiderhiser, L., and DeLuca, N.A. (1998). Persistence and expression of the herpes simplex virus genome in the absence of immediate-early proteins. J Virol *72*, 3307-3320.

Samaniego, L.A., Wu, N., and DeLuca, N.A. (1997). The herpes simplex virus immediate-early protein ICP0 affects transcription from the viral genome and infected-cell survival in the absence of ICP4 and ICP27. J Virol *71*, 4614-4625.

Sanjana, N.E., Shalem, O., and Zhang, F. (2014). Improved vectors and genome-wide libraries for CRISPR screening. Nat Methods *11*, 783-784.

Sartori, A.A., Lukas, C., Coates, J., Mistrik, M., Fu, S., Bartek, J., Baer, R., Lukas, J., and Jackson, S.P. (2007). Human CtIP promotes DNA end resection. Nature *450*, 509-514.

Schaffer, P., Vonka, V., Lewis, R., and Benyesh-Melnick, M. (1970). Temperature-sensitive mutants of herpes simplex virus. Virology *42*, 1144-1146.

Schaller, T., Bulli, L., Pollpeter, D., Betancor, G., Kutzner, J., Apolonia, L., Herold, N., Burk, R., and Malim, M.H. (2017). Effects of Inner Nuclear Membrane Proteins SUN1/UNC-84A and SUN2/UNC-84B on the Early Steps of HIV-1 Infection. J Virol *91*.

Seth, R.B., Sun, L., Ea, C.K., and Chen, Z.J. (2005). Identification and characterization of MAVS, a mitochondrial antiviral signaling protein that activates NF-kappaB and IRF 3. Cell *122*, 669-682.

Shah, G.A., and O'Shea, C.C. (2015). Viral and Cellular Genomes Activate Distinct DNA Damage Responses. Cell *162*, 987-1002.

Shang, G., Zhang, C., Chen, Z.J., Bai, X.C., and Zhang, X. (2019). Cryo-EM structures of STING reveal its mechanism of activation by cyclic GMP-AMP. Nature *567*, 389-393.

Shieh, S.Y., Ikeda, M., Taya, Y., and Prives, C. (1997). DNA damage-induced phosphorylation of p53 alleviates inhibition by MDM2. Cell *91*, 325-334.

Shirata, N., Kudoh, A., Daikoku, T., Tatsumi, Y., Fujita, M., Kiyono, T., Sugaya, Y., Isomura, H., Ishizaki, K., and Tsurumi, T. (2005). Activation of ataxia telangiectasia-mutated DNA damage checkpoint signal transduction elicited by herpes simplex virus infection. J Biol Chem *280*, 30336-30341.

Showalter, S.D., Zweig, M., and Hampar, B. (1981). Monoclonal antibodies to herpes simplex virus type 1 proteins, including the immediate-early protein ICP 4. Infect Immun *34*, 684-692.

Silva, L., Cliffe, A., Chang, L., and Knipe, D.M. (2008). Role for A-type lamins in herpesviral DNA targeting and heterochromatin modulation. PLoS Pathog *4*, e1000071.

Silva, L., Oh, H.S., Chang, L., Yan, Z., Triezenberg, S.J., and Knipe, D.M. (2012). Roles of the nuclear lamina in stable nuclear association and assembly of a herpesviral transactivator complex on viral immediate-early genes. MBio *3*.

Smith, G. (2012). Herpesvirus transport to the nervous system and back again. Annual review of microbiology *66*, 153-176.

Smith, S., Reuven, N., Mohni, K.N., Schumacher, A.J., and Weller, S.K. (2014). Structure of the herpes simplex virus 1 genome: manipulation of nicks and gaps can abrogate infectivity and alter the cellular DNA damage response. J Virol *88*, 10146-10156.

Song, Z.M., Lin, H., Yi, X.M., Guo, W., Hu, M.M., and Shu, H.B. (2020). KAT5 acetylates cGAS to promote innate immune response to DNA virus. Proc Natl Acad Sci U S A *117*, 21568-21575.

Stabell, A.C., Meyerson, N.R., Gullberg, R.C., Gilchrist, A.R., Webb, K.J., Old, W.M., Perera, R., and Sawyer, S.L. (2018). Dengue viruses cleave STING in humans but not in nonhuman primates, their presumed natural reservoir. Elife *7*.

Stewart, G.S., Wang, B., Bignell, C.R., Taylor, A.M., and Elledge, S.J. (2003). MDC1 is a mediator of the mammalian DNA damage checkpoint. Nature *421*, 961-966.

Stracker, T.H., Carson, C.T., and Weitzman, M.D. (2002). Adenovirus oncoproteins inactivate the Mre11-Rad50-NBS1 DNA repair complex. Nature *418*, 348-352.

Stucki, M., Clapperton, J.A., Mohammad, D., Yaffe, M.B., Smerdon, S.J., and Jackson, S.P. (2005). MDC1 directly binds phosphorylated histone H2AX to regulate cellular responses to DNA double-strand breaks. Cell *123*, 1213-1226.

Sun, L., Wu, J., Du, F., Chen, X., and Chen, Z.J. (2013). Cyclic GMP-AMP synthase is a cytosolic DNA sensor that activates the type I interferon pathway. Science *339*, 786-791.

Sun, Y., Jiang, X., Chen, S., Fernandes, N., and Price, B.D. (2005). A role for the Tip60 histone acetyltransferase in the acetylation and activation of ATM. Proc Natl Acad Sci U S A *102*, 13182-13187.

Tang, K.W., Norberg, P., Holmudden, M., Elias, P., and Liljeqvist, J. (2014). Rad51 and Rad52 are involved in homologous recombination of replicating herpes simplex virus DNA. PLoS One *9*, e111584.

Taylor, T.J., and Knipe, D.M. (2004). Proteomics of herpes simplex virus replication compartments: association of cellular DNA replication, repair, recombination, and chromatin remodeling proteins with ICP8. J Virol *78*, 5856-5866.

Theard, D., Coisy, M., Ducommun, B., Concannon, P., and Darbon, J.M. (2001). Etoposide and adriamycin but not genistein can activate the checkpoint kinase Chk2 independently of ATM/ATR. Biochem Biophys Res Commun *289*, 1199-1204.

Tibbetts, R.S., Brumbaugh, K.M., Williams, J.M., Sarkaria, J.N., Cliby, W.A., Shieh, S.Y., Taya, Y., Prives, C., and Abraham, R.T. (1999). A role for ATR in the DNA damage-induced phosphorylation of p53. Genes Dev *13*, 152-157.

Trigg, B.J., Lauer, K.B., Fernandes Dos Santos, P., Coleman, H., Balmus, G., Mansur, D.S., and Ferguson, B.J. (2017). The Non-Homologous End Joining Protein PAXX Acts to Restrict HSV-1 Infection. Viruses *9*.

Unterholzner, L., Keating, S.E., Baran, M., Horan, K.A., Jensen, S.B., Sharma, S., Sirois, C.M., Jin, T., Latz, E., Xiao, T.S.*, et al.* (2010). IFI16 is an innate immune sensor for intracellular DNA. Nat Immunol *11*, 997-1004.

Vassilev, L.T., Vu, B.T., Graves, B., Carvajal, D., Podlaski, F., Filipovic, Z., Kong, N., Kammlott, U., Lukacs, C., Klein, C.*, et al.* (2004). In vivo activation of the p53 pathway by small-molecule antagonists of MDM2. Science *303*, 844-848.

Verpooten, D., Ma, Y., Hou, S., Yan, Z., and He, B. (2009). Control of TANK-binding kinase 1-mediated signaling by the gamma(1)34.5 protein of herpes simplex virus 1. J Biol Chem *284*, 1097-1105.

Wang, H., Shi, L.Z., Wong, C.C., Han, X., Hwang, P.Y., Truong, L.N., Zhu, Q., Shao, Z., Chen, D.J., Berns, M.W.*, et al.* (2013a). The interaction of CtIP and Nbs1 connects CDK and ATM to regulate HR-mediated double-strand break repair. PLoS genetics *9*, e1003277.

Wang, S., Wang, K., Lin, R., and Zheng, C. (2013b). Herpes simplex virus 1 serine/threonine kinase US3 hyperphosphorylates IRF3 and inhibits beta interferon production. J Virol *87*, 12814-12827.

Wang, Y., Schwedes, J.F., Parks, D., Mann, K., and Tegtmeyer, P. (1995). Interaction of p53 with its consensus DNA-binding site. Mol Cell Biol *15*, 2157-2165.

Ward, I.M., and Chen, J. (2001). Histone H2AX is phosphorylated in an ATR-dependent manner in response to replicational stress. J Biol Chem *276*, 47759-47762.

West, A.P., Khoury-Hanold, W., Staron, M., Tal, M.C., Pineda, C.M., Lang, S.M., Bestwick, M., Duguay, B.A., Raimundo, N., MacDuff, D.A.*, et al.* (2015). Mitochondrial DNA stress primes the antiviral innate immune response. Nature *520*, 553-557.

Wilcock, D., and Lane, D.P. (1991). Localization of p53, retinoblastoma and host replication proteins at sites of viral replication in herpes-infected cells. Nature *349*, 429-431.

Wilkinson, D.E., and Weller, S.K. (2004). Recruitment of cellular recombination and repair proteins to sites of herpes simplex virus type 1 DNA replication is dependent on the composition of viral proteins within prereplicative sites and correlates with the induction of the DNA damage response. J Virol *78*, 4783-4796.

Wilkinson, D.E., and Weller, S.K. (2006). Herpes simplex virus type I disrupts the ATR-dependent DNA-damage response during lytic infection. J Cell Sci *119*, 2695-2703.

Wilson, A.C., and Mohr, I. (2012). A cultured affair: HSV latency and reactivation in neurons. Trends in microbiology *20*, 604-611.

Wu, J., Sun, L., Chen, X., Du, F., Shi, H., Chen, C., and Chen, Z.J. (2013). Cyclic GMP-AMP is an endogenous second messenger in innate immune signaling by cytosolic DNA. Science *339*, 826-830.

Xia, T., Yi, X.M., Wu, X., Shang, J., and Shu, H.B. (2019). PTPN1/2-mediated dephosphorylation of MITA/STING promotes its 20S proteasomal degradation and attenuates innate antiviral response. Proc Natl Acad Sci U S A *116*, 20063-20069.

Yin, X., Liu, M., Tian, Y., Wang, J., and Xu, Y. (2017). Cryo-EM structure of human DNA-PK holoenzyme. Cell Res *27*, 1341-1350.

You, Z., Chahwan, C., Bailis, J., Hunter, T., and Russell, P. (2005). ATM activation and its recruitment to damaged DNA require binding to the C terminus of Nbs1. Mol Cell Biol *25*, 5363-5379.

Zannini, L., Delia, D., and Buscemi, G. (2014). CHK2 kinase in the DNA damage response and beyond. Journal of molecular cell biology *6*, 442-457.

Zhang, J., Willers, H., Feng, Z., Ghosh, J.C., Kim, S., Weaver, D.T., Chung, J.H., Powell, S.N., and Xia, F. (2004). Chk2 phosphorylation of BRCA1 regulates DNA double-strand break repair. Mol Cell Biol *24*, 708-718.

Zhang, J., Zhao, J., Xu, S., Li, J., He, S., Zeng, Y., Xie, L., Xie, N., Liu, T., Lee, K.*, et al.* (2018). Species-Specific Deamidation of cGAS by Herpes Simplex Virus UL37 Protein Facilitates Viral Replication. Cell Host Microbe *24*, 234-248.e235.

Zou, L., and Elledge, S.J. (2003). Sensing DNA damage through ATRIP recognition of RPA-ssDNA complexes. Science *300*, 1542-1548.